NONINVASIVE AORTIC PRESSURE DERIVATION FROM PERIPHERAL ARTERIAL SITES: A COMPARATIVE STUDY

By

PRIYA RANJANI MOHAN

A thesis submitted to the

Graduate School- New Brunswick

Rutgers, The State University of New Jersey

And

The Graduate School of Biomedical Sciences

In partial fulfillment of the requirements

For the completion of the

Master of Science

Graduate Program in Biomedical Engineering

Written under the direction of

Professor John K-J. Li

And approved by

New Brunswick, New Jersey

May, 2016.

ABSTRACT OF THE THESIS

Noninvasive Aortic Pressure Derivation from Peripheral Arterial Sites:

A Comparative Study

By **PRIYA MOHAN**

Thesis Director: Professor John K-J. Li

In the United States approximately 73 million people 20 and older, i.e. 1 in every 3 person, suffer from high blood pressure. Hypertensive subjects have significantly increased stiffness in their arteries, making it harder for blood to flow through. Anti-hypertensive drugs such as beta blockers and calcium channel blockers are used for their treatment with the aim to lower blood pressure through reducing vascular stiffness or increasing arterial compliance. The efficacy of the drugs' effects on each patient cannot be accurately determined by the commonly used blood pressure cuff, which provides just systolic and diastolic pressures. In order to accurately diagnose certain severe cases of cardiovascular disorders, invasive and costly catheterization is performed. This thesis develops a model-based noninvasive diagnostic technique for personalized treatment. The methodology utilizes noninvasively measured peripheral artery pulse waveforms as an input to a transfer function in order to compute central aortic pressure waveforms. This is because aortic pressure cannot be obtained directly by noninvasive means and large vessel compliance or stiffness is critical in determining proper function and treatment of hypertensive patients. A cardiovascular system model allows critical parameters, such as large artery compliance and blood pressure augmentation index, to be readily computed.

Many research groups have attempted to produce the aortic waveform noninvasively, while some have succeeded, most of the existent models have flaws which limit the accuracy of the synthesized waveforms. Therapeutic drug efficacy can be easily monitored at regular intervals through this new model-based noninvasive hypertension evaluation system. This project also evaluates the preferred site for noninvasive blood pressure measurements such as radial artery, carotid artery and femoral artery through comparison of their respective transfer functions. Evaluating the physiological advantages of the various peripheral arterial sites for noninvasive blood pressure measurements, radial arterial sites seems to be ideal as it provides best stability during tonometry due to its anatomical advantage of bone packing in the area and increased accessibility compared to other sites such as carotid and femoral. The scope of the thesis limits direct comparison of noninvasively derived with directly invasively measured aortic pressure waveform. Future testing of this step will allow the eventual system to have many advantages, in that it is noninvasive, accurate and low-cost, and affords personalized care for hypertensive patients.

Acknowledgement

I would like to thank my research mentor Dr. John K-J. Li for giving me the opportunity to perform research in his Cardiovascular Engineering Lab and for his exceptional guidance. I would also like to thank Tim Phan, a graduate student in the Lab, for spending time with me to explain core concepts that played a key role in helping me to perform my research successfully. I would also like to thank the Aresty Research Center for funding the project. The input from my thesis committee members Dr. Drzewiecki and Dr. Shoane are also appreciated.

I dedicate my success to my mother- Subashini Mohan, my father- Mohan Shankaran and my extended family for all their support.

Table of Contents

Chapter 1: Introduction

1.1 Cardiovascular Disease- Hypertension

Hypertension, is characterized by a condition in which the arteries have elevated blood pressure. The force of blood in the arteries when the heart contracts is known as systolic and the force exerted while the heart relaxes is the diastolic pressure. Hypertension is classified as a blood pressure level of 140/90 mmHg or higher. Blood pressure levels between 120/80 mmHg and 139/89 mmHg are classified as *prehypertension*. Hypertension is treated using catheters and oral medications in order to lower systemic resistance; however, these drugs such as beta blockers and calcium channel blockers may potentially affect vascular arterial compliance, an index of stiffness of the arteries. The efficacy of the drugs is difficult to determine using generic sphygmomanometer (blood pressure cuff) measurements which only provide systolic and diastolic pressures. Pressure waveforms are often used to quantify the functioning of the heart and its responses to treatments as it provides a more accurate data of the blood flow to the heart during a certain time interval.

Table 1.1 Illustration of the different systolic and diastolic pressures which correspond to various levels of hypertension.

Category	**Systolic** mm Hg (upper #)		**Diastolic** mm Hg (lower #)
Normal	less than **120**	and	less than **80**
Prehypertension	**120 – 139**	or	**80 – 89**

Hypertension Stage 1	**140 – 159**	or	**90 – 99**
Hypertension Stage 2	**160** or higher	or	**100** or higher
Severe Hypertension – Medical Attention Needed	Higher than **180**	or	Higher than **110**

1.2 Blood Pressure Measurements

Blood pressure is usually monitored using a sphygmomanometer, or colloquially known as a blood pressure cuff, which outputs systolic and diastolic pressure measurements along with heart rate. There are other ways to determine blood pressure such palpation, auscultatory method or invasive methods. The auscultatory method (from the Latin word for "listening") uses a stethoscope and a sphygmomanometer (Mathers, 2003). This is an inflatable cuff which is attached to a mercury manometer and is called *Riva-Rocci.* It is placed around the upper arm approximately at the same height as the heart. Systolic blood pressure is the first sound that is heard. At the diastolic pressure the cuff pressure is further released until no sound can be heard. In order to accurately diagnose certain severe cases of cardiovascular disorders, physicians have their patients undergo a type of cardiac catheterization procedure called the arterial-line or A-line procedure. Several patients who undergo medication for these cardiovascular conditions also require cardiac catheterization for constant monitoring of their arterial blood pressure. The process of invasively obtaining aortic blood pressure waveform is very expensive, time consuming and prone to infection. Catheter insertions will output blood pressure waveforms which are more accurate in quantifying the characteristics of a heart’s physical properties and functioning.

1.3 Automated Blood Pressure Measurement Monitor

One of the widely used blood pressure measuring devices is Omron Healthcare HEM-780 Automatic Blood Pressure Monitor which contains Intellisense technology for more accurate, memory with date/time stamp, more comfortable readings, hypertension indicator, detects irregular heartbeat, and has 84 base memory per user. Similarly, the MABIS deluxe air release valve has an accurate deflation rate, which features heavy-duty vulcanized bladder and thick-walled inflation bulb along with calibrated nylon cuff (Visser, 1995). Range markings on the cuff helps the practitioner to facilitate the placement of the cuff properly and aids in selecting the right size. Similarly, The American Diagnostics Corporation manual blood pressure kit has a self-adjusting D-Ring cuff which can be used with one hand. The cuff range is 24-33.6 and the blood pressure reading is accurate to 3mmHg of reading (Visser, 1995). Through these devices only systolic and diastolic pressures can be obtained.

1.4 Central Aortic and Peripheral Arterial Waveform Measurements

The shockwave known as arterial pressure wave is generated from the blood that's released from the left ventricle, carried from aorta, away to the peripheral arteries. Figure 1.1 represents the impulse from left ventricular contraction that passes though the aortic valve and vessels travelling down along a path of blood. The pulse then is detected by a catheter and passes through another hard tubing which consists of fluid and finally into the pressure transducer.

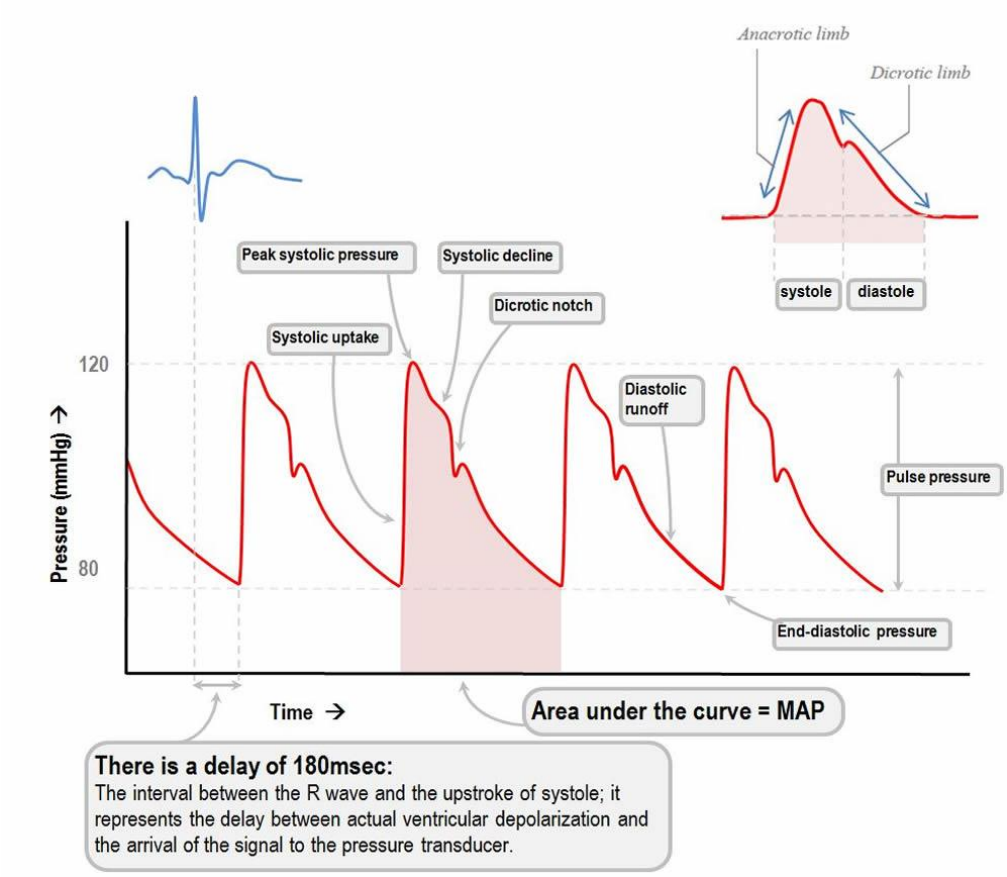

Figure 1.1: Illustration of aortic waveform and its components. Reproduced with permission from (John Wiely and Sons. Ruiz, 2013)**.**

A very narrow pulse pressure might indicate chances of various conditions such as severe cardiogenic shock or pulmonary embolism.

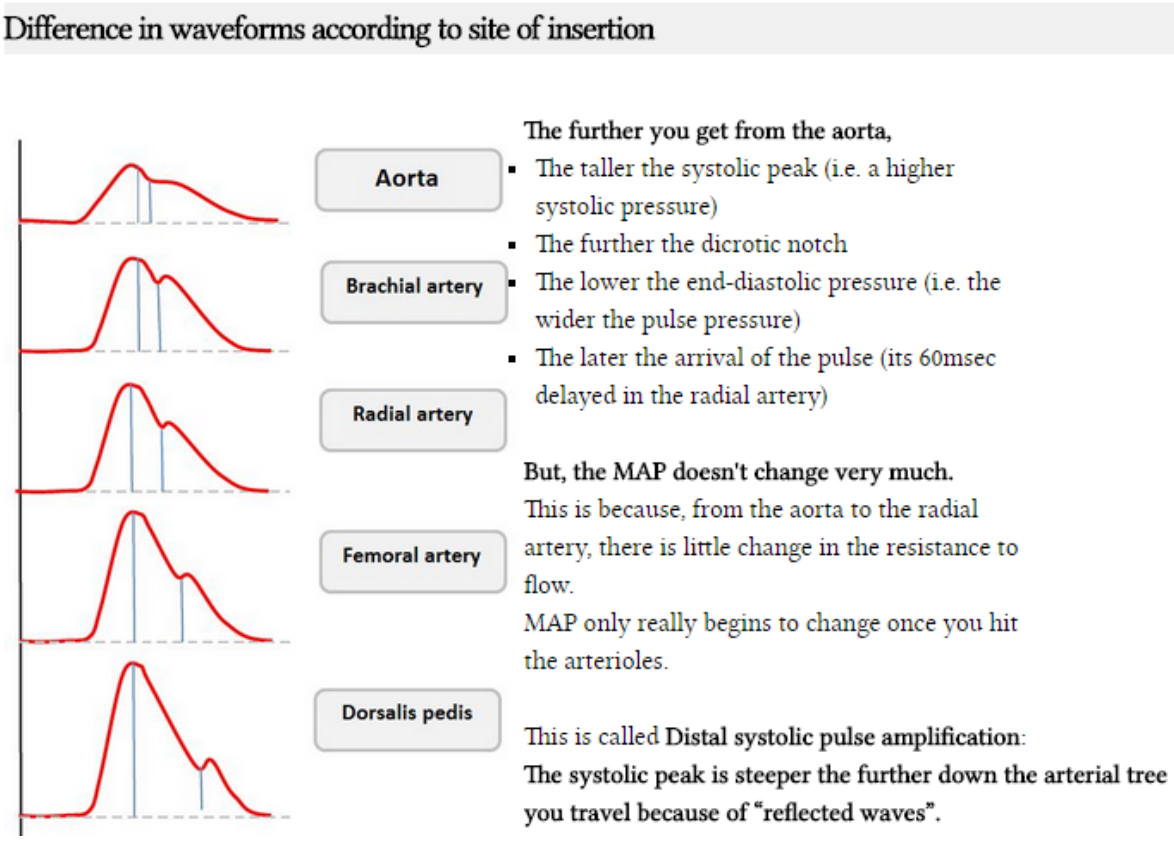

Figure 1.2: Waveforms in different arterial sites. Notice morphological changes in radial arterial waveform is compared to the aortic waveform. Reproduced with permission from (John Wiely and Sons. Ruiz, 2013)**.**

Compared to aorta, there could be as much as a 20mmHg increase in the systolic BP by the time the blood gets to the radial artery.

1.5 Anti-Hypertensive Drug Treatment: *The ACE inhibitor- Ramipril*

In 2000, *The Lancet* published a research article written by The Heart Outcome Prevention Evaluation (HOPE) study investigators, who conducted an experiment that investigates the effects of the angiotensin-converting-enzyme inhibitor (ACE inhibitor) drug called Ramipril's effects on altering the risk of acquiring cardiovascular diseases in

patients with diabetes mellitus. It was proven that despite having unpleasant side effects, Ramipiril significantly reduced the risk of cardiovascular disease in diabetic patients.

In 1960s, one the earliest forms of ACE inhibitors was discovered through the venom properties of the snake (Patlak, 2004). The Nobel Prize winner, John Vane, performed studies at the Royal College of Surgeons laboratories which demonstrate that peptides from the Brazilian viper's venom inhibited the activity of ACE from dog lung.[4] Since then ACE inhibitors have been used as vasodilators that relax the blood vessel and improve hemodynamic functioning of the heart. ACE inhibitors, especially, Ramipril have been shown to have adverse side effects on patients such as severe fits of cough, hypotension and angioedema (Visser, 1995). Out of the 1808 patients who were administered Ramipril during the double blind experiment conducted by HOPE, 133 (7%) of participants discontinued the study due to discomfort caused by excessive cough and another 2% withdrew from the study due to hypotension or dizziness (HOPE study investigators, 2000). Also 3% withdrew due to Angioedema, swelling of the deep skin layers (HOPE study investigators, 2000). While, those participants who belonged to the control group had less withdrawal rates with attributions to the aforementioned side effects.

Although Ramipril have been shown to have several side effects, its benefits outweigh the minor discomforts. HOPE recruited 3577 diabetic patients aged 55 years or older who were had at least one cardiovascular diseases. In the experiment conducted by HOPE, Ramipril was shown to reduce the risk of cardiovascular diseases by 25-30% in middle-aged to old people who were affected by diabetes mellitus. The investigators of the HOPE experiment conclude that ACE inhibitor, Ramipril, was able to achieve the

benefits due to its ability to lower the levels of angiotensin-II, a vasoconstrictor that is powerful enough to cause smooth-muscle growth and promote plaque rupture in the arteries (HOPE study investigators, 2000).

It is also important to note that although the study strongly suggest that Rampiril is an effective ACE inhibitor that reduces the risk of cardiovascular complications in diabetic patients, the adherence rate of the participants to Ramipril was 65% by the end of the study, which might potentially differ if the adherence rate was higher (HOPE study investigators, 2000). Also, Ramipril was studied by HOPE as an effort to monitor the results of the cardiovascular outcomes in patients when the drug was added to the current treatment course and was not designed to provide a specific level of blood pressure. Thus, the study shows the effect of Ramipril as a preventive method with several benefits that are brought about by the vasodilation which reduces blood pressure. While medications such as Ramipril reduce the risk, life style choices such as diet, smoking and drinking habits may affect the risk factors in patients with diabetes mellitus as well.

Chapter 2: Specific Aims and Significance of the Thesis

2.1 Specific Aims

The overall objective of the thesis is to identify pulse waveform differences in normal and diseased conditions and to establish methods to quantify central and peripheral pulse contour changes. The thesis also aims to identify the advantages and disadvantages of obtaining blood pressure waveform at radial, carotid and femoral arteries as the input to produce the aortic blood pressure waveform.

The specific aims are:

1. To obtain distinct transfer functions for radial, carotid and femoral artery in order to produce the aortic blood pressure waveform.
2. To compare the transfer function of subjects who are normal, hypertensive and or with severe heart failure.
3. To identify the ideal site by comparing and contrasting the transfer functions at various sites.
4. Analyze the transfer function for different pathological conditions and drug treatments.

2.2 Significance

Hypertensive subjects have significantly increased stiffness in their arteries, making it harder for blood to flow through. Some of the anti-hypertensive drugs such as ACH inhibitors and calcium channel blockers are used for their treatment with the aim to lower blood pressure through reducing vascular stiffness or increasing arterial compliance. The efficacy of the drugs' effects on each patient cannot be accurately

determined by the commonly used blood pressure cuff which provides just systolic and diastolic pressures. Personalized treatment to obtain the arterial waveform from clinical catheterization is invasive and costly, thus impractical as an evaluation tool. The results of this will lead to a diagnostic technique for personalized treatment based on non-invasive radial artery pressure pulse. The transfer function will then allow computation of central aortic pressure for further diagnosis of reduced large artery stiffness- a hallmark of hypertension. Therapeutic drug efficacy can be easily monitored at regular intervals through this new model-based hypertension evaluation approach. The analysis of the ideal site from which the noninvasive measurements can be obtained can produce better estimation of the aortic blood pressure waveform. Although each site (radial, carotid and femoral) have their own advantages and disadvantages, it could be beneficial to compare the results and calibrate the system for each individual patient to produce an accurate aortic estimation.

Chapter 3: Methods

3.1 Blood Pressure Data from Digitized Waveform

Theoretically speaking, the aortic pressure can be reconstructed by measuring the radial artery pressure and knowing the transfer function between the two waveforms. This approach is most useful for computing central aortic pressure which cannot be measured directly through noninvasive means. This thesis concentrates on this method.

A series of harmonic sine waves were fit into each pressure wave at heart rate frequencies during Fourier Frequency analysis. The transfer function is a ratio in phase and amplitude of the harmonics of radial and aortic BP data. Below is the generalized transfer function where Y(z) is the output and X(z) is the input.

$$H(z) = \frac{Y(z)}{X(z)} \tag{3.1}$$

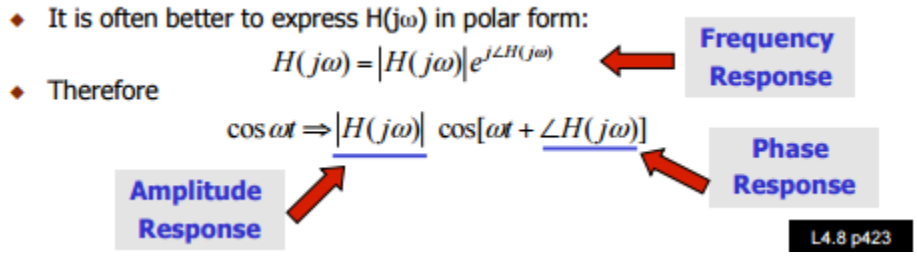

(3.2)

In order to establish the transfer function, simultaneously measured radial carotid and femoral arterial and aortic waveforms from various previously published research papers were digitized using a software known as WebPlotDigitizer. The software facilitates extraction of data from plot images. It has automatic and manual features which allow the user to add, delete or manually manipulate each data point. The automatic mode allows the user to highlight a section of the plot image, select a sample

pixel which contains the data and when the software is run it quantifies the data according to the input from the user regarding data location, after which the user may alter the data positions. To perform FFT the radial arterial and aortic data points must be interpolated such that the sampled data points are 2^n points. Therefore the data was interpolated using MATLAB software, with a time interval of 0.01 sec between each data point. Radial and aortic pressure waveforms do not start at the same time, as expected, since aortic pulse appears ahead of the radial pulse. There is a pulse transit time delay between the aortic pressure as it propagates to the radial artery. The pulse transit delay can be calculated using the following formula (Zhang, 2011):

Pulse transit time (PPT) = Distance traveled by the pulse * Pulse wave velocity

The average PPT from aorta to radial artery was calculated to be about 116 ±0.022 ms in a study conducted by Dr. Zhang's team on a group of 266 healthy adults (Zhang, 2011). Therefore, a PPT of 140 ms/ 0.01 sec was used to process the radial pressure data. A PPT of 14.28 ms for carotid and 46.15 ms for femoral arterial data.

Then FFT was performed on the interpolated radial and aortic data set to produce the magnitudes. The ratio of these magnitudes were obtained into order to derive a generalized amplitude.

$$\text{Amplitude} = \frac{MRadial}{MAorta} \qquad (3.3)$$

Now that a generalized amplitude matrix with the ratio of magnitude is established, the radial blood pressure data of 4 other subjects were processed again with FFT to obtain the radial magnitude. Using the generalized amplitude and radial magnitude, the magnitude values of aorta was computed as follows:

$$MAorta = \frac{MRadial}{Amplitude} \quad (3.4)$$

After the aortic magnitude values were obtained, Inverse Fourier Transform was performed to convert the signal from frequency domain to time domain. The resulting aortic blood pressure in time domain was graphed simultaneously along with the original aortic waveform of each corresponding patient to compare accuracy. 2-D correlation coefficient was calculated using the MATLAB function called corr2 to further quantify the validity of the derived aortic blood pressure waveform.

A research team from St. Vincent's Hospital, Australia, led by Karamanoglu et. al (1996) used a similar technique, however his team used discrete fourier transform (DFT). We chose FFT since it's a faster algorithm for calculation than DFT. The equation for computing fourier series analysis of digitized data has a summation in instead of integration. While DFT computation of N points takes about $\Theta(n^2)$ time, FFT produces that same result in Θ (n log n) time steps, which is much more efficient. Therefore, FFT was used instead of DFT.

Therefore we interpolate the data using a time interval of 0.01 sec between each data point, as shown below:

```
t_interp = 0:0.01:0.9

radial_interp = interp1(radial(:,1),radial(:,2), t_interp)';
radial_interp(end) = radial_interp(1);

aortic_interp = interp1(aortic(:,1),aortic(:,2), t_interp)';
```

Radial and aortic pressure waveforms do not start at the same time, as expected, since aortic pulse appears ahead of the radial pulse. There is a pulse transit time delay between

the aortic pressure to propagate and the radial artery. An assumption was made that the delay from aorta to radial artery is about 140 milliseconds. This pulse transit delay time is important as this allow the phase relations between aortic and radial pulse waveforms to be more accurately computed.

```
delay = 0.14/0.01; % delayed time = 140 ms/ 0.01 sec = 14
radial_delayed = circshift(radial_interp,uint64(delay));
```

3.2 Introduction to Fast Fourier Transform (FFT)

A Fast Fourier Transform (FFT) must be performed on radial pressure data and the aortic pressure data to obtain amplitude and phase measures. A discrete Fourier transform algorithm called the Fast Fourier transform (FFT) decreases the number of computations needed for N points. FFT is used to convert signals in time domain to frequency domain. The response of an FFT resembles a sine function if the function being transformed is unrelated to sampling frequency. Fast Fourier transform algorithms could be of two categories such as decimation in time, and decimation in frequency. By breaking up a transform of length N into two transforms of length N/2 using the below identity we obtain the Cooley-Tukey FFT algorithm which creates an output transform that represents decimation in time (Backle, 1986).

$$\sum_{n=0}^{N-1} a_n\, e^{-2\pi i n k/N} = \sum_{n=0}^{N/2-1} a_{2n}\, e^{-2\pi i (2n) k/N}$$

$$+ \sum_{n=0}^{N/2-1} a_{2n+1}\, e^{-2\pi i (2n+1) k/N}$$

$$= \sum_{n=0}^{N/2-1} a_n^{\text{even}}\, e^{-2\pi i n k/(N/2)}$$

$$+ e^{-2\pi i k/N} \sum_{n=0}^{N/2-1} a_n^{\text{odd}}\, e^{-2\pi i n k/(N/2)},$$

(3.5)

Once the FFT amplitude and phase has been obtained, an estimation of transfer function that quantifies the radial arterial pressure data to aortic pressure approximation using the following equations:

Amplitude: $\frac{MRadial}{MAorta}$ (3.6)

Phase: $\theta(Radial) - \theta(Aorta)$ (3.7)

3.3 Creating FFT using MATLAB

1. Take the FFT by calling the fft() function and storing the output in variable fft_radial:

```
• fft_radial = fft(radial);
```

2. Create the vector of frequencies in Hertz using n and fs (n is the number of points in the waveform and fs is the sampling frequency at which the waveform was acquired):

```
• n = length(radial);
• fs = 100;
```

Create the x-axis frequencies using the following formula

```
• f = (0:n-1)*(fs/n);
```

3. Obtain the magnitude by taking the absolute value of fft_radial after dividing it by n:

```
• radial_fft = fft(radial_delayed);
• aortic_fft = fft(aortic_interp);
• gtf_a_r = radial_fft./aortic_fft;
• magnitude  = abs(gtf_a_r);
```

4. Obtain the phase by using phase():

```
• phase = phase(gtf_a_r);
```

The magnitude and phase plots of the FFT can be thought of as cosines at different magnitudes, frequencies, and phase shifts. The magnitude (M) and phase (Φ) from the FFT plots are put it into the formula: M ∗ cos (2Π ∗ *f* ∗ t + Φ), where *f* is the frequency (x-axis) of the point. Individual cosines are added up to see how

many it takes to approximate the pressure waveforms. It is later discussed in Results (Chapter 4) that just sum of 6 cosines are required to match the pressure waveforms.

5. Resolving the x axis of frequency in hertz

```
• m = length(t_interp); %91 points
• fs = 100; %sampling frequency f=1/dt =1/0.01
• f = (0:m-1)*(fs/m);
```

6. Data points at 0Hz and the first 10 harmonics (a net of 11 points of the magnitude and phase) are plotted:

- figure();
- subplot(2,1,1);
- plot(f, magnitude (1:11));
- xlabel('Frequency (Hz)'); ylabel('Magnitude (mmHg)');
- subplot(2,1,2);
- plot(f, phase (1:11));
- xlabel('Frequency (Hz)'); ylabel('Phase (rad)');

Only 0Hz and the first 10 harmonics are taken into account because most of the published generalized transfer functions are only reported up to ~10Hz. This is because frequencies above 10Hz do not contain significant information and are hard to separate from noise.

Chapter 4: Results

Simultaneously recorded aortic and radial artery pressure waveforms that were digitize, as well as the corresponding computed transfer function magnitude and phase relations are shown below:

Radial Artery to Aortic Pressure Transfer Function

Normal Subjects:

Subject 1 – Graph 1 a

Used to produce generalized TF magnitude for (Radial to Aorta)

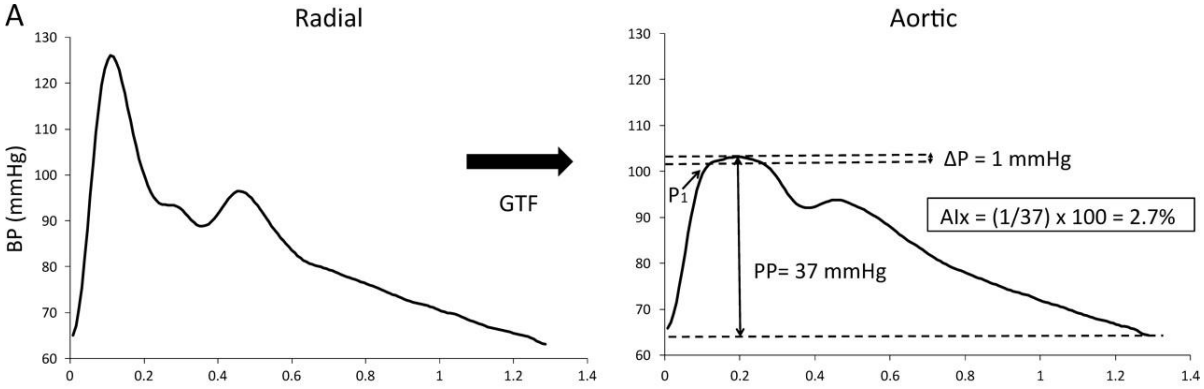

Figure 4.1: Radial artery pressure waveforms (left panels) and the corresponding generalized transfer function (GTF) transformed central aortic pressure waveforms (right panels) from a young man (age 24, brachial BP 126/65 mmHg). Reproduced with permission from Oxford University Press. (Williams, 2011**).**

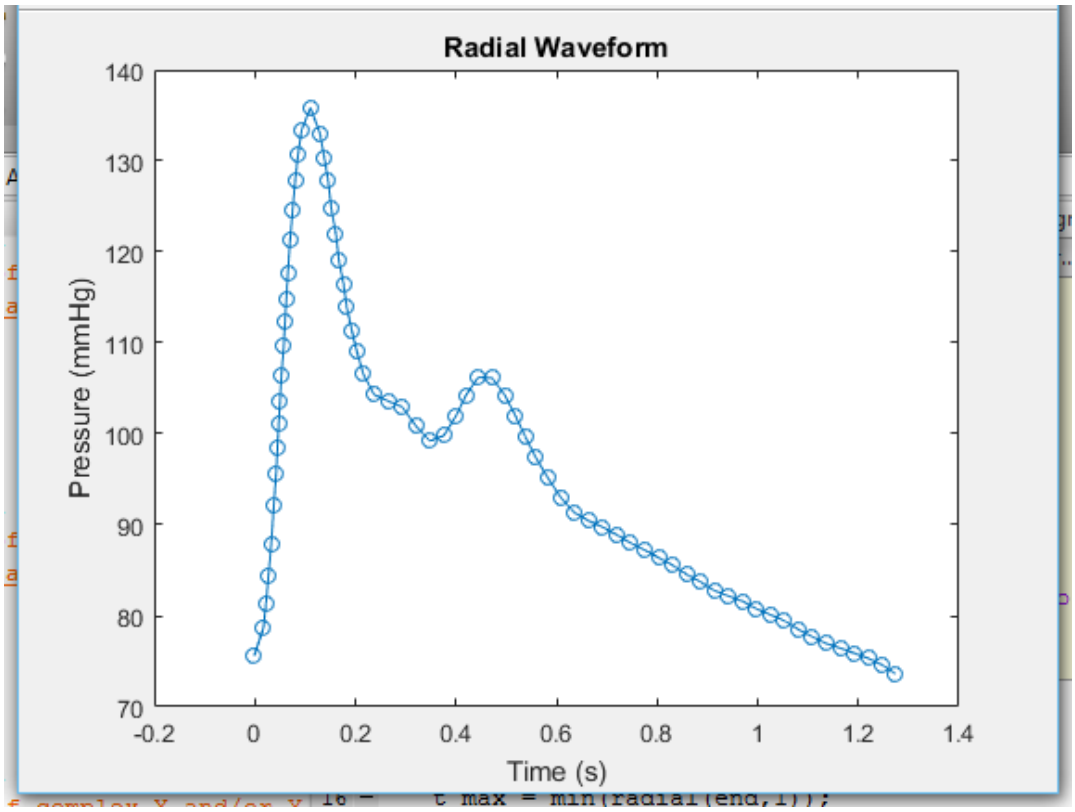

Figure 4.2: Digitized waveform of the normal individual whose original waveform can be seen in figure 4.1.

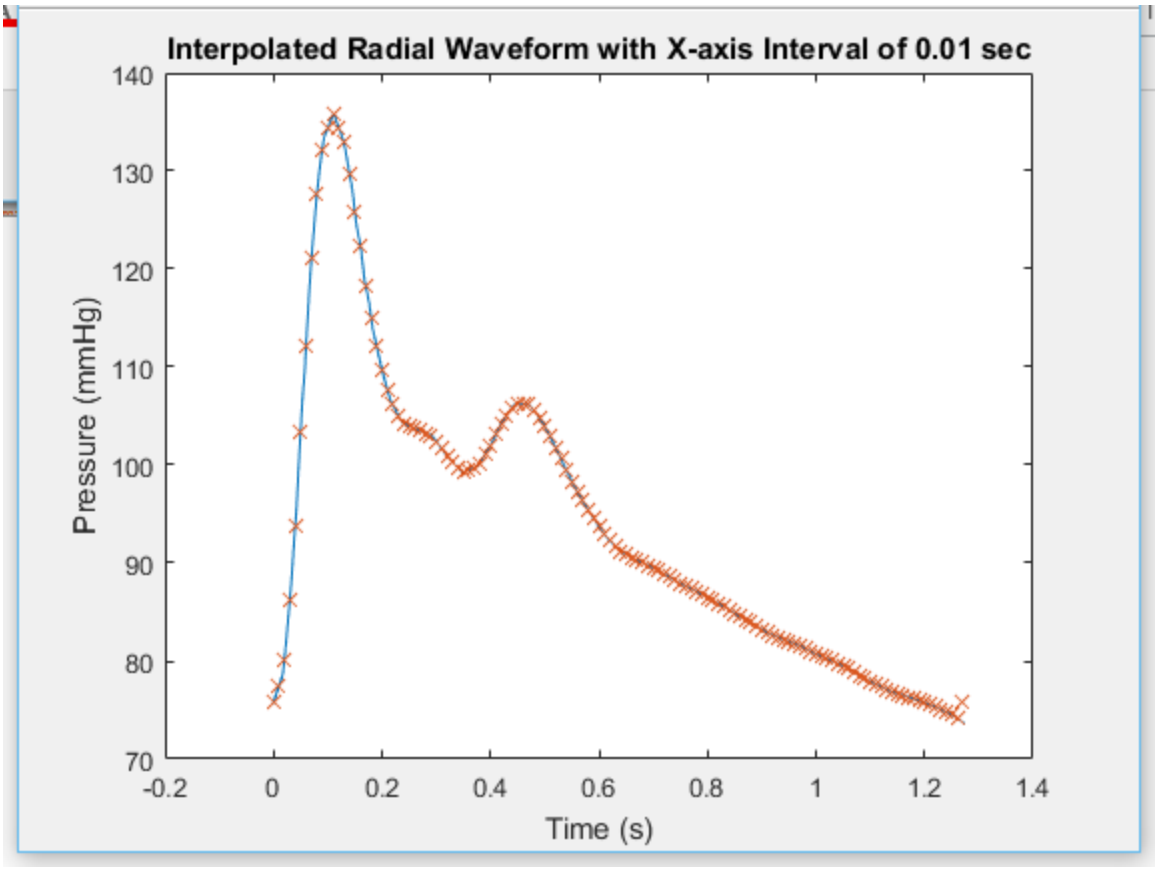

Figure 4.3: Digitized and interpolated waveform of the normal individual whose original waveform can be seen in figure 4.1.

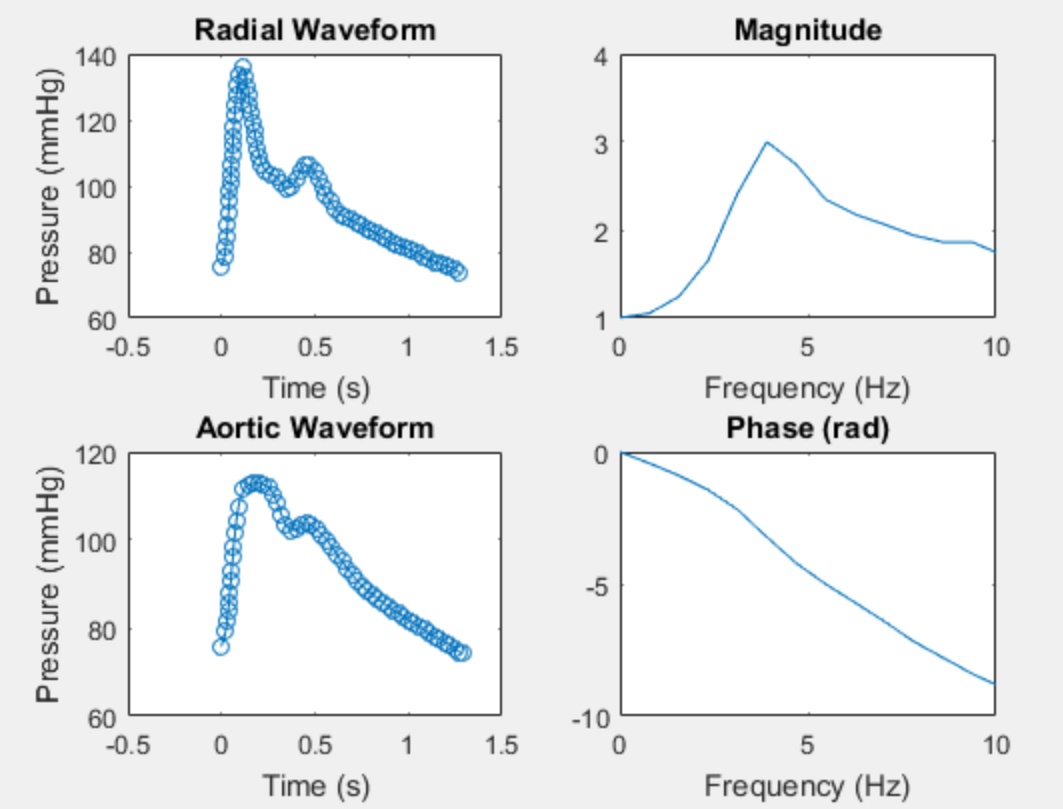

Figure 4.4 Transfer function magnitude and phase in frequency domain of the blood pressure waveform data of the normal individual discussed in figure 4.1. It is evident that the magnitude plateaus towards maximum and the phase declines almost linearly.

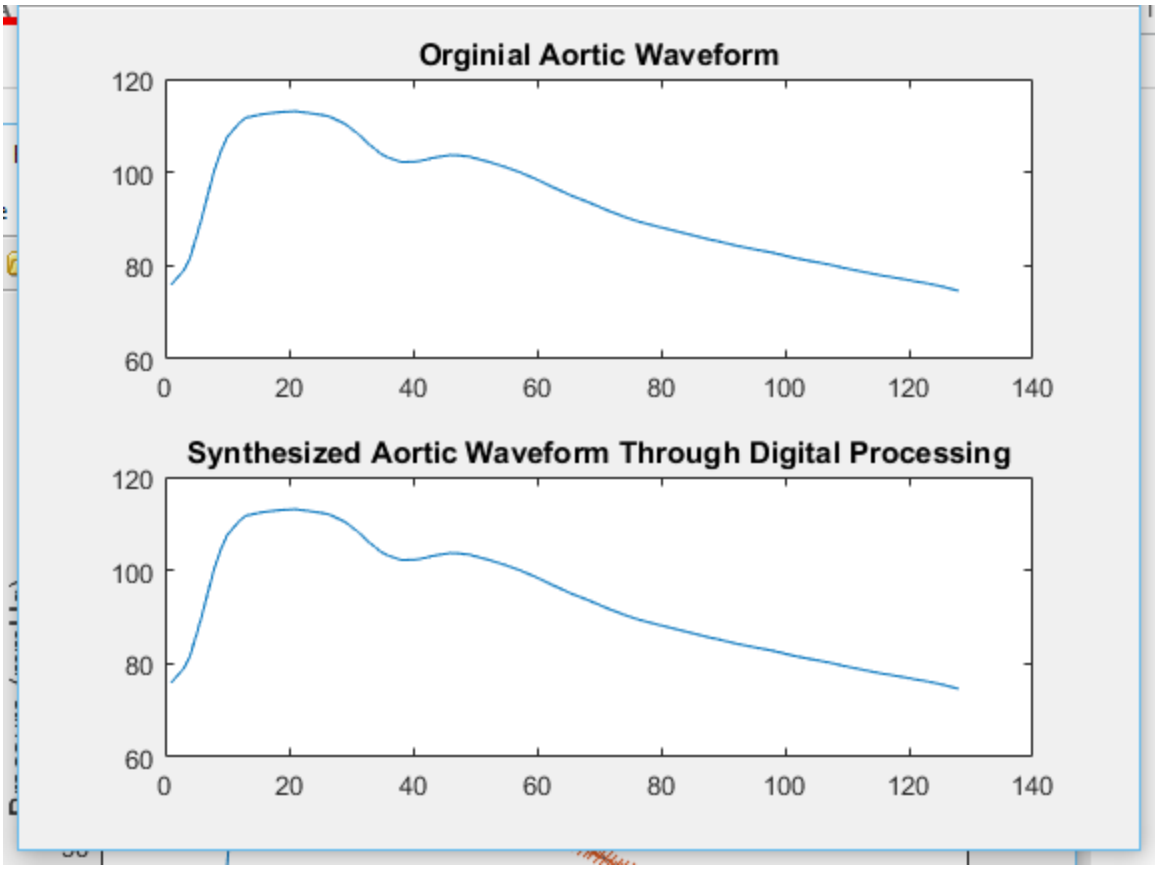

Reconstructed waveform correlation to original digitized waveform is 100%

Figure 4.5 The transfer function magnitude was used to reproduce the aortic waveform of this individual. The generalized magnitude used to compute the inverse fast fourier transform was the magnitude shown in figure 4.3. The synthesized aortic waveform shown above is the waveform produced by performing an ifft on the subject's radial blood pressure data.

Normal Subject 2: (Graph 4)

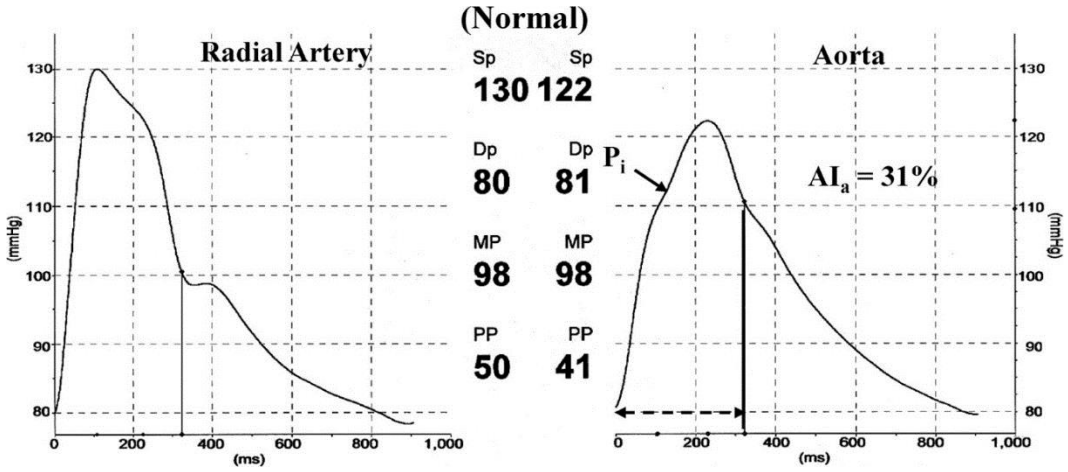

Figure 4.6 Noninvasively measured radial artery and synthesized aortic pressure waves in a patient of a normal subject (upper panel) with similar heart rate, height and age. Reproduced with permission from (Wolters Kluwer Health, Inc. Denardo, 2010)**.**

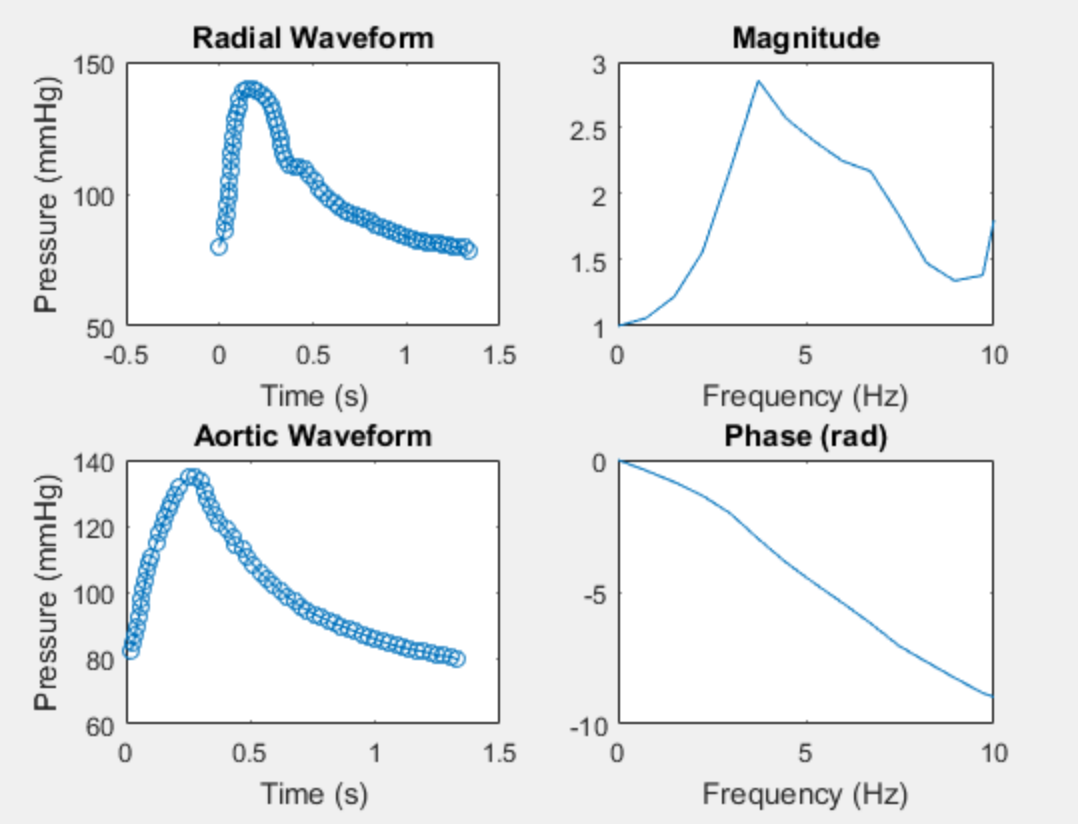

Figure 4.7 Transfer function magnitude and phase in frequency domain of the blood pressure waveform data of the normal individual discussed in figure 4.1. It is evident that the magnitude plateaus towards maximum and the phase declines almost linearly.

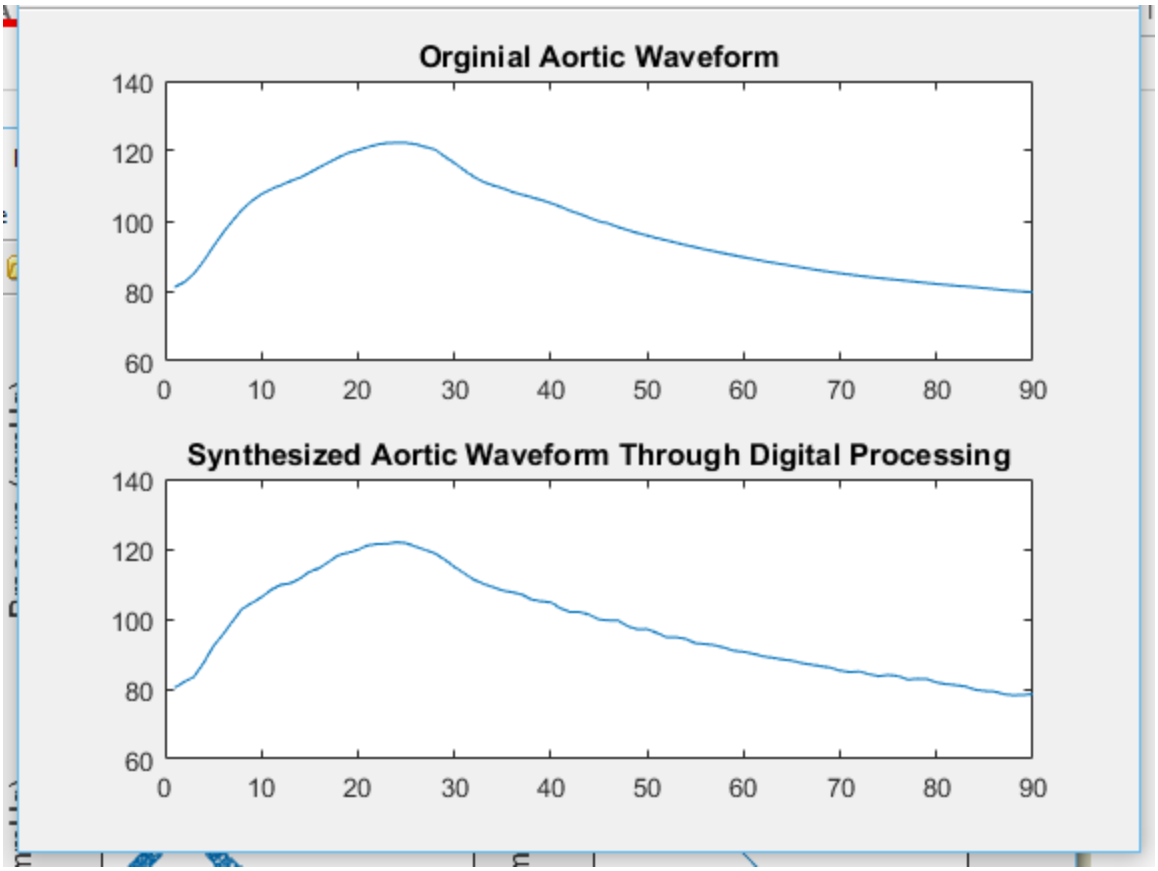

Reconstructed waveform correlation to original digitized waveform is 99.8189 %

Figure 4.8 The transfer function magnitude was used to reproduce the aortic waveform of this individual. The generalized magnitude used to compute the inverse fast fourier transform was the magnitude shown in figure 4.3. The synthesized aortic waveform shown above is the waveform produced by performing an ifft on the subject's radial blood pressure data.

Normal Subject 3 (graph 8):

http://heart.bmj.com/content/99/suppl_2/A79.2

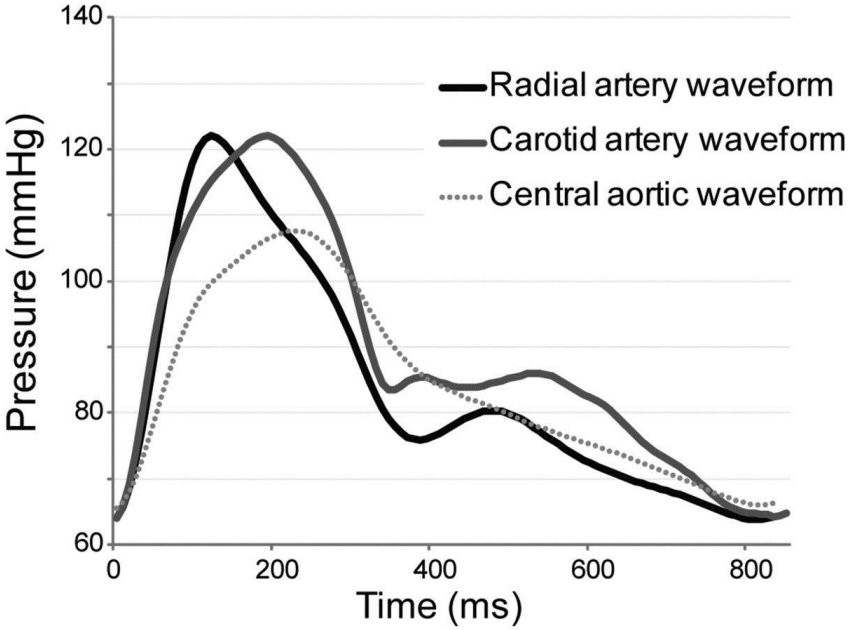

Figure 4.9 Radial, carotid and aortic pressure waveforms were available in 201 patients enrolled into the Alternative Risk Markers in Coronary Artery Disease (ARM-CAD) study with follow-up data at a mean of 1.2 years. Peripheral waveforms were obtained over 12 s using a Millar tonometer.

Reproduced with permission from (BMJ Publishing Group Ltd. Lewis, 2013)**.**

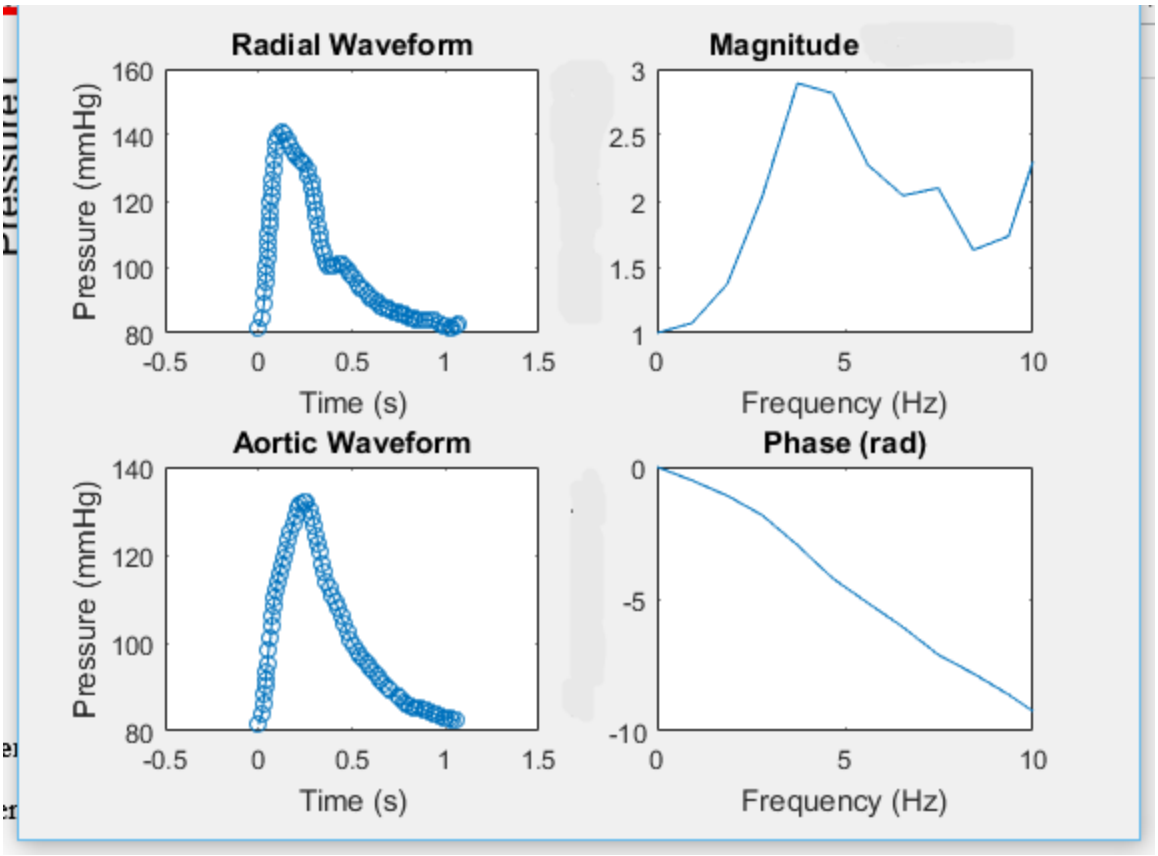

Figure 4.10 Transfer function magnitude and phase in frequency domain of the blood pressure waveform data of the normal individual discussed in figure 4.1. It is evident that the magnitude plateaus towards maximum and the phase declines almost linearly.

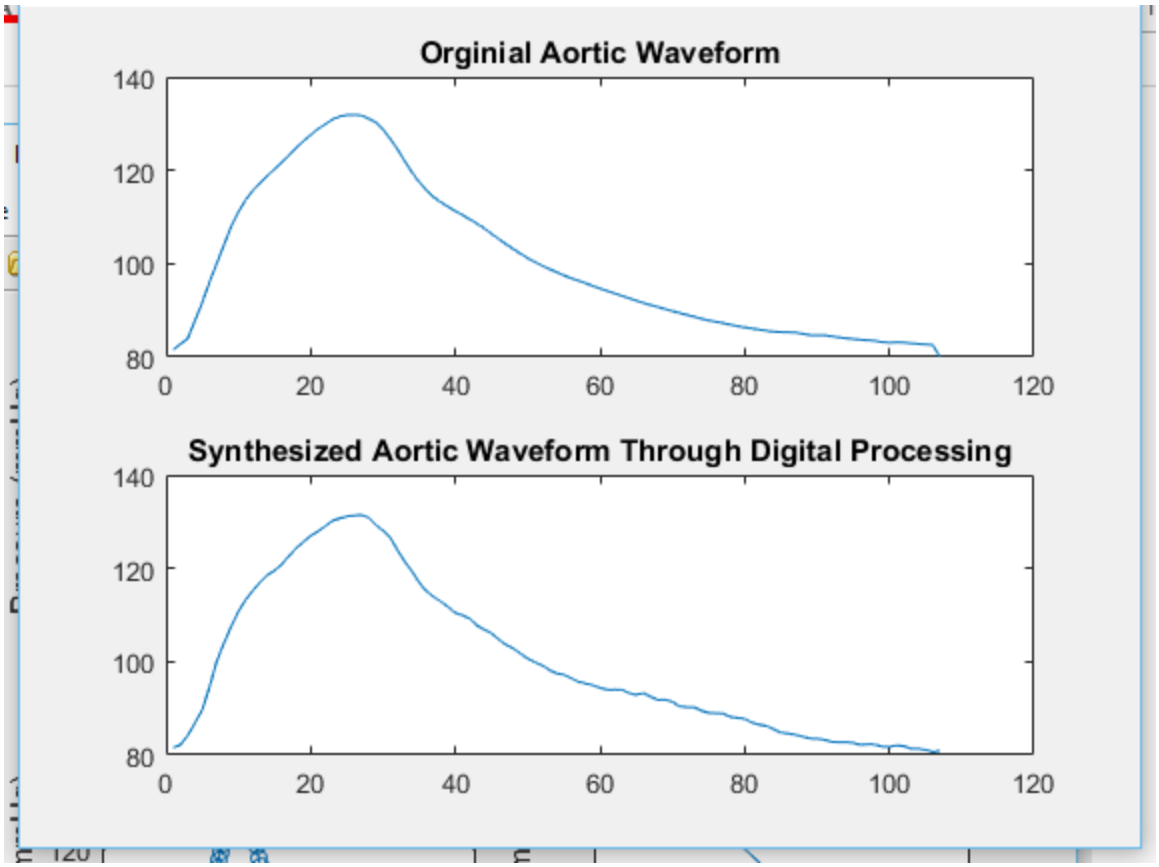

Reconstructed waveform correlation to original digitized waveform is 99.8523 %

Figure 4.11 The transfer function magnitude was used to reproduce the aortic waveform of this individual. The generalized magnitude used to compute the inverse fast fourier transform was the magnitude shown in figure 4.3. The synthesized aortic waveform shown above is the waveform produced by performing an ifft on the subject's radial blood pressure data.

Normal Subject 4 (Graph 10)

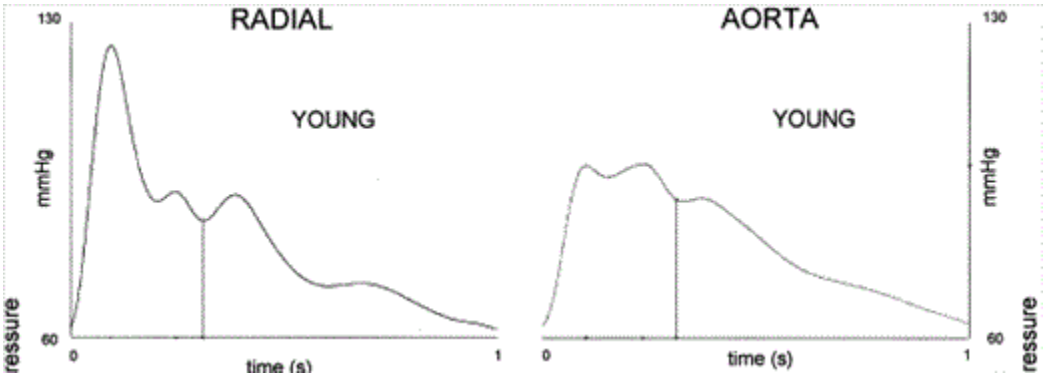

Figure 4.12 Arm and Aortic Pressure Waves in a young subject. Radial (left) and aortic (right) pressure waves in a 36-year-old man calibrated to the same brachial cuff values of systolic and diastolic pressure. Millar tonometer used for recording radial wave, SphygmoCor for analysis.

Reproduced with permission from (Journal of American College of Cardiology. O'Rourke, 2007)**.**

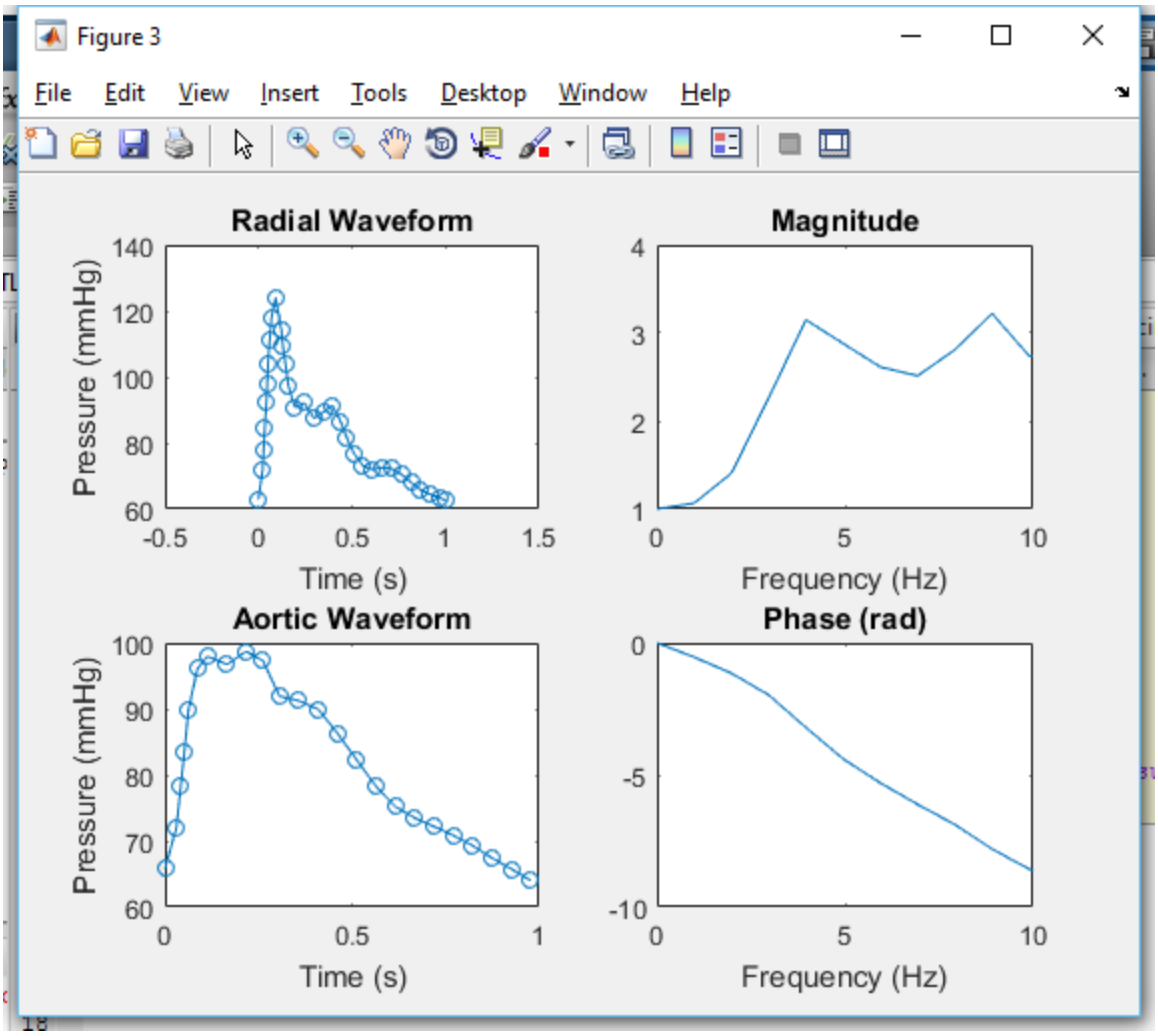

Figure 4.13 Transfer function magnitude and phase in frequency domain of the blood pressure waveform data of the normal individual discussed in figure 4.1. It is evident that the magnitude plateaus towards maximum and the phase declines almost linearly.

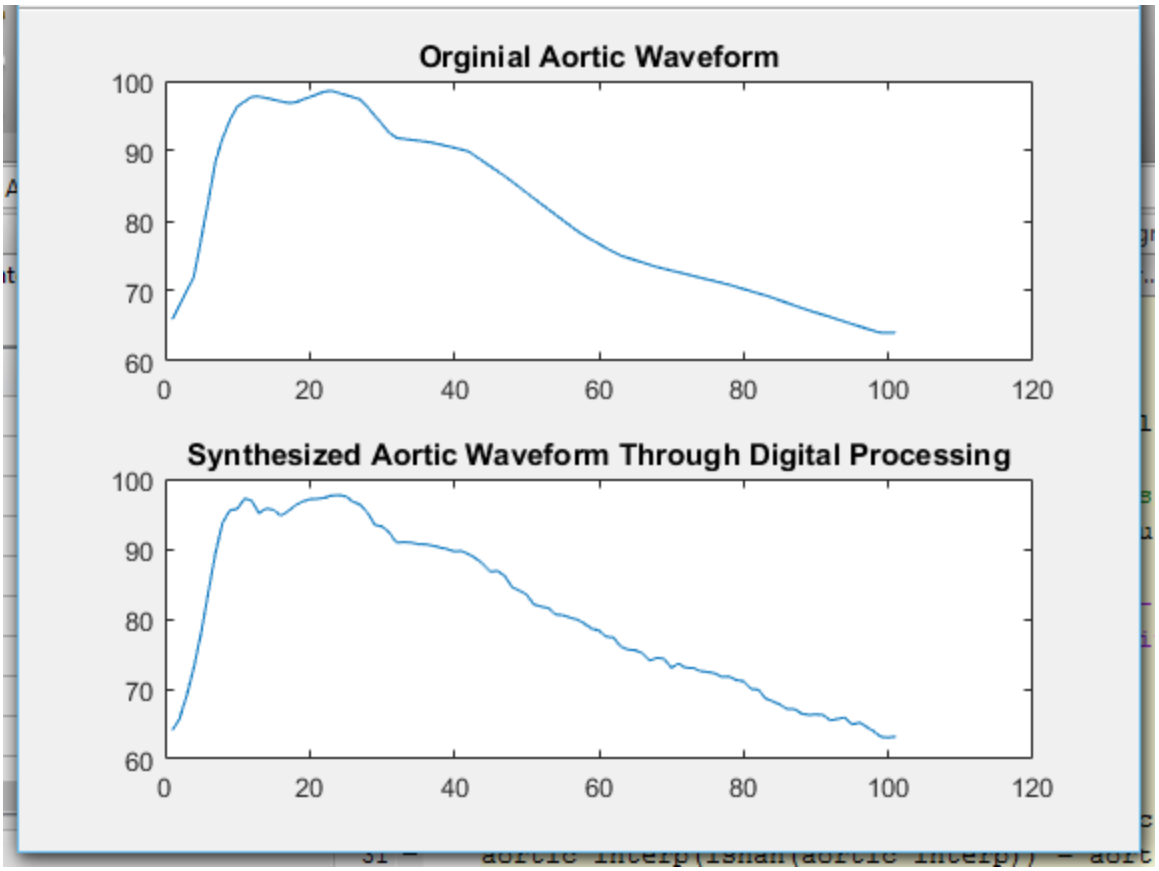

Reconstructed waveform correlation to original digitized waveform is 99.6824 %

Figure 4.14 Transfer function magnitude was used to reproduce the aortic waveform of this individual. The generalized magnitude used to compute the inverse fast fourier transform was the magnitude shown in figure 4.3. The synthesized aortic waveform shown above is the waveform produced by performing an ifft on the subject's radial blood pressure data.

Severe Heart Failure

Severe Heart Failure Patient 1 (Graph 5)

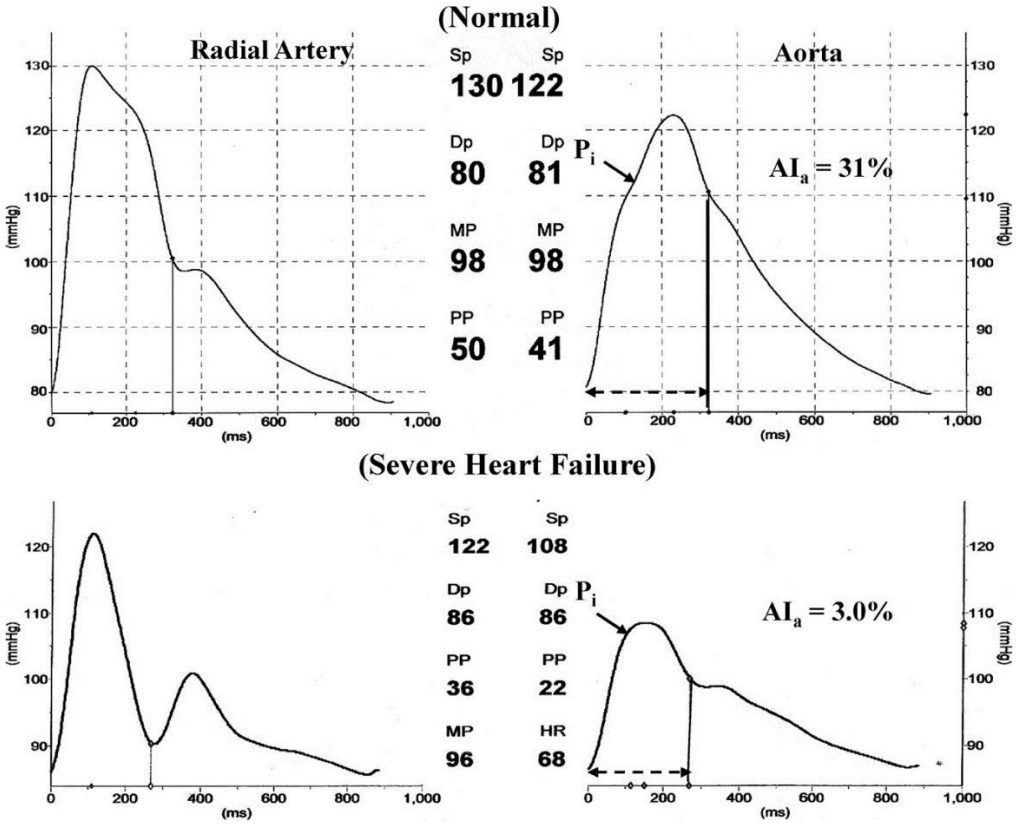

Figure 4.15 Noninvasively measured radial artery and synthesized aortic pressure waves in a patient with heart failure and severe LVSD (lower panel) compared to a normal subject (upper panel) with similar heart rate, height and age. Mean arterial pressure was similar between the two (96 versus 98 mm Hg) while both peripheral (36 versus 50 mm Hg) and central (22 versus 41 mm Hg) pulse pressures were less in the heart failure patient. P_i is the inflection point and denotes the beginning upstroke of the reflected wave. The radial artery pressure wave of the heart failure patient displays a dicrotic wave while the aortic pressure wave does not. Reproduced with permission from (Wolters Kluwer Health, Inc. Denardo, 2010).

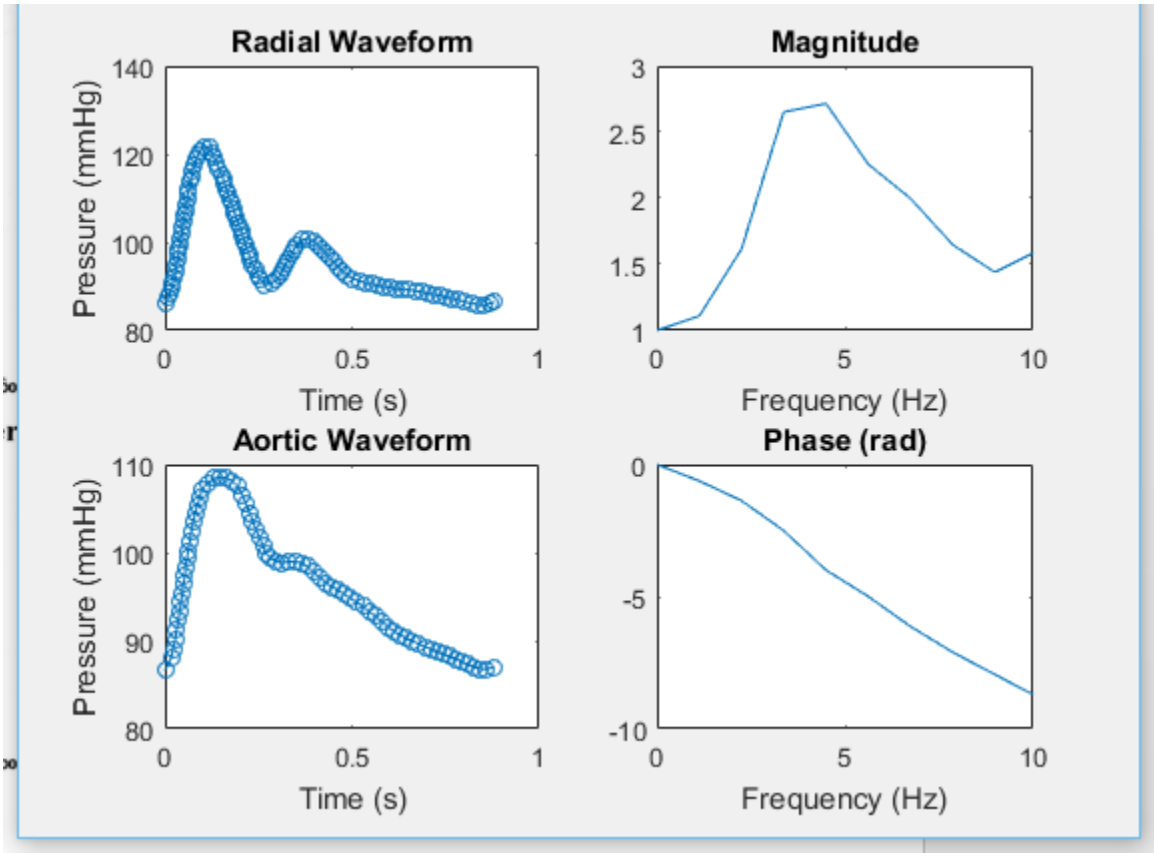

Figure 4.16 Transfer function magnitude and phase in frequency domain of the blood pressure waveform data of the individual with heart failure discussed in figure 4.11. It is evident that the magnitude increased towards maximum and declines sharply. The phase declines almost linearly similar to that of the normal patient.

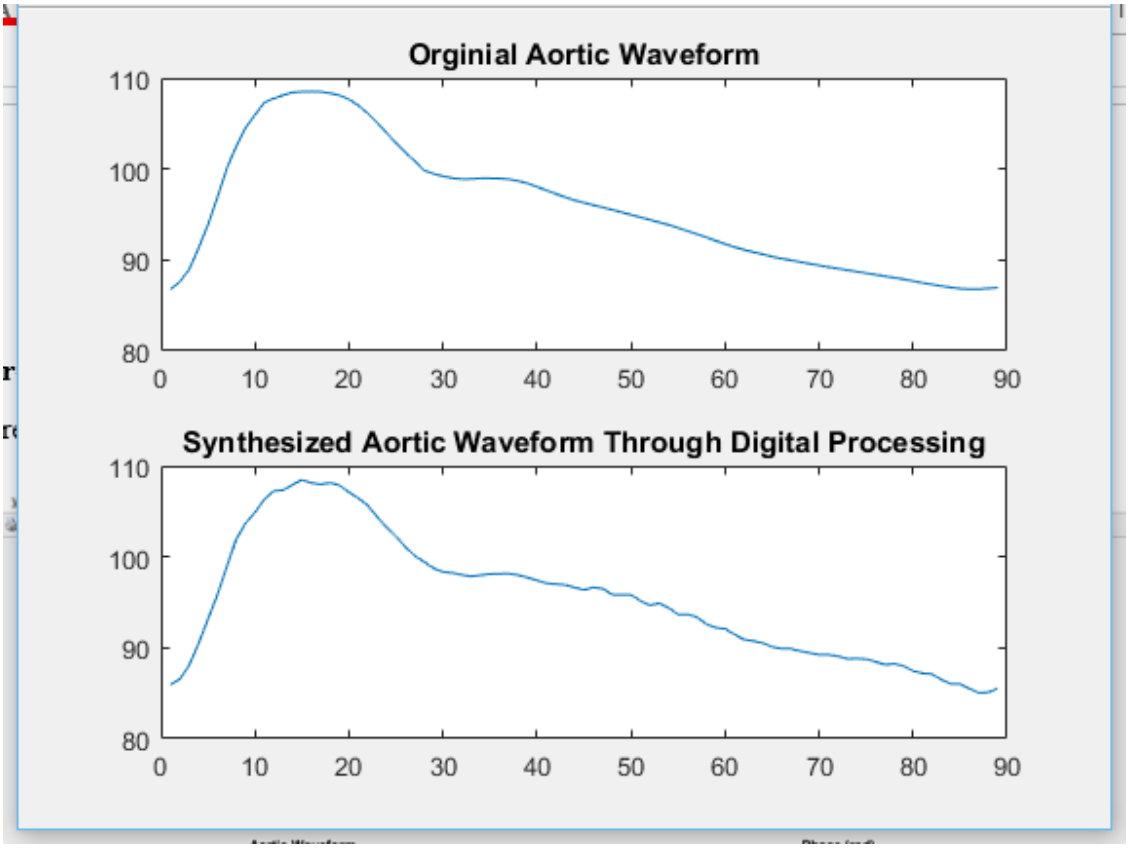

Reconstructed waveform correlation to original digitized waveform **is** 99.6744 %

Figure 4.17 The transfer function magnitude was used to reproduce the aortic waveform of this individual. The generalized magnitude used to compute the inverse fast fourier transform was the magnitude shown in figure 4.3. The synthesized aortic waveform shown above is the waveform produced by performing an ifft on the subject's radial blood pressure data.

Hypertensive Subjects:

Hypertensive Subject 1 (Graph 2):

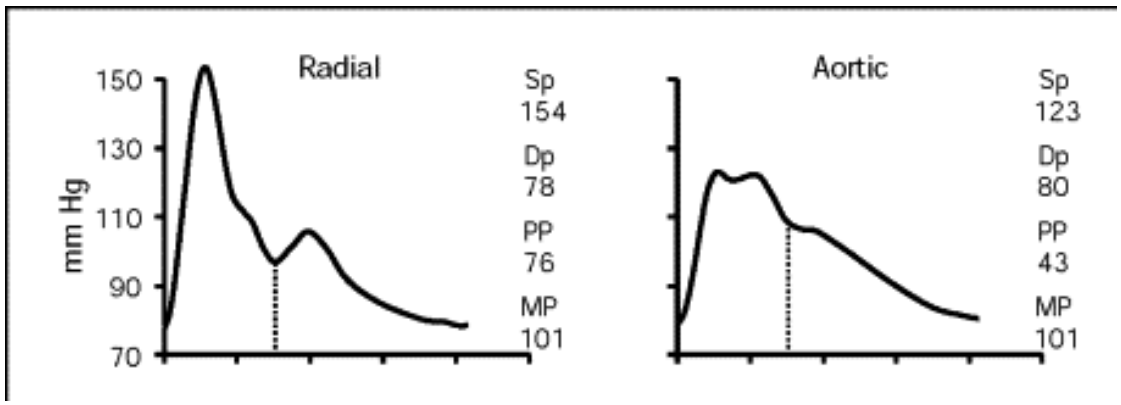

Figure 4.18 The data obtained from SphygmoCor is from a person with spurious systolic hypertension. Top, The radial artery waveform (left) and synthesized aortic wave (right). Dp = diastolic pressure; MP = mean pressure; PP = pulse pressure; Sp = systolic pressure. Reproduced with permission from (Elsevier. O'Rourke, 2006)**.**

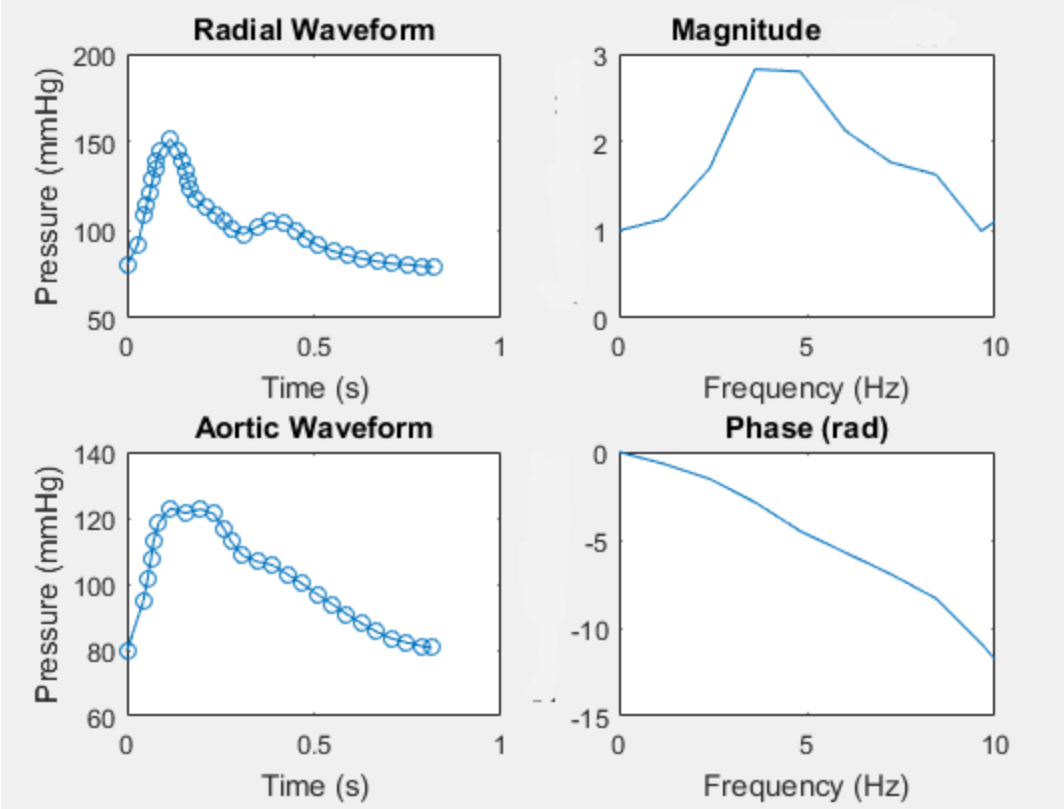

Figure 4.19 Transfer function magnitude and phase in frequency domain of the blood pressure waveform data of the individual with hypertension discussed in figure 4.15. It is evident that the magnitude increased towards maximum and declines sharply. The phase declines almost linearly similar to that of the normal patient.

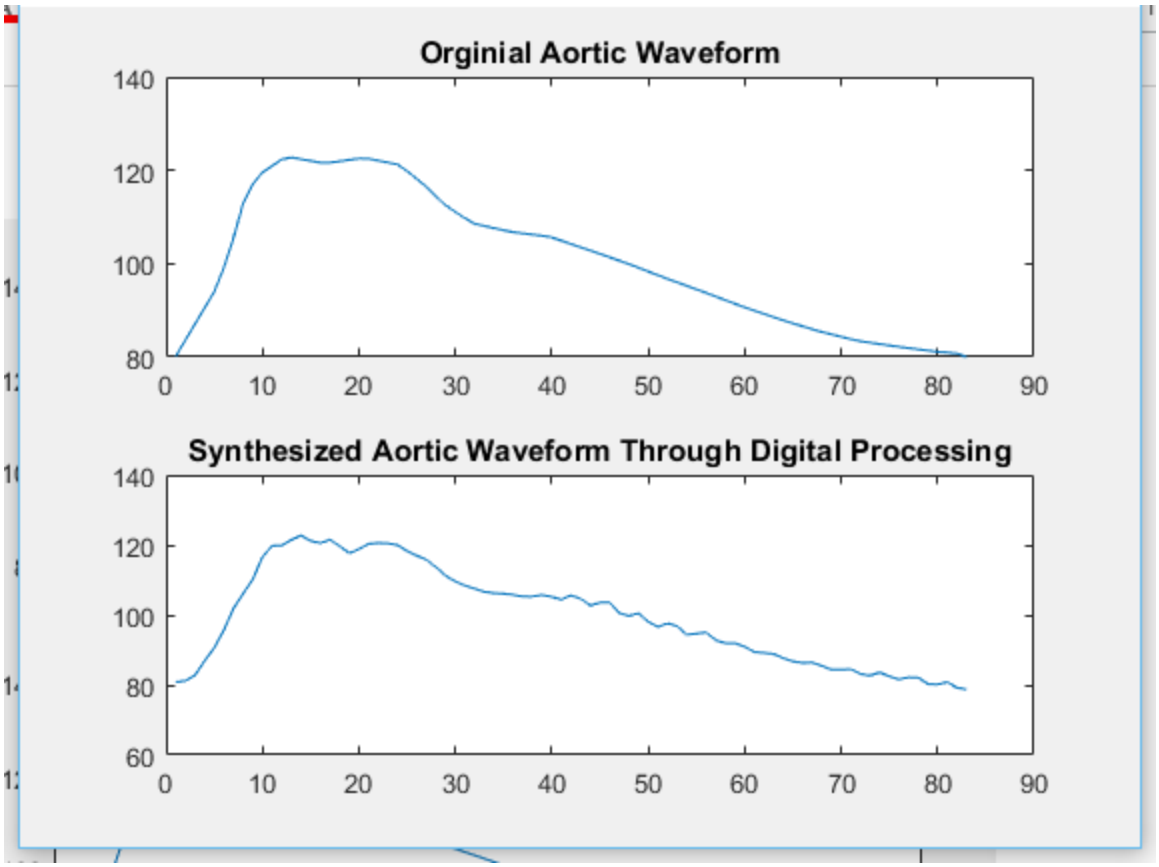

Reconstructed waveform correlation to original digitized waveform is 99.3980 %

Figure 4.20 Transfer function magnitude was used to reproduce the aortic waveform of this individual. The generalized magnitude used to compute the inverse fast fourier transform was the magnitude shown in figure 4.3. The synthesized aortic waveform shown above is the waveform produced by performing an ifft on the subject's radial blood pressure data.

Hypertensive Subject 2 (Graph 3):

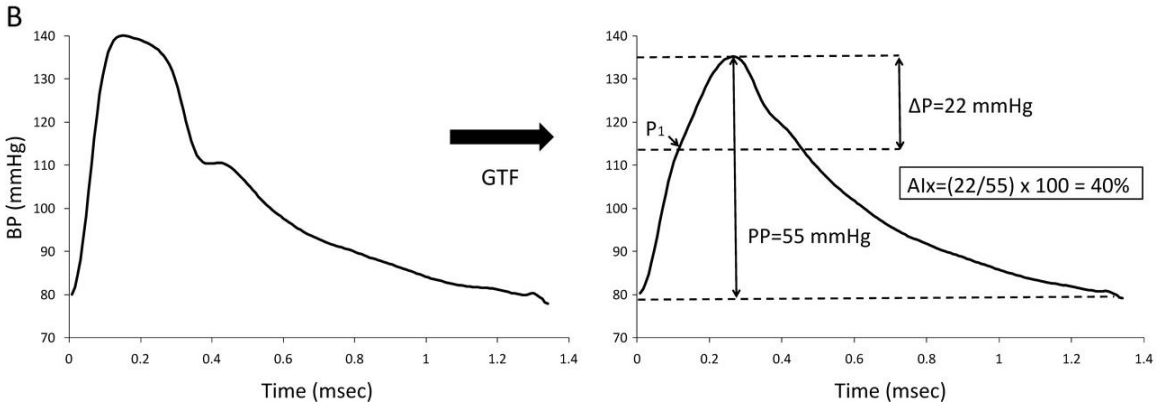

Figure 4.21 The above radial and aortic blood pressure waveforms were obtained from an older man (age 72, brachial BP 140/80 mmHg).

Reproduced with permission from (Wolters Kluwer Health, Inc. Chen, 1997)**.**

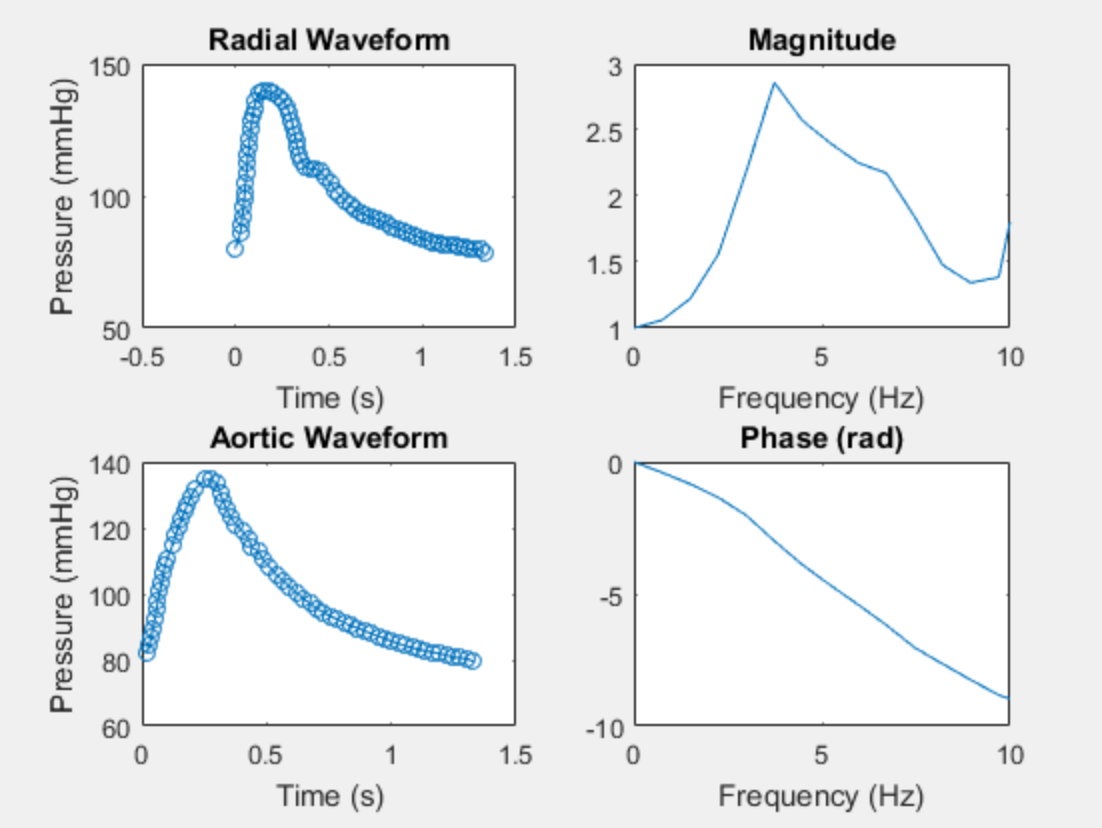

Figure 4.22 Transfer function magnitude and phase in frequency domain of the blood pressure waveform data of the individual with hypertension discussed in figure 4.18. It is evident that the magnitude increased towards maximum and declines sharply. The phase declines almost linearly similar to that of the normal patient.

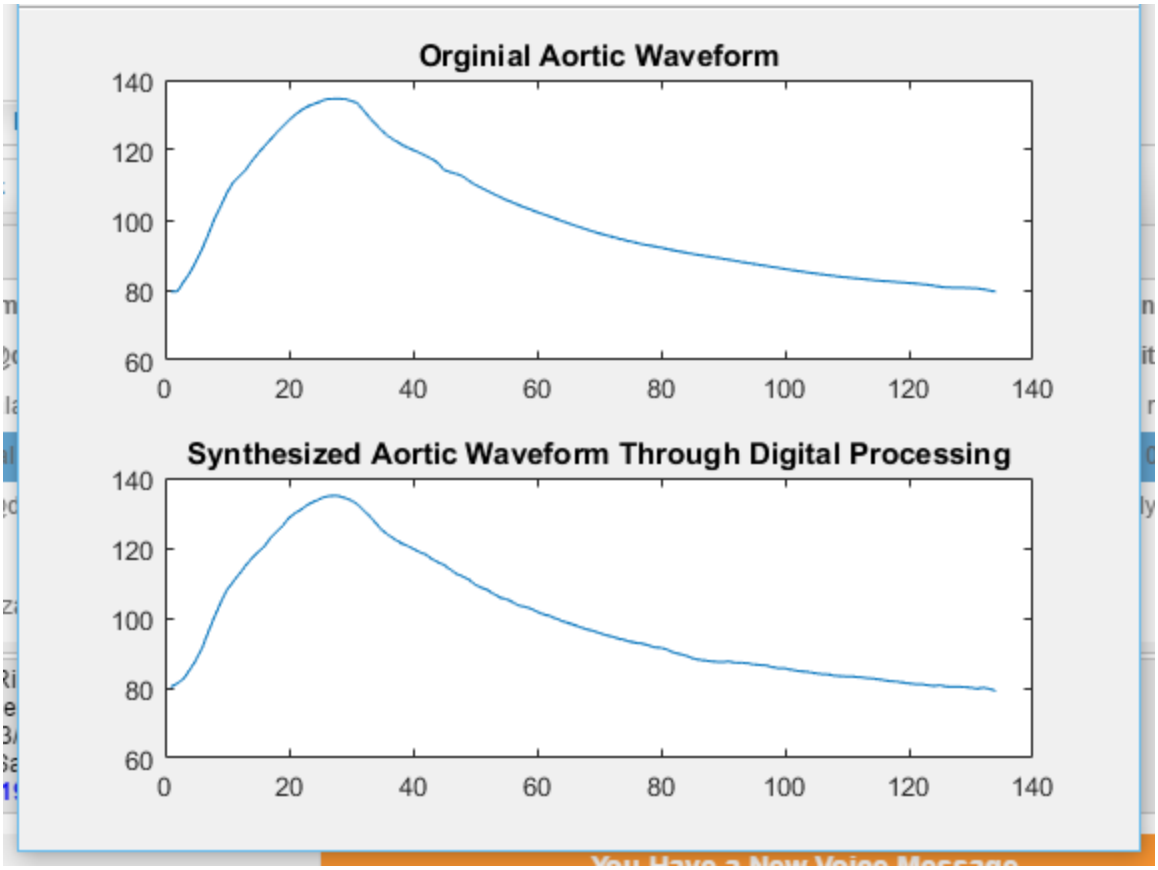

Reconstructed waveform correlation to original digitized waveform **is** 99.3917 %

Figure 4.23 The transfer function magnitude was used to reproduce the aortic waveform of this individual. The generalized magnitude used to compute the inverse fast fourier transform was the magnitude shown in figure 4.3. The synthesized aortic waveform shown above is the waveform produced by performing an ifft on the subject's radial blood pressure data.

Hypertensive Subject 3 (Graph 11):

ACE Inhibitor

Ramipril- Treats high blood pressure and heart failure after a heart attack. Reduces the risk of heart attack, stroke, and death. This medicine is an ACE inhibitor.

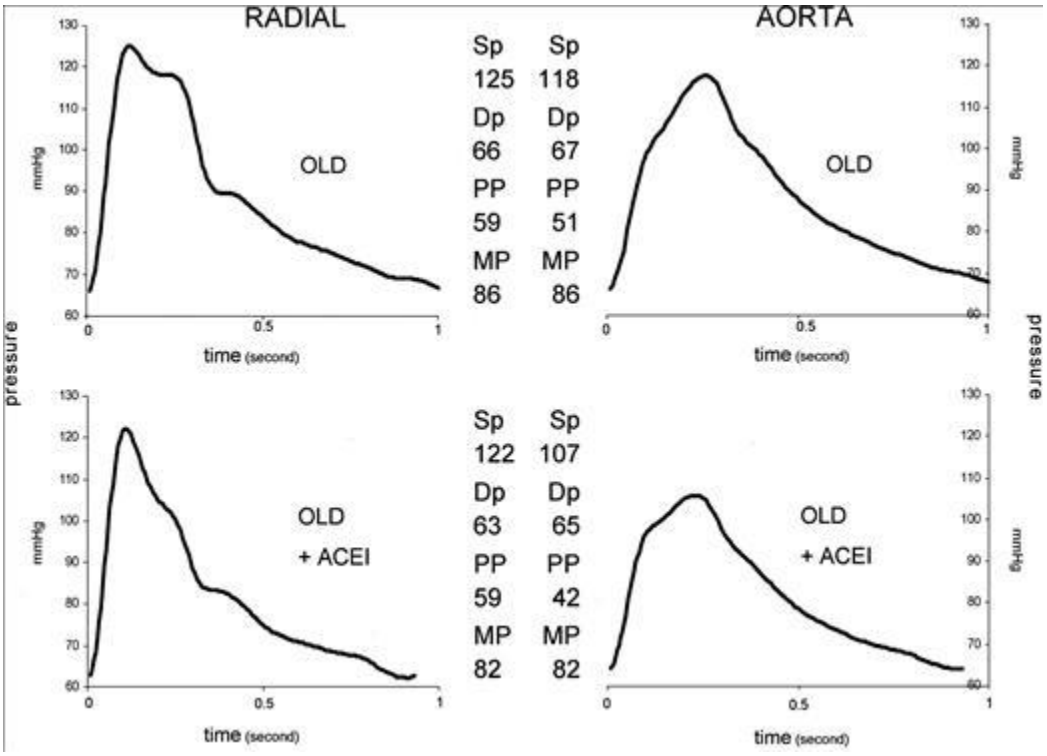

Figure 4.24 Arm and Aortic Pressure Waves in Old Subject Before and After Administration of Ramipril. Radial (left) and aortic (right) pressure waves in a 68-year-old man under control conditions (top) and 2 h after administration of ramipril 10 mg orally. Ramipril caused greater (8 mm Hg) reduction of aortic than brachial systolic pressure. ACEI = angiotensin-converting enzyme inhibitor; DP = diastolic pressure; MP = mean pressure; PP = pulse pressure; SP = systolic pressure.

Reproduced with permission from (Elsevier. O'Rourke, 2007)**.**

Before Ramipril

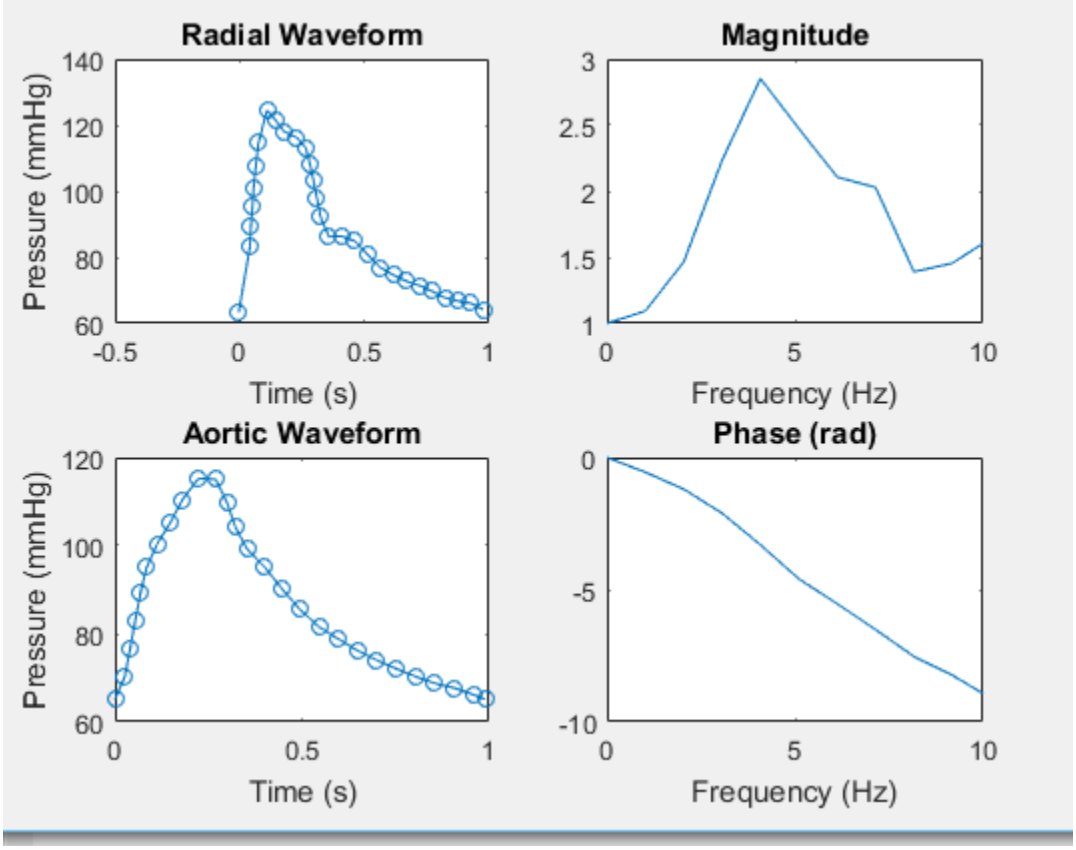

Figure 4.25 Transfer function magnitude and phase in frequency domain of the blood pressure waveform data of the individual with hypertension discussed in figure 4.21. It is evident that the magnitude increased towards maximum and declines sharply. The phase declines almost linearly similar to that of the normal patient.

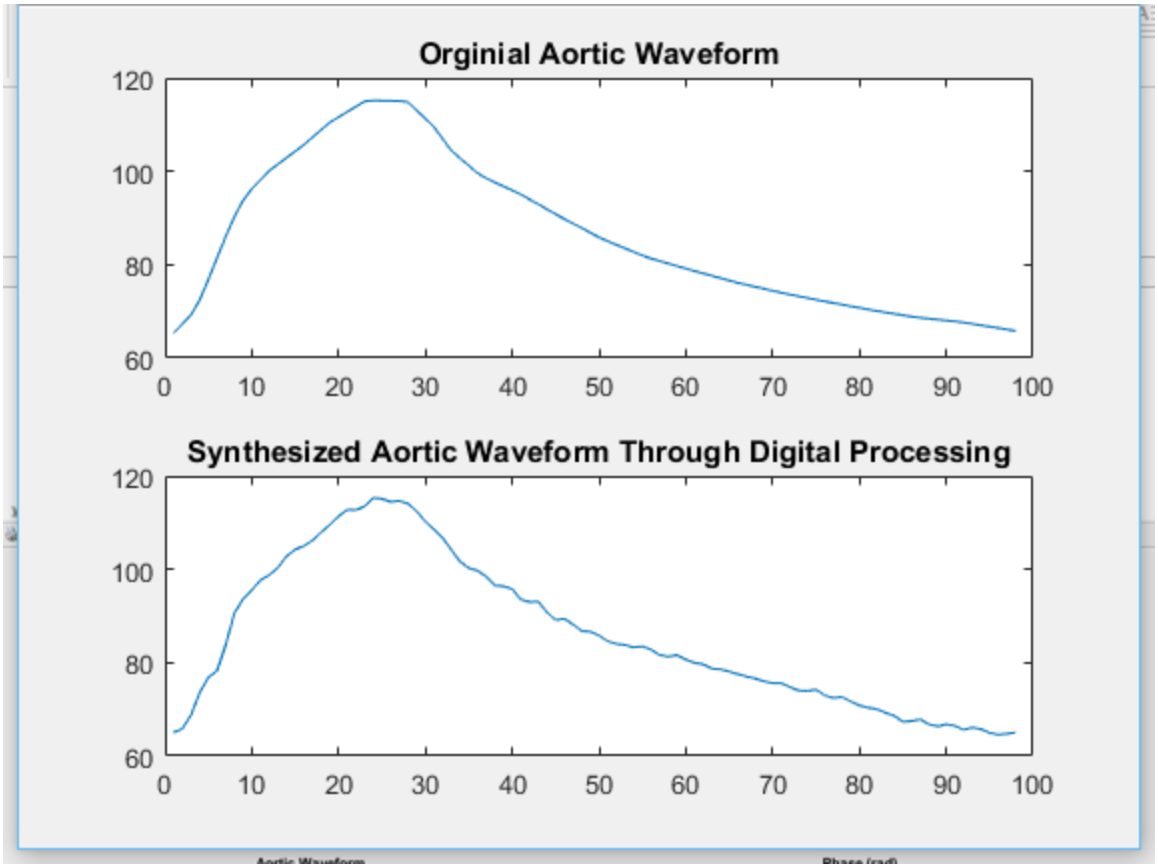

Reconstructed waveform correlation to original digitized waveform is 99.7102 %

Figure 4.26 The transfer function magnitude was used to reproduce the aortic waveform of this individual. The generalized magnitude used to compute the inverse fast fourier transform was the magnitude shown in figure 4.3. The synthesized aortic waveform shown above is the waveform produced by performing an ifft on the subject's radial blood pressure data.

After: ACE inhibitor Rampril- 2 hrs after administration of Rampril

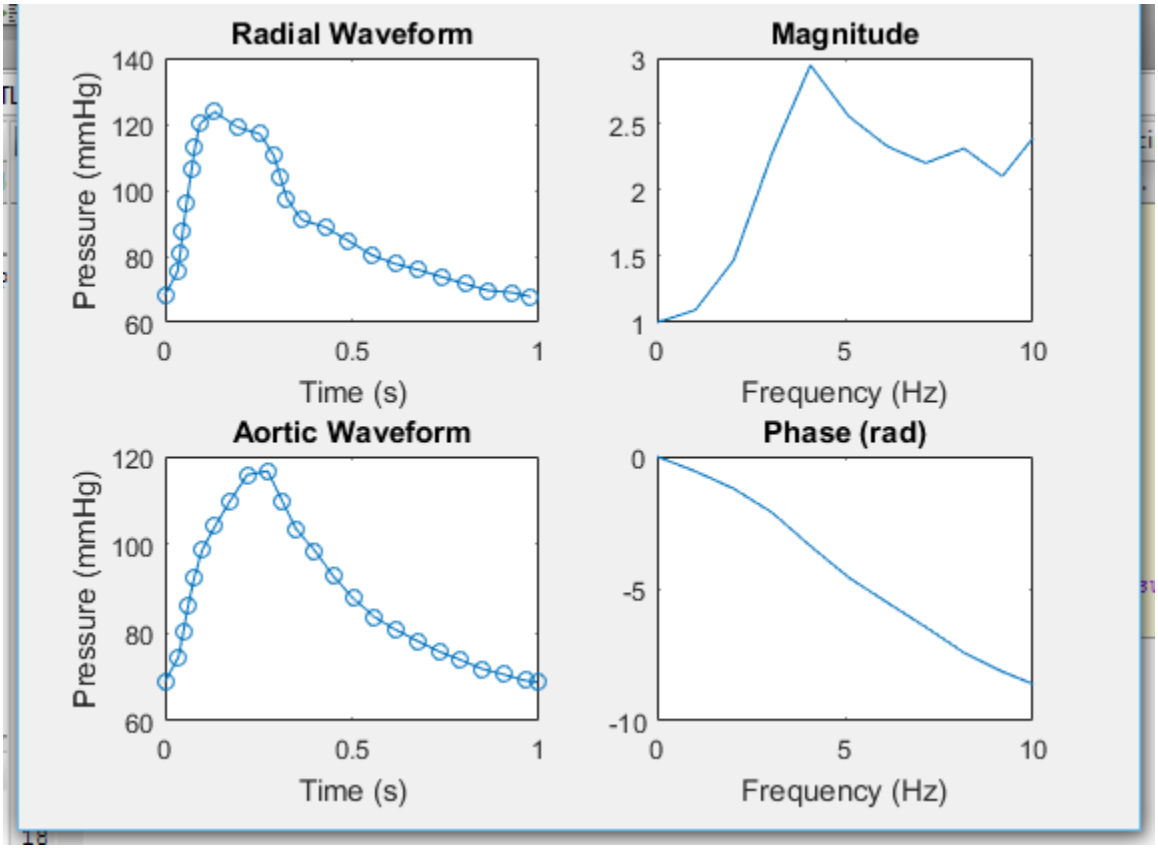

Figure4.27 shows the transfer function magnitude and phase in frequency domain of the blood pressure waveform data of the hypertensive individual discussed in figure 4.31. It is evident that the magnitude plateaus towards maximum just as it would for a normal patient due to the decrease in the blood pressure. The phase declines almost linearly.

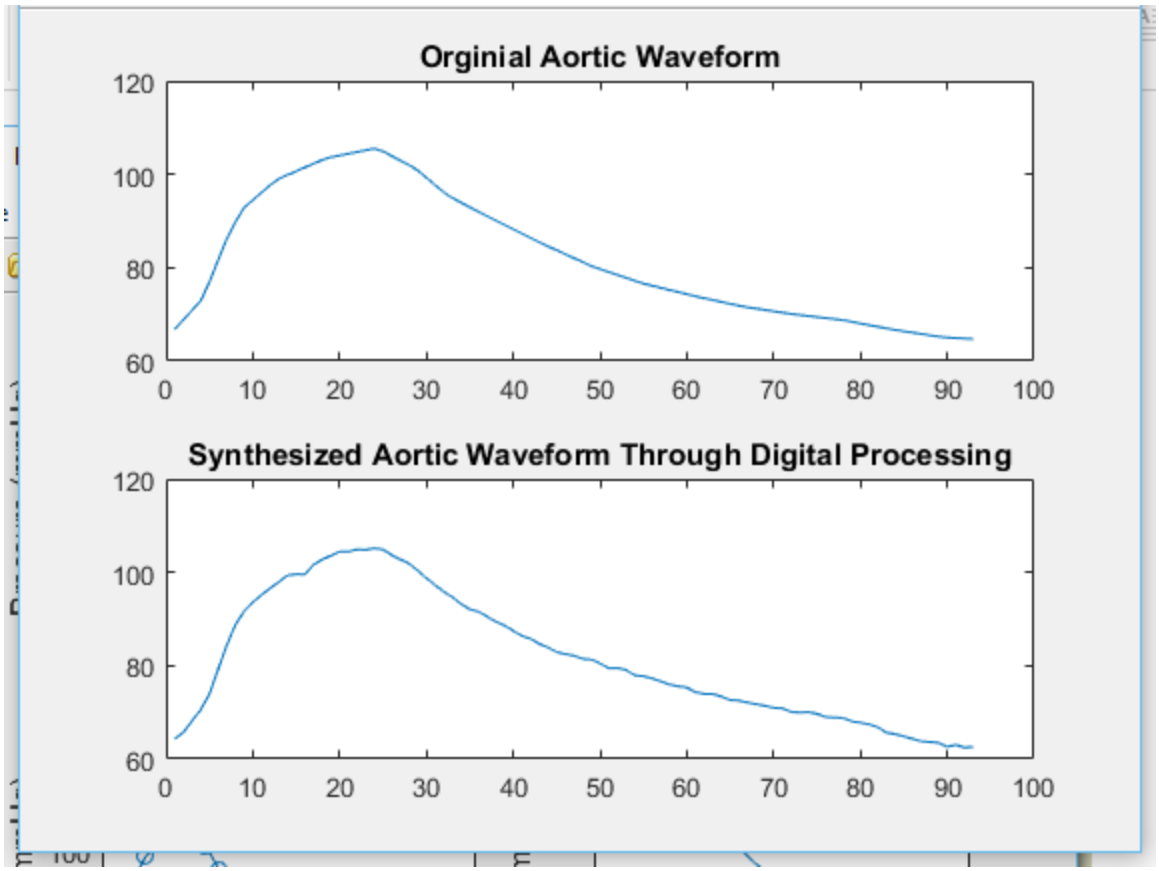

Reconstructed waveform correlation to original digitized waveform is 99.7934 %

Figure 4.28 The transfer function magnitude was used to reproduce the aortic waveform of this individual. The generalized magnitude used to compute the inverse fast fourier transform was the magnitude shown in figure 4.3. The synthesized aortic waveform shown above is the waveform produced by performing an ifft on the subject's radial blood pressure data.

Carotid Data

Subject 1

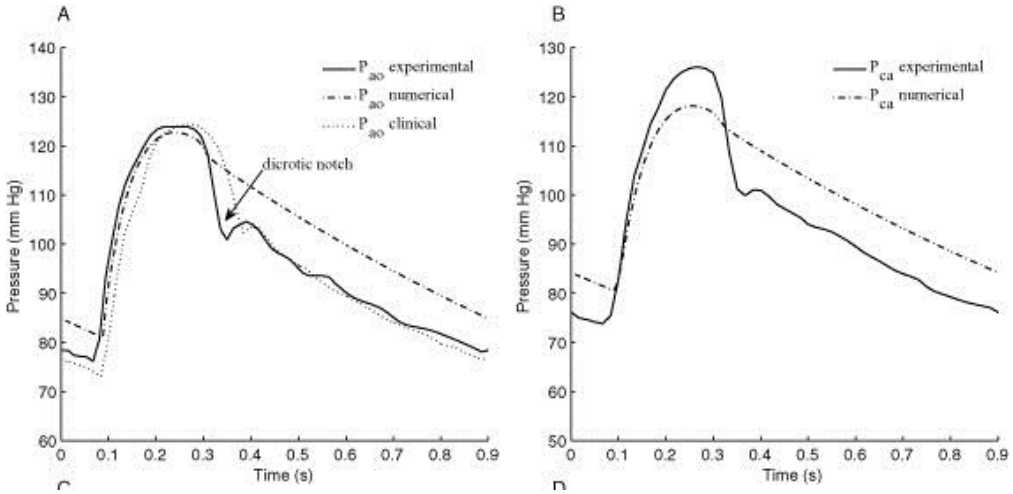

Figure 4.29 Comparison of pressure and flow time histories in aortic, carotid during control condition is shown. Aortic pressure 124/76 mm Hg, carotid pressure 126/74 mm Hg, cardiac output 5.1 L/min, and heart rate 66.67 bpm.

Reproduced with permission from (John Wiely and Sons. Ruiz, 2013)**.**

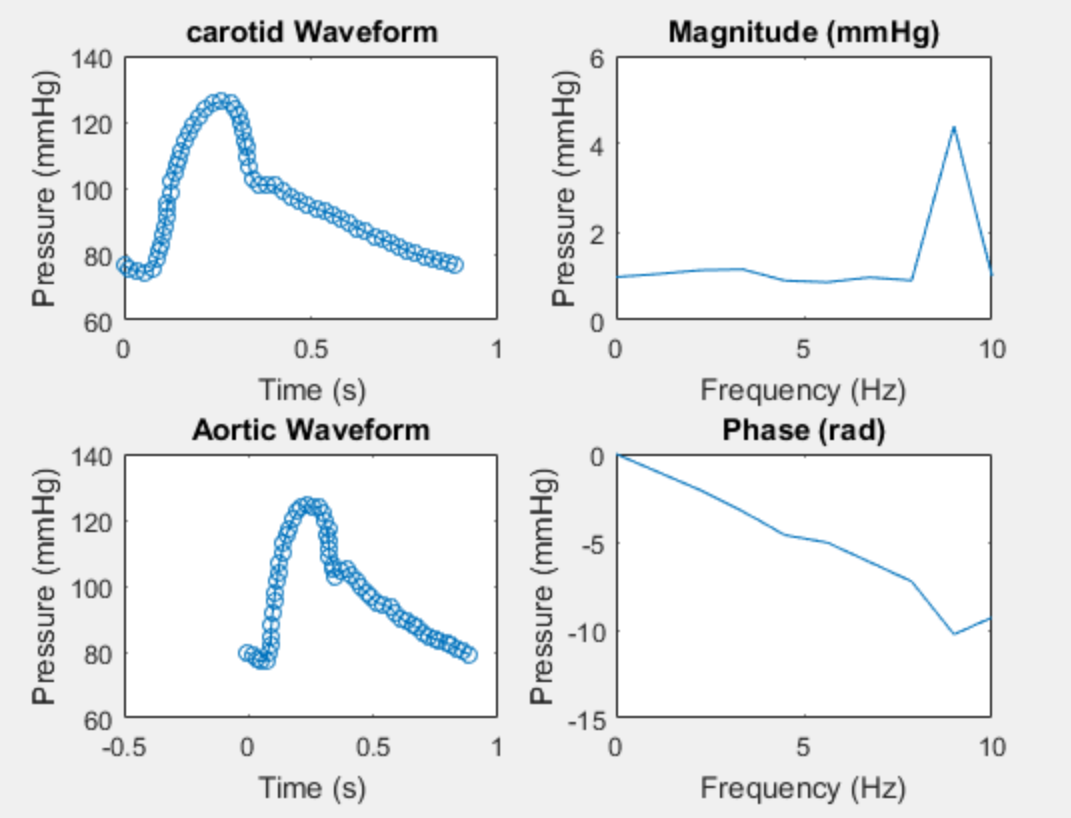

Figure 4.30 Transfer function magnitude and phase in frequency domain of the carotid blood pressure waveform data of the normal individual discussed in figure 4.26. It is evident that the magnitude has a sharp peak around 9Hz then declines and the phase declines almost linearly.

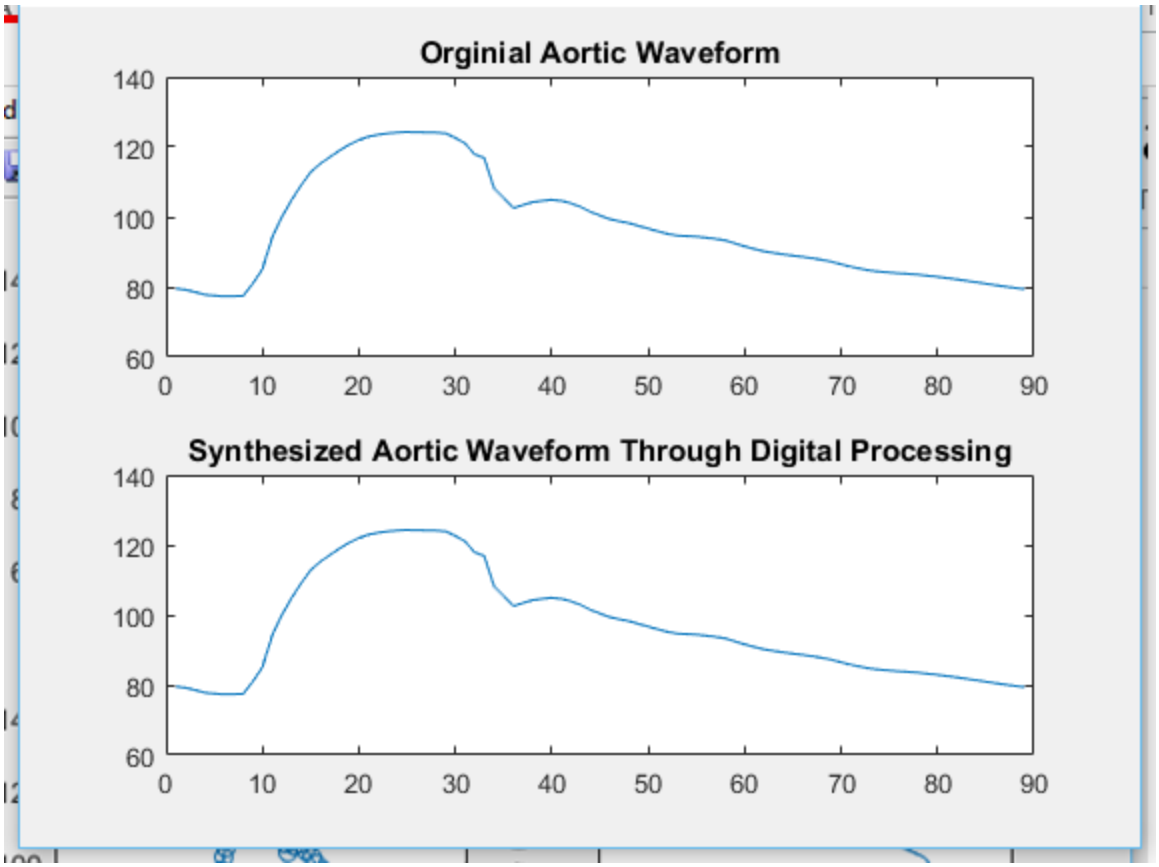

Reconstructed waveform correlation to original digitized waveform **is** 100.0000 %

Figure 4.31 Transfer function magnitude was used to reproduce the aortic waveform of this individual. The generalized magnitude used to compute the inverse fast fourier transform was the magnitude shown in figure 4.27. The synthesized aortic waveform shown above is the waveform produced by performing an ifft on the subject's carotid blood pressure data.

Subject 2

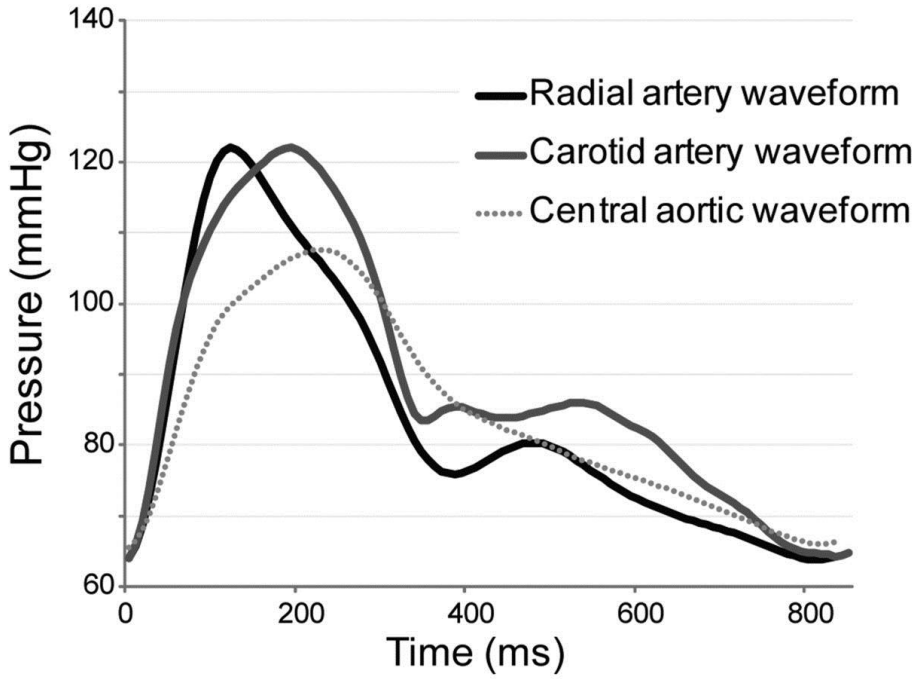

Figure 4.32 Radial, carotid and aortic pressure waveforms were available in 201 patients enrolled into the Alternative Risk Markers in Coronary Artery Disease (ARM-CAD) study with follow-up data at a mean of 1.2 years. Peripheral waveforms were obtained over 12 s using a Millar tonometer.

Reproduced with permission from (BMJ Publishing Group Ltd. Lewis, 2013)**.**

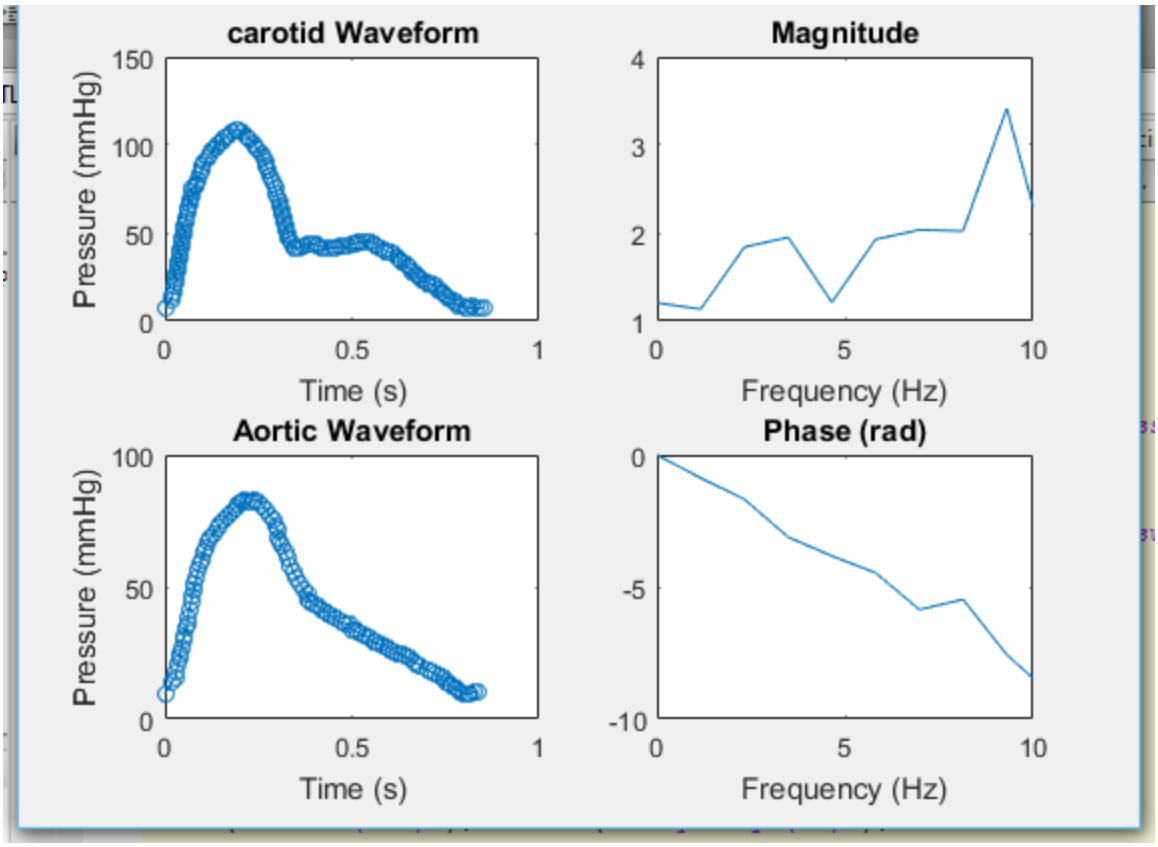

Figure 4.33 Transfer function magnitude and phase in frequency domain of the carotid blood pressure waveform data of the normal individual discussed in figure 4.29. It is evident that the magnitude has a sharp peak around 9Hz then declines and the phase declines almost linearly.

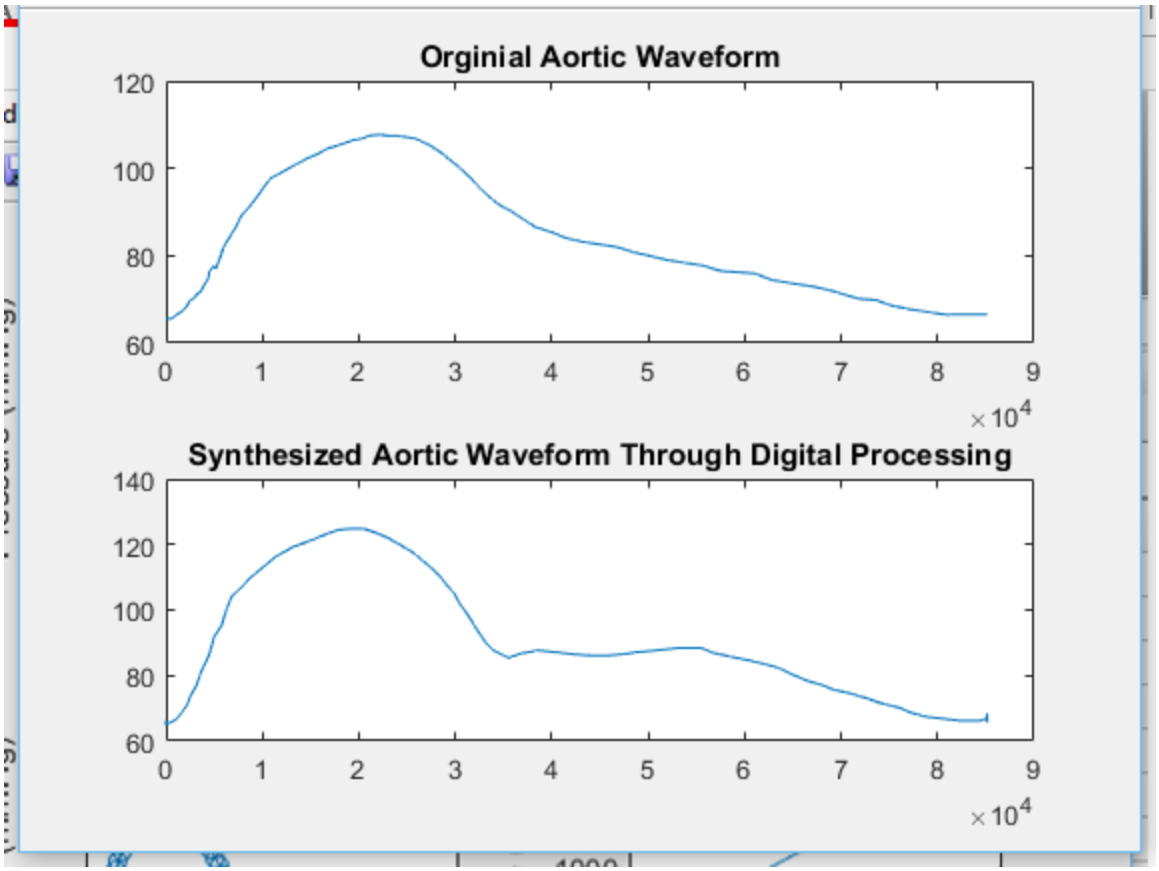

Reconstructed waveform correlation to original digitized waveform **is** 94.9223 %

Figure 4.34 The transfer function magnitude was used to reproduce the aortic waveform of this individual. The generalized magnitude used to compute the inverse fast fourier transform was the magnitude shown in figure 4.27. The synthesized aortic waveform shown above is the waveform produced by performing an ifft on the subject's carotid blood pressure data.

Subject 3

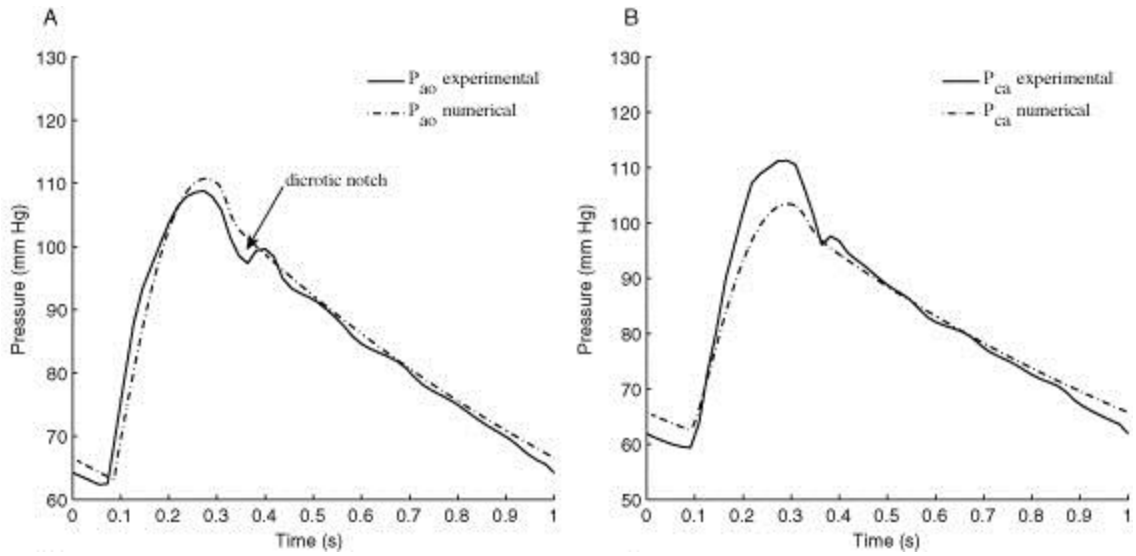

Figure 4.35 Comparison of pressure and flow time histories in aortic and carotid arteries during congestive heart failure condition is shown. Aortic pressure 110/62 mm Hg, carotid pressure 112/59 mm Hg, pulmonary pressure 34/24 mm Hg, cardiac output 2.6 L/min, and heart rate 60 bpm.

Reproduced with permission from (John Wiely and Sons. Ruiz, 2013)**.**

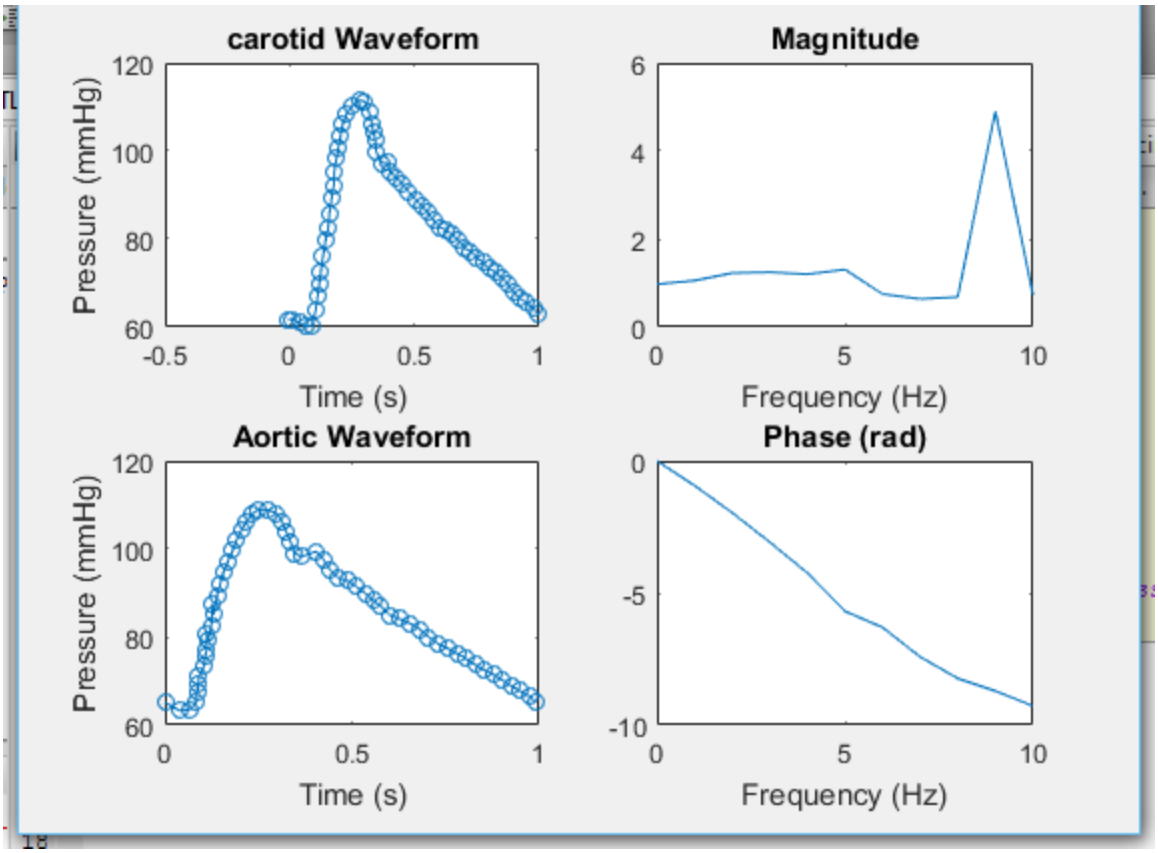

Figure 4.36 Above shows the transfer function magnitude and phase in frequency domain of the carotid blood pressure waveform data of the normal individual discussed in figure 4.32. It is evident that the magnitude has a sharp peak around 9Hz then declines and the phase declines almost linearly.

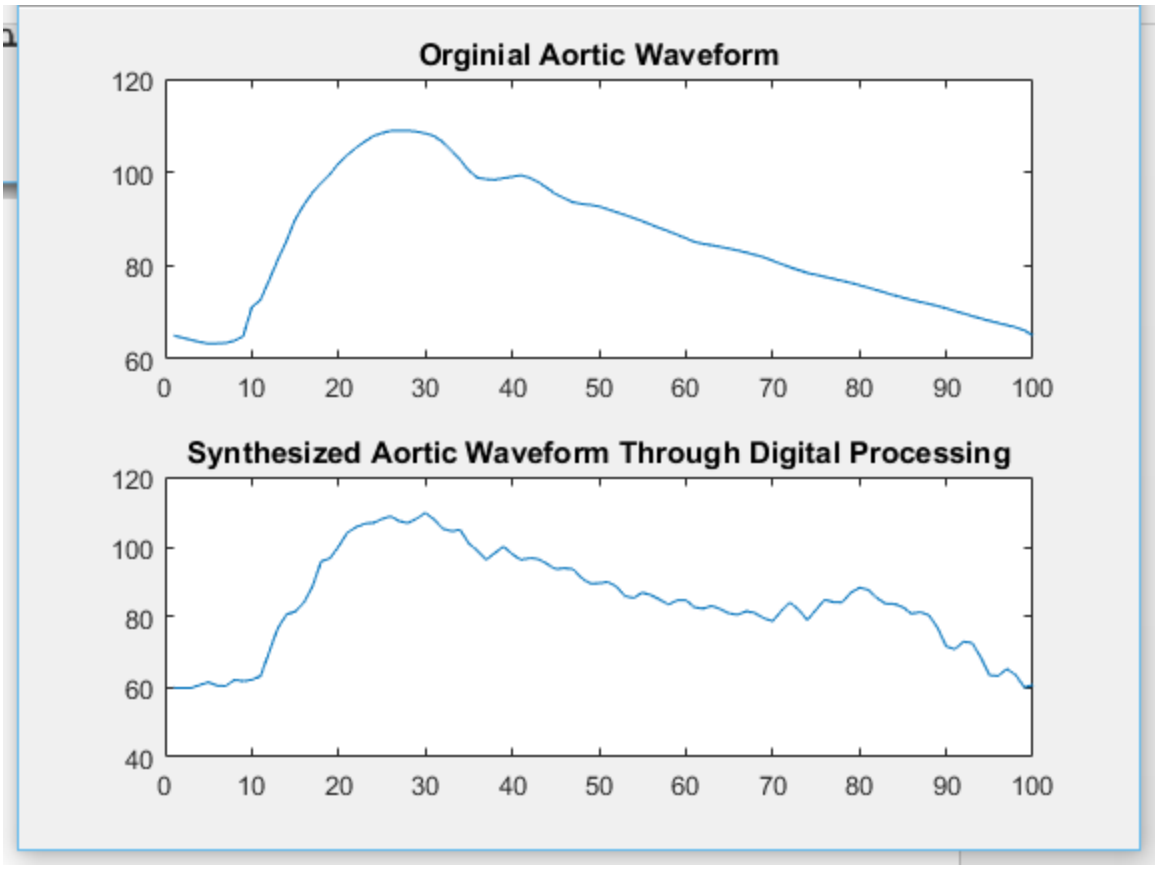

Reconstructed waveform correlation to original digitized waveform **is** 94.4225 %

Figure 4.37 The transfer function magnitude was used to reproduce the aortic waveform of this individual. The generalized magnitude used to compute the inverse fast fourier transform was the magnitude shown in figure 4.27. The synthesized aortic waveform shown above is the waveform produced by performing an ifft on the subject's carotid blood pressure data.

Femoral Data

Subject 1

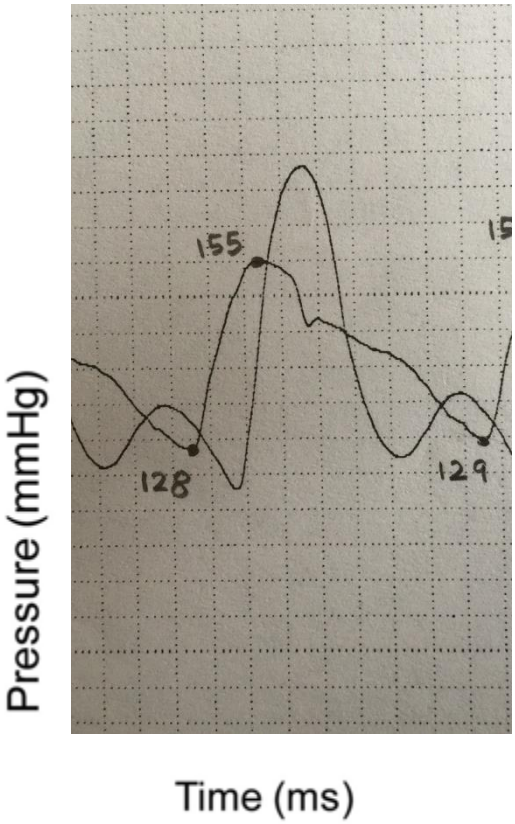

Figure 4.38 The above femoral arterial blood pressure data is obtained from a normal individual. (Courtesy of Professor John K-J. Li)

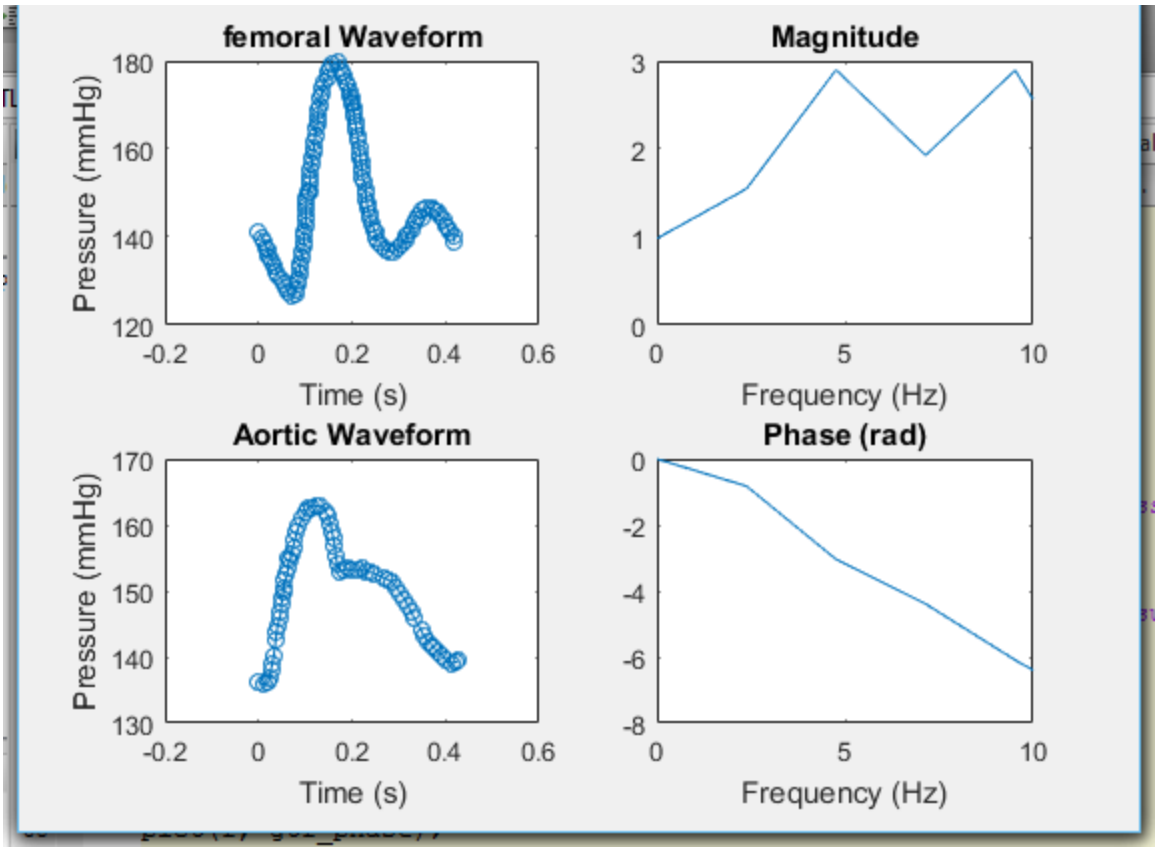

Figure 4.39 above shows the transfer function magnitude and phase in frequency domain of the carotid blood pressure waveform data of the normal individual discussed in figure 4.35. It is evident that the magnitude has two sharp peaks around 5Hz and 9Hz then declines and the phase declines almost linearly.

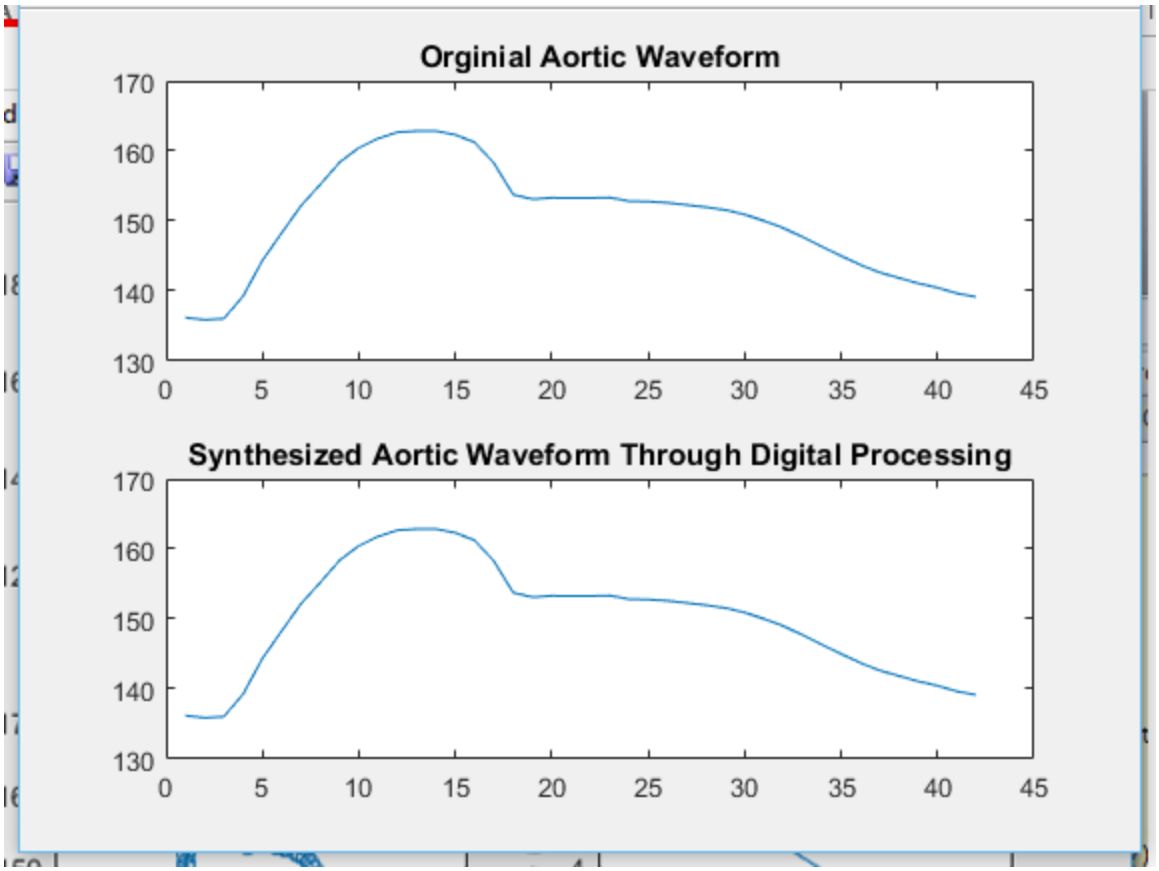

Waveform_correlation =

100.0000

Figure 4.40 The transfer function magnitude was used to reproduce the aortic waveform of this individual. The generalized magnitude used to compute the inverse fast fourier transform was the magnitude shown in figure 4.36. The synthesized aortic waveform shown above is the waveform produced by performing an ifft on the subject's femoral blood pressure data.

Subject 2

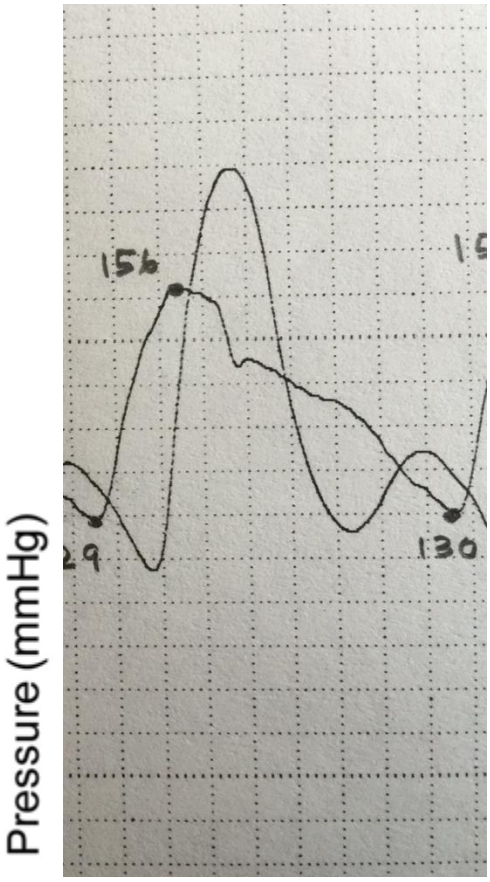

Figure 4.41 The above femoral arterial blood pressure data is obtained from a normal individual. (Courtesy of Professor John K-J. Li)

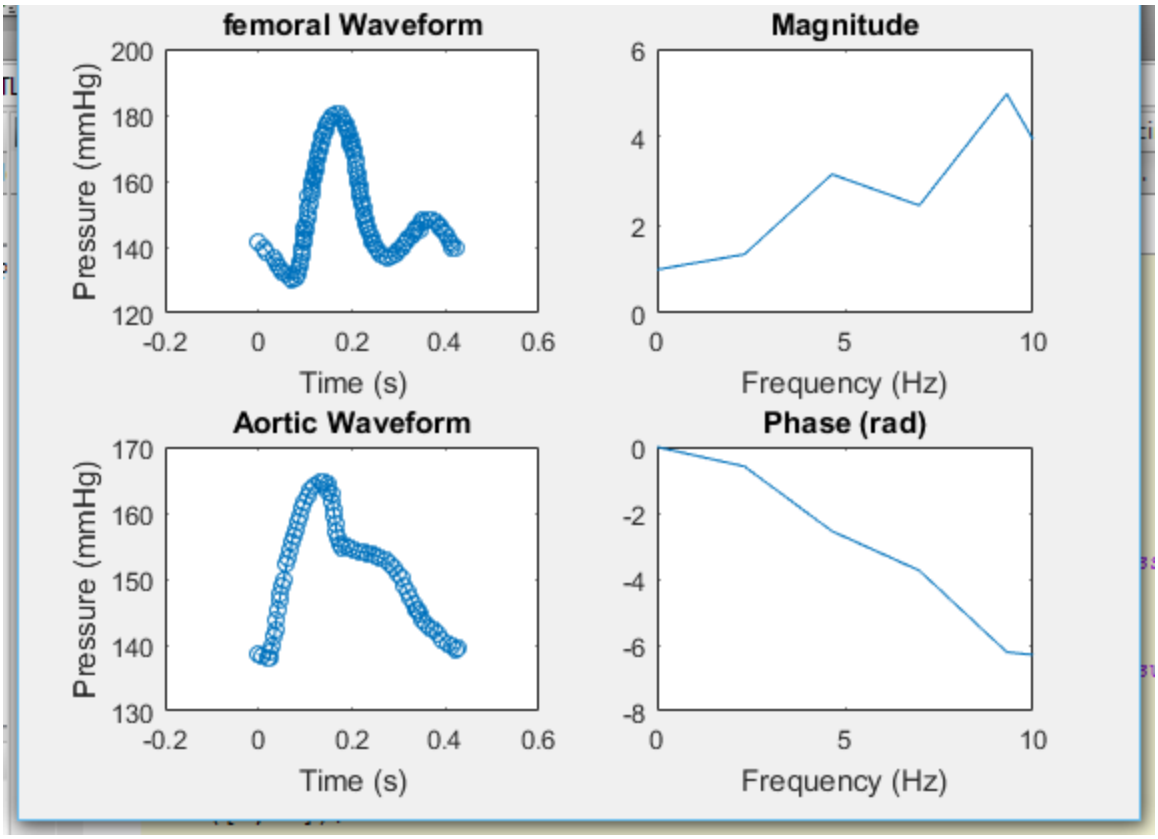

Figure 4.42 above shows the transfer function magnitude and phase in frequency domain of the carotid blood pressure waveform data of the normal individual discussed in figure 4.38. It is evident that the magnitude has two sharp peaks around 5Hz and 9Hz then declines and the phase declines almost linearly.

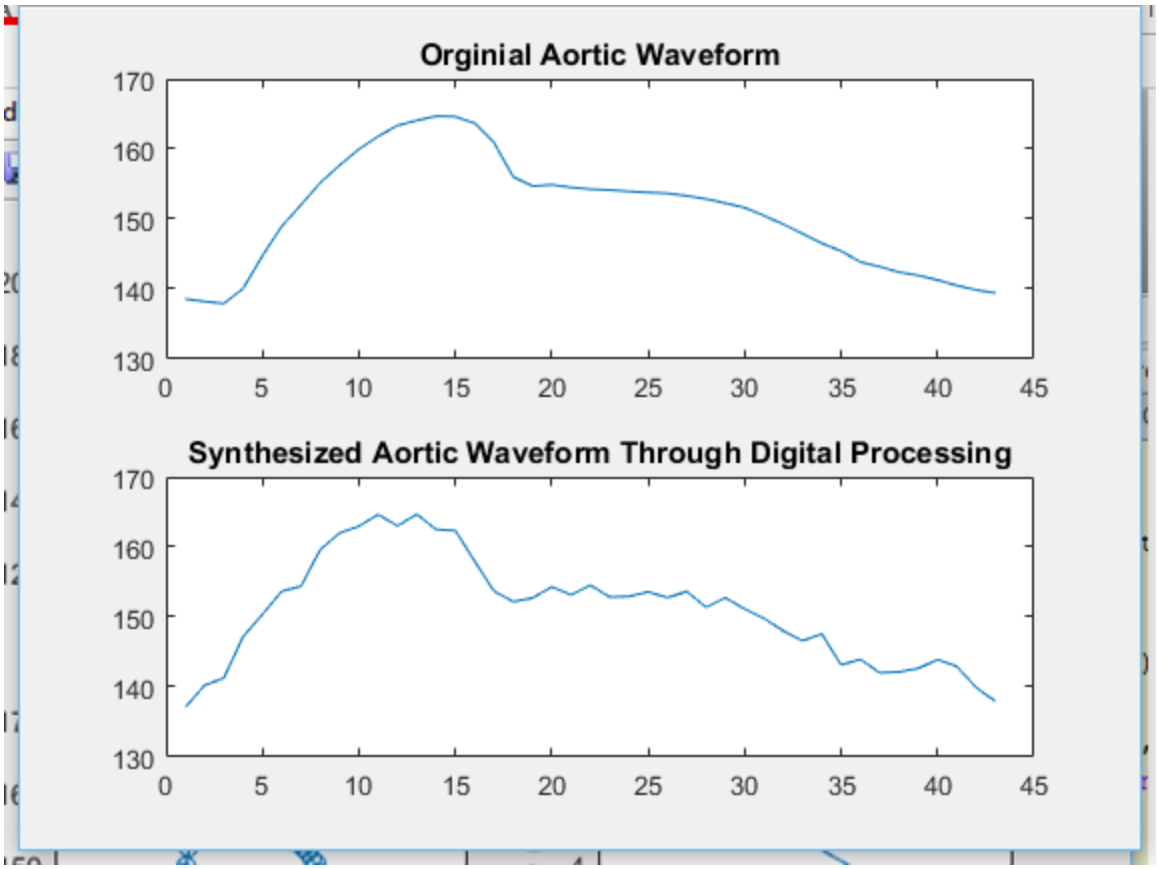

Waveform_correlation =

94.6110

Figure 4.43 The transfer function magnitude was used to reproduce the aortic waveform of this individual. The generalized magnitude used to compute the inverse fast fourier transform was the magnitude shown in figure 4.36. The synthesized aortic waveform shown above is the waveform produced by performing an ifft on the subject's femoral blood pressure data.

Subject 3

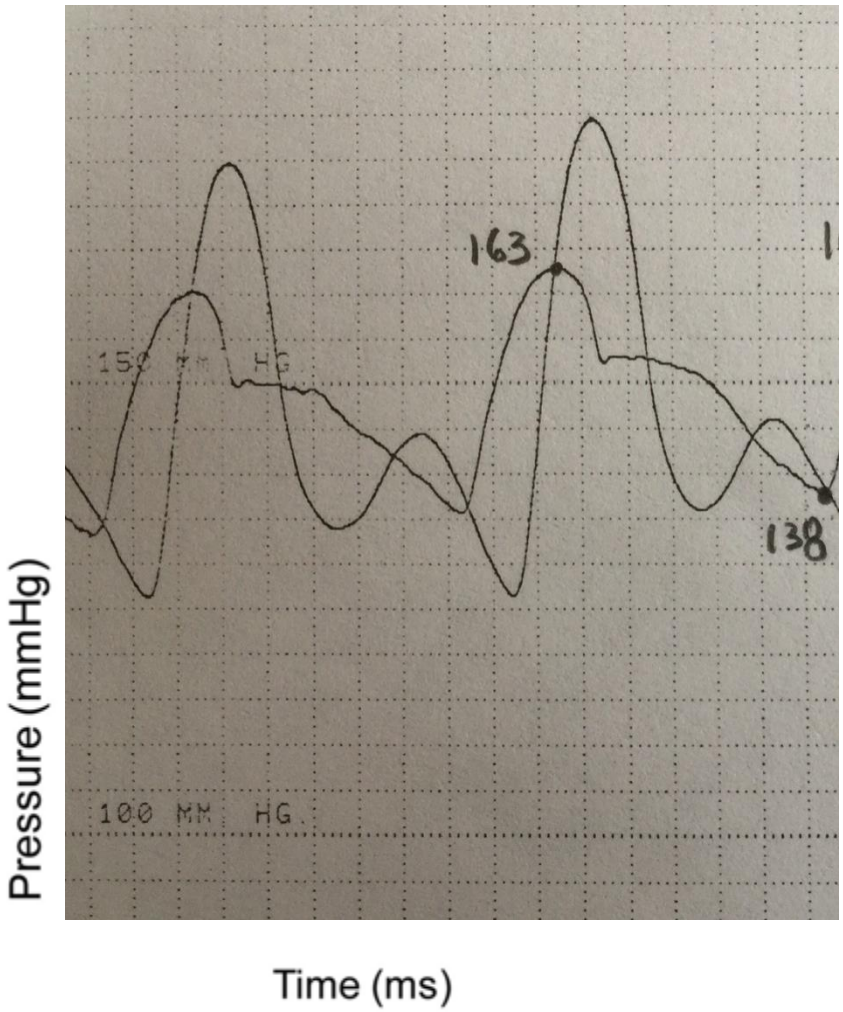

Figure 4.44 The above femoral arterial blood pressure data is obtained from a normal individual. (Courtesy of Professor John K-J. Li)

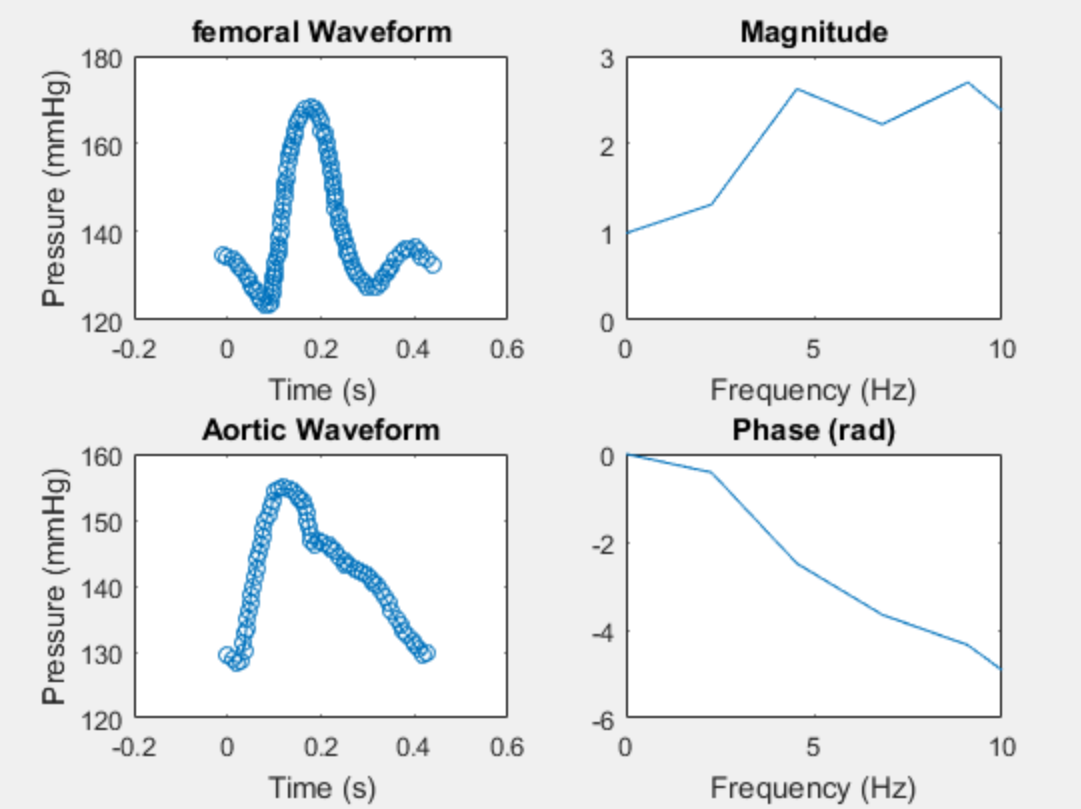

Figure 4.45 above shows the transfer function magnitude and phase in frequency domain of the carotid blood pressure waveform data of the normal individual discussed in figure 4.38. It is evident that the magnitude has two sharp peaks around 5Hz and 9Hz then declines and the phase declines almost linearly.

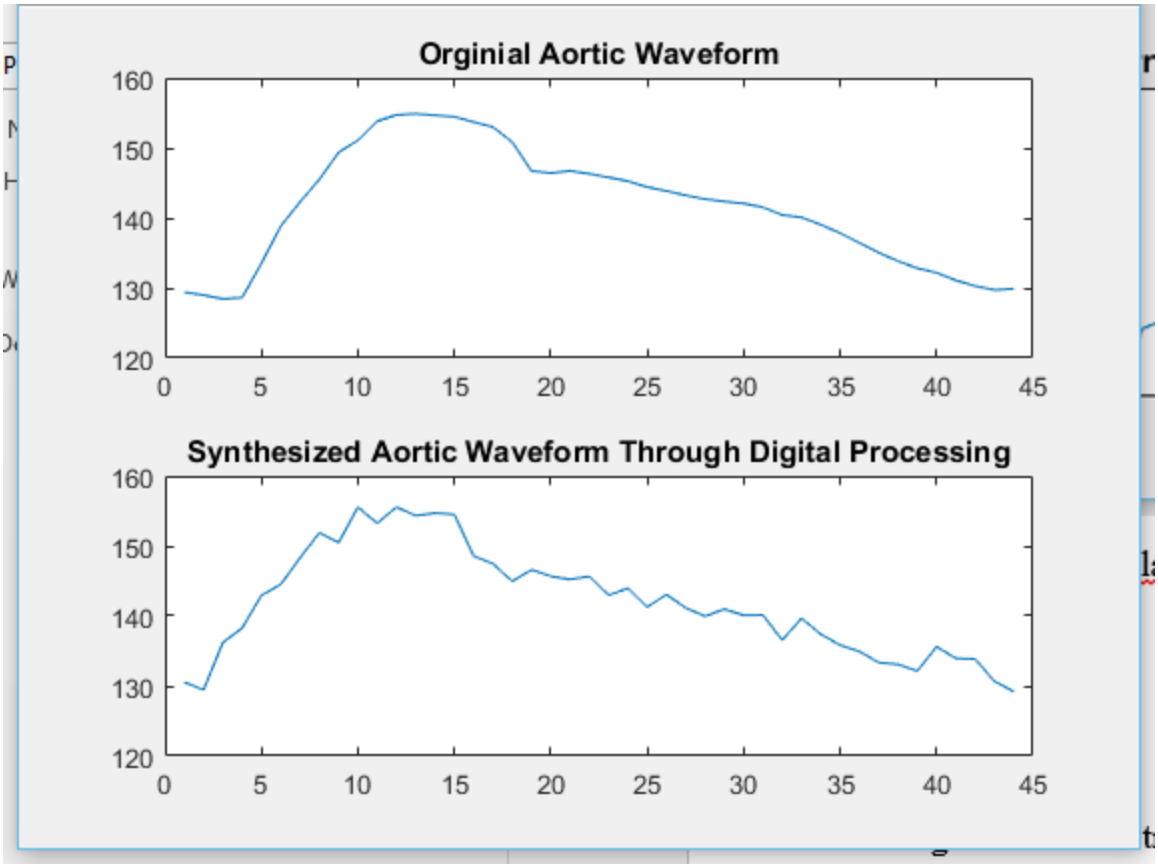

Waveform_correlation =

90.2675

Figure 4.46 The transfer function magnitude was used to reproduce the aortic waveform of this individual. The generalized magnitude used to compute the inverse fast fourier transform was the magnitude shown in figure 4.36. The synthesized aortic waveform shown above is the waveform produced by performing an ifft on the subject's femoral blood pressure data.

Superimposition of Transfer Functions

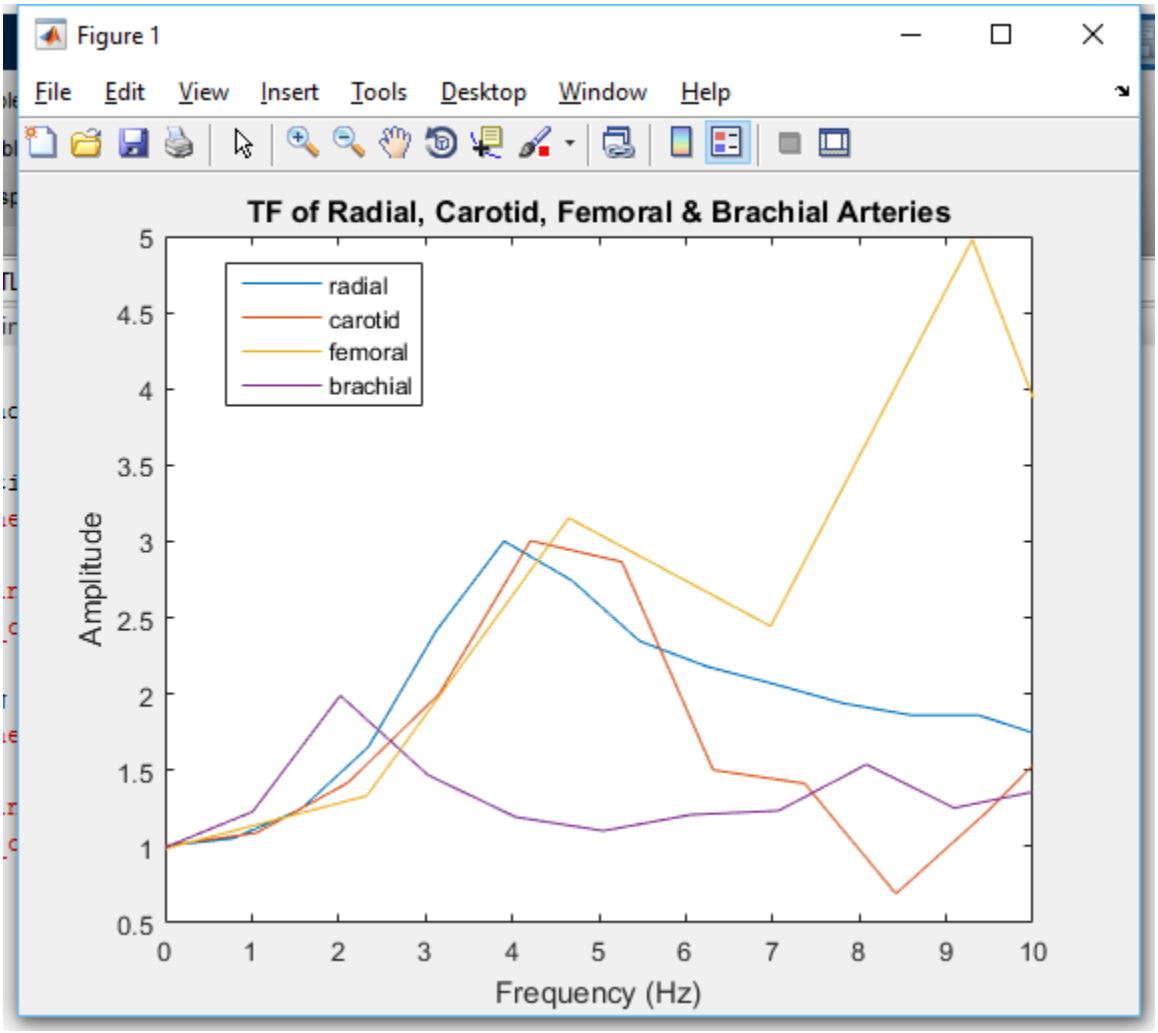

Figure 4.47 The magnitudes of the TF are superimposed to show the differences in the amplitudes.

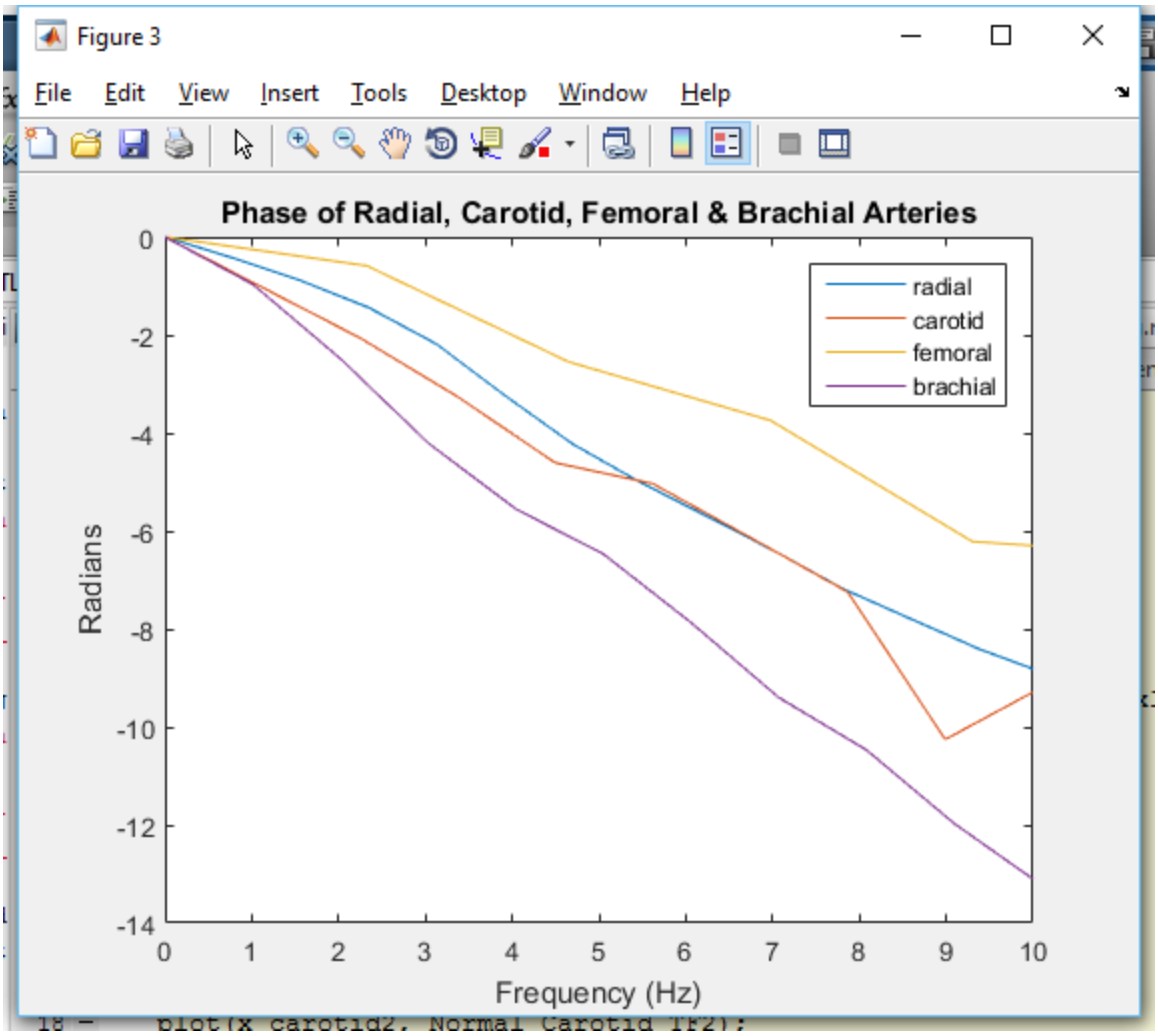

Figure 4.48 The phases of the TF are superimposed to show the differences in the radians.

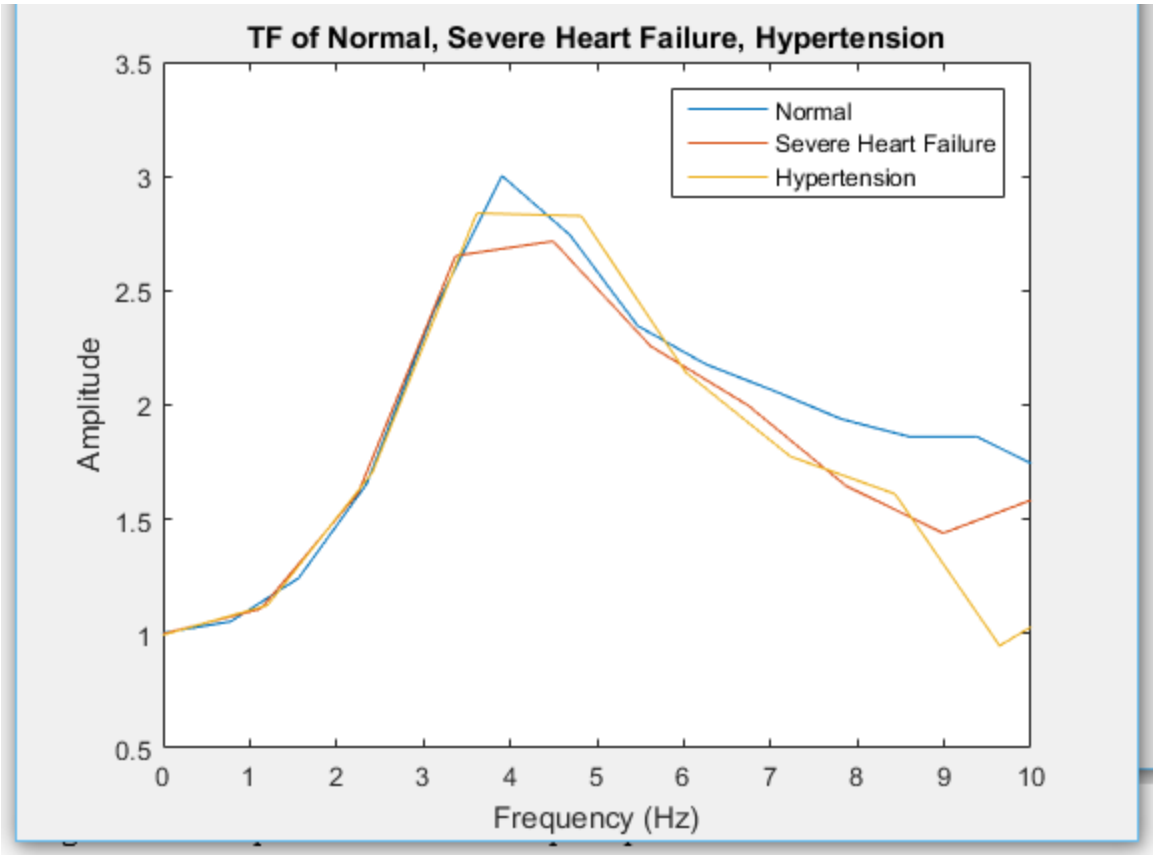

Figure 4.49 The magnitudes of the TF are superimposed to show the differences in the amplitudes obtained from patients with various conditions. Surprisingly, there is little difference except at the amplitude peak and at higher frequencies.

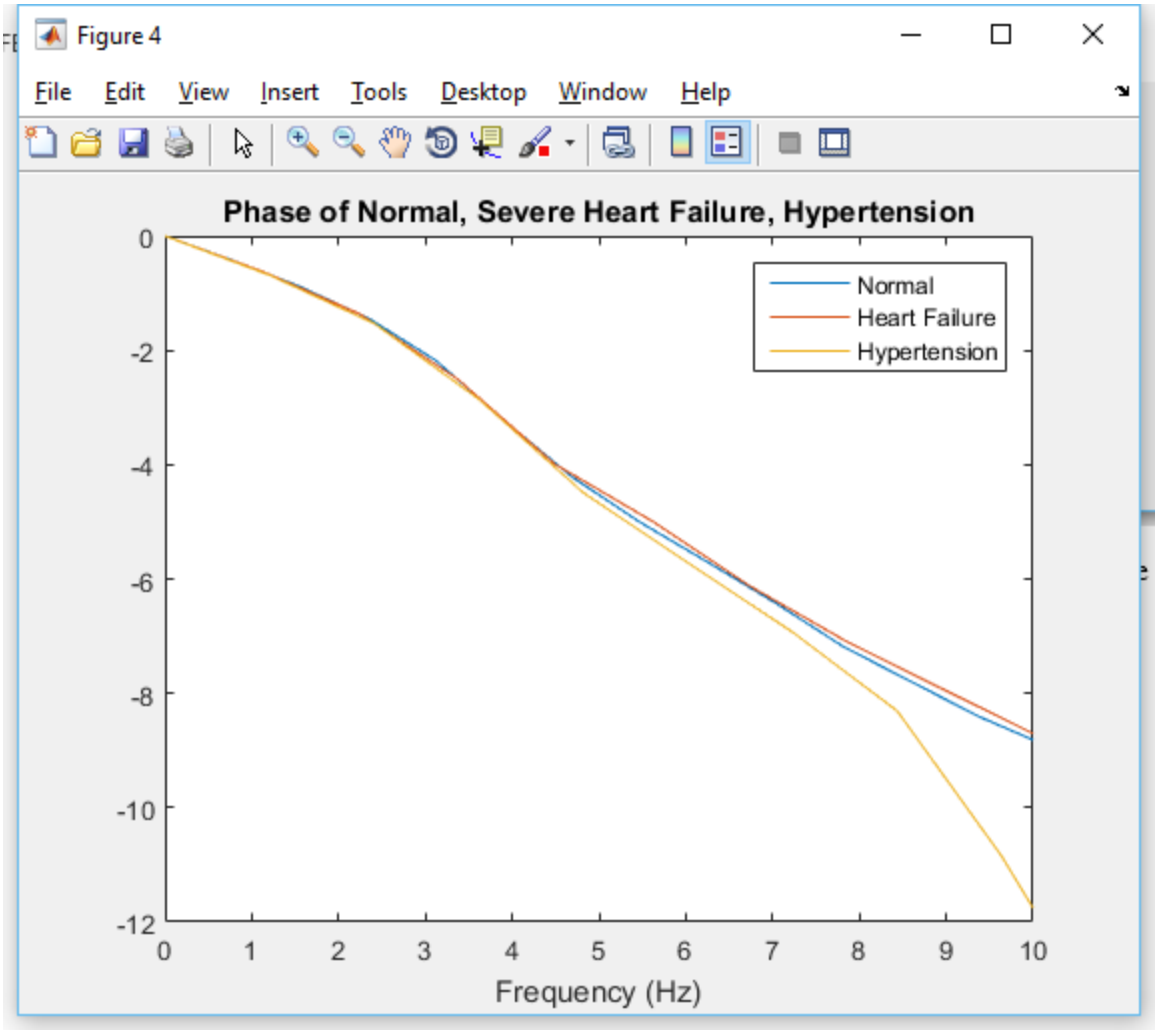

Figure 4.50 The phases of the TF are superimposed to show the differences in the radians of those patients with various cardiovascular conditions. Surprisingly, little change is seen at most frequencies.

Spectral analysis through FFT converts blood pressure from time series to frequency domain, where M(Radial) is the input signal and M(Aorta) is the output signal. Similarly, the IFFT converts the data from frequency domain back to time domain once the M(Aorta) is calculated using M(Radial) and amplitude ratio established. The larger the increase in proximity of the peripheral artery from that of the aorta, the larger the

amplitude of the pressure data. Also, with increasing frequency, phase lags. In terms of physiological representation of the transfer function results obtained above, cardiovascular conditions such as hypertension create a decrease in arteria compliance and an increase in vascular resistance which cause effective damping of increments in blood pressure resulting in lower gain or magnitude values, compared to that of the normal subject. Similarly, vasodilation causes a lowering in phase and an increased gain since there is less damping of the effect of blood pressure changes in the peripheral blood flow.

Chapter 5: Discussion, Conclusion and Suggestions for Future Work

5.1 Discussion of Results

Among the 10 leading causes of death listed by World Health Organization (WHO), cardiovascular conditions such as ischemic heart disease, stroke, diabetes mellitus and hypertension were some of the major causes of death (Nwankow, 2013). Hypertension is commonly treated with oral medications in order to lower systemic resistance; however, these drugs such as beta blockers, calcium channel blockers, and more recently created angiotensin-converting enzyme inhibitors. The efficacy of the drugs on blood vessels in many cases is not known since generic sphygmomanometer measurements only provide systolic and diastolic pressures. In this thesis unique radial and aortic blood pressure waveforms, of each subject, were obtained from previously published research and journal articles. These waveforms were digitized and interpolated to obtain pressure data values with consistent time intervals. The data was then processed through FFT to obtain transfer function magnitude and phase in the frequency domain. These, magnitude and phase data hold key information to obtain aortic blood pressure from the radial arterial blood pressure data. The arterial line or a-line is the most popular method used currently in the intensive care unit and anesthesiologist, to monitor aortic blood pressure, where a catheter is inserted through an artery up to the aorta. However, this method is time consuming, expensive and invasive compared to the modeling techniques discussed in this research thesis.

Waveforms of patients who are normal, hypertensive, have severe heart failure and those who were administered the ACH inhibitor called Ramipril were analyzed**.** It is evident from the FFT results that the frequency magnitude of those with hypertension and severe heart failure had sharp peaks as pressure increases in the frequency domain and the pressure dropped abruptly unlike that of normal patients or of those who were administered Ramipril. The magnitude data of the patients who were normal plateaued around the value of 3 mmHg and did not decline sharply. The phase decrease was constant and almost linear in both normal and hypertensive patients. When blood pressure data of a 36 year old man and his 68 year old father was analyzed, it evident that the aortic blood pressure significantly increases with age. The transfer function magnitude of the 36 year old man stabilized around the value of 3 mmHg indicating that his blood pressure falls under the normal range. Whereas, that of the 68 year old man decreased steeply once it reached the magnitude value of 3 mmHg around 5 Hz, indicating that he suffers from hypertension.

Similarly, when blood pressure measurements were taken before administering ACH inhibitor Ramipril to the 68 year old man, the transfer function magnitude pressure value declined sharply after reaching peak. However, when blood pressure measurements were obtained two hours after administering Ramipril, his aortic blood pressure decreased from around 120 mmHg to 109 mmHg. Also, the transfer function magnitude pressure data values also plateaued around peak with each subsequent frequency, similar to the behavior of magnitude data seen in a normal patient. This indicates that the ACH inhibitor, Ramipril is effective in reducing the aortic blood pressure.

The pressure data obtained from the frequency and phase domain of the several waveforms can be categorized and averaged to obtain amplitude and phase values which can then be applied to the following equations:

$$M_{Aorta} = \frac{MRadial}{Amplitude} \quad (5.1)$$

$$\theta(Aorta) = \theta(Radial) - Phase$$

The magnitude and phase information of the arterial line from the aorta can be extrapolated. These values can then be implemented into the inverse FFT to obtain pressure values of the aortic waveform in the time domain.

It is evident from the results that when correlation coefficients were calculated, the correlation of normal patients' synthesized aortic blood pressure waveforms were 99.85% proving that the model can indeed produce the aortic waveform given the radial blood pressure data as input. In cases with severe heart failure and hypertension, as shown in figure 4.6 and figure 4.8, the correlation coefficients were 99.33% and 99.398% which were expected since the blood pressure waveforms of those with arterial stiffness which leads to these disorders so they indeed have blood pressure waveforms that differ from normal patients. Furthermore, the amplitude ratio was derived from a normal patient and this ratio was what that was used to obtain the aortic waveform of these subject with the cardiovascular diseases so the 0.4% (r = 0.004) difference in correlation of normal subjects and subjects with the diseases was anticipated. Although this model proves to be highly accurate in noninvasively producing aortic blood pressure data, if a large number of subjects' blood pressure data were analyzed and if the results were indeed consistent with the above findings then we can safely conclude that using this model if a patient's correlation coefficient was r = 0.99398 (or 99.398%) it is highly likely that the patient is

at high risk for cardiovascular disease. Physicians can also further use the characteristics of the aortic waveform to provide specific diagnosis and treatment.

5.2 Comparison with Other Studies

Although this study did not include raw data collected directly from patients, these blood pressure data obtained from the published waveforms when processed using the above signal processing methods, provided reasonable results. Many research groups have attempted to produce the aortic waveform noninvasively, while many have succeeded, most of the existent models have several flaws which limit the accuracy of the synthesized waveforms. The ARX (AutoRegresive Exogenous) parametric model described in Chen et al.'s (1997) paper uses the present and previous output of the radial blood pressure measurements, however the a's and b's, also known as the parameters of the ARX parametric model, $T(t) = -a_1T(t-1) – a_2T(t-2)-\ldots- a_{na}T(t-2) + b_1P(t-1)+\ldots+ b_1P(t-nb)$, differs for each patient. The values of a and b were obtained using curve fitting for each of the transfer function estimate, making the generalizability of this model difficult, as the values have to be calibrated for each case.

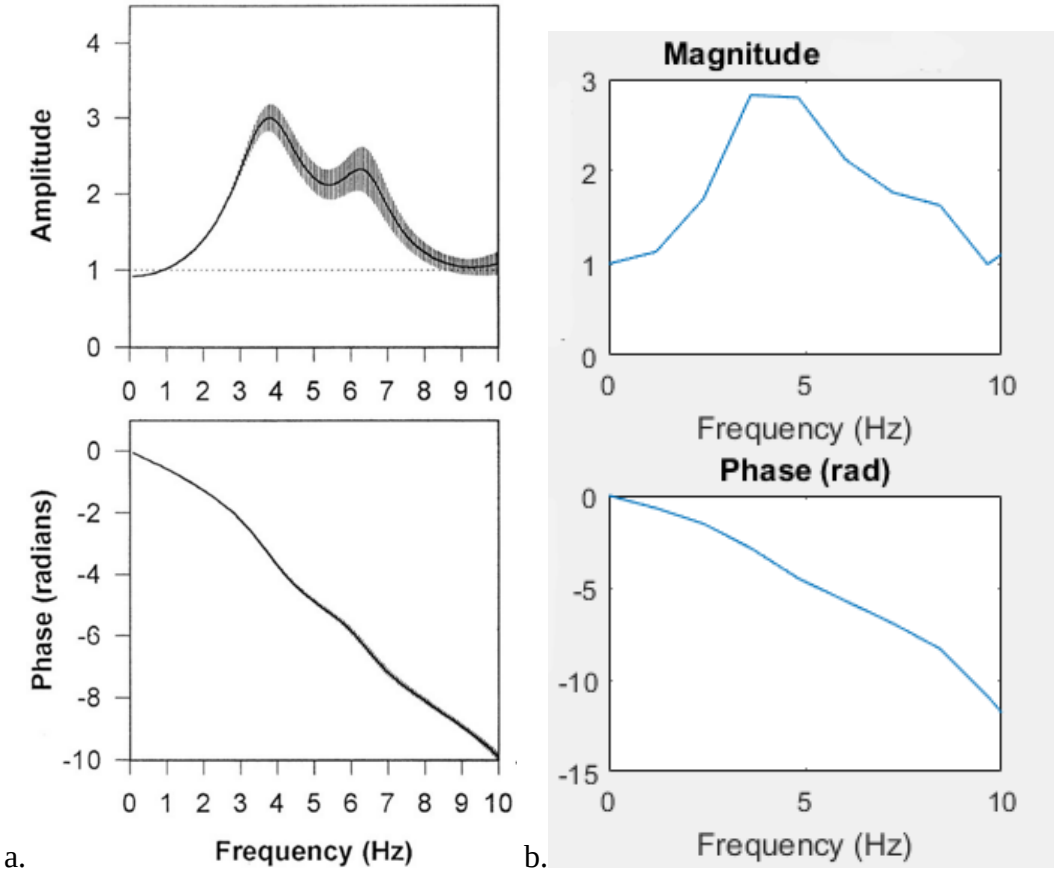

a. b.

Figure 5.1 Comparison of the transfer function magnitudes and phases. The transfer function magnitude and phase from Chen et al.'s (1997) ARX estimation is shown to the left in a. The TF magnitudes and phase obtained through this project by using radial blood pressure data are shown to the right in b. Reproduced with permission from (Wolters Kluwer Health, Inc. Chen, 1997)**.**

The transfer function magnitude that was derived noninvasively through this thesis has an amplitude of 3 around 4Hz similar to the magnitude peak obtained by Chen et al. (1997) through the ARX estimation, as shown in figure 5.1. The magnitudes decline to an amplitude of 1 after reaching the peak. There is a slight difference in that they have a

second peak around 6Hz. Similarly, phase declines towards -10 rads as frequency increases in both methods.

Compared to other non-invasive methods of obtaining aortic waveform such as that of Takazawa et al.(1998) who used augmentation index, the correlation results obtained through this generalized FFT method were better as their method's correlation coefficient of radial AI and aortic AI were $r = 0.91$ and $r = 0.70$ before and after administration of a vasodilator, Nicorandil, respectively, as opposed to the correlation coefficient of $r = 0.998$ that we were able to achieve through the digital processing method discussed in this thesis. Similarly, there have been research done in the past which analyze the pulse volume plethysmography (PVP) waveform with brachial cuff-based technologies as opposed to tonometry based techniques but there is a risk of the accuracy of the estimated systolic blood pressure being compromised since the cuff is elastic and might trap compressed air causing damped pressure signals. This in turn might cause a lack of sufficient high frequency components to produce accurate BP waveforms. Although Chen et al.'s (1997) ARX parametric model has flaws as discussed in the introduction, their parametric model was developed by averaging the transfer functions produced with their data sets, and it might be highly beneficial to implement their averaging technique into our current signal processing method (Chen et al.,1997). In the future, by obtaining a large number of data sets and averaging them for each category of patients such as normal, hypertensive and ischemic heart disease would provide specific amplitude ratios for each condition and may lead to a much specialized non-invasive diagnostic standard.

5.3 Conclusion

Distinct transfer functions for radial, carotid and femoral artery were computed in order to produce the aortic blood pressure waveform noninvasively. Also, the transfer function components of subjects who are normal, hypertensive and or with severe heart failure were compared. Radial artery was identified to be one of the ideal sites for acquiring noninvasive blood pressure data, by comparing and contrasting the transfer functions of blood pressure data from various peripheral arterial various sites. Similarly, transfer function for different pathological conditions and drug treatments were also analyzed.

Blood pressure data from arterial sites such as radial, carotid and femoral were used to produce aortic blood pressure waveform of each corresponding patient noninvasively. The synthesized aortic blood pressure data were then compared to that of the original aortic blood pressure data. From the results radial seems to be the ideal site for noninvasive measurement of blood pressure data. This could be explained due to the anatomy of the radial arterial site which is packed with bones and thus allows for better stability during tonometer blood pressure recording. The radial artery is also very accessible compared to femoral artery. However, femoral artery has an advantage as the aorta continues to the femoral artery unlike radial and carotid. Similarly, although carotid is also accessible it might not be the ideal site as it has less bone packing and the artery is relatively not as superficial as the radial artery. It is crucial to derive aortic blood pressure waveform noninvasively since arterial compliance is directly proportional to the functioning and structural condition of aorta. Large vessel stiffness also depends on the ability of aorta to pump blood. Augmentation index, which is a ratio that reflects the

arterial stiffness and facilitates the inference of wave reflection is also calculated from the aortic pressure. The arterial load of the left ventricle, otherwise known as the ejecting heart, is also dependent on aortic pressure. Therefore, by deriving aortic pressure noninvasively it is possible to quantify various characteristics of the heart which can make the diagnostic process more efficient.

5.4 Limitations and Suggestions for Future Work

The findings in this thesis is limited by the fact that the invasively aortic obtained blood pressure data readings could not be repeating again on the same person to assess exact correlation as a means of validating the noninvasively reproduced aortic BP waveform, because the data used in this thesis were obtained by digitizing the blood pressure waveforms from previously published research. Due to the inability to collect data from the same patient again the blood pressure data from one subject was used to obtain the amplitude ratio discussed in equation 3.1 as the basis for the transfer function, and this generalized amplitude was used on the BP data sets from several other subjects to derive the aortic blood pressure waveforms noninvasively. Another limitation is the fact that the peaks from peripheral blood pressure waveforms were not perfectly aligned with the peaks of the aortic blood pressure waveforms. It is possible that the aortic waveform might be spread out in comparison to peripheral BP waveforms. By aligning the peaks and notches of the waveforms, we could potentially achieve better transfer function estimates. Similarly, most the transfer function magnitudes had sharp peaks instead of a smooth magnitude curves, this could potentially have been the result of using high sampling rate and taking into consideration only 10Hz. There is a possibility that

some of the high frequency data were discarded. A possible solution for the issue would be to use a lower sampling rate of 50ms/ sample and to provide a sampling rate of 20Hz, which would be twice the Nyquist frequency of the 10Hz range of interest. This would give a better resolution on the magnitude plots.

In order to obtain better statistical significance, directly collected pressure waveform and data from patients of a wide range of race, age and cardiovascular conditions would be ideal. Also obtaining a larger sample size from a randomized pool of patients would help to obtain better validity. Incorporating pressure waveform data from patients who were administered a variety of anti-hypertensive drugs such as ACE inhibitor and beta blockers would augment the statistical significance and can facilitate the understanding of the reactions to these drugs. Although a limited number of waveforms were analyzed, aortic waveforms were successfully derived through non-invasive signal processing methods. This noninvasive method could help address the specific needs of each individual patient with cardiovascular conditions or could potentially help physicians to develop personalized course of treatments and can thus lead to a better quality of care. Although the generalized transfer functions used, produced an aortic BP waveform correlation of about 98% for normal subjects whose radial arterial BP data was processed, these transfer functions could be calibrated to produce more accurate aortic blood pressure estimations If the pulse transit time can be inputted according to the anatomy of each patient by obtaining the exact distance from aorta to the peripheral arterial sites, a personalized therapeutic strategy can be planned to tailor the needs of each patient and provide long term compliance improvement.

References:

Adji, A., & O'Rourke, M. F. (2004). Determination of central aortic systolic and pulse pressure from the radial artery pressure waveform. *Blood pressure monitoring*, *9*(3), 115-121.

Asmar, R., Rudnichi, A., Blacher, J., London, G. M., & Safar, M. E. (2001). Pulse pressure and aortic pulse wave are markers of cardiovascular risk in hypertensive populations. *American journal of hypertension*, *14*(2), 91-97.

Bakhle YS. "Conversion of angiotensin I to angiotensin II by cell-free extracts of dog lung". Nature 1968;220:919–21.

Cameron, J. D., McGrath, B. P., & Dart, A. M. (1998). Use of radial artery applanation tonometry and a generalized transfer function to determine aortic pressure augmentation in subjects with treated hypertension. *Journal of the American College of Cardiology*, *32*(5), 1214-1220.

Chen, C. H., Nevo, E., Fetics, B., Pak, P. H., Yin, F. C., Maughan, W. L., & Kass, D. A. (1997). Estimation of central aortic pressure waveform by mathematical transformation of radial tonometry pressure validation of generalized transfer function. *Circulation*, *95*(7), 1827-1836.

Davies, J. I., Band, M. M., Pringle, S., Ogston, S., & Struthers, A. D. (2003). Peripheral blood pressure measurement is as good as applanation tonometry at predicting ascending aortic blood pressure. *Journal of hypertension*, *21*(3), 571-576.

Denardo, S. J., Nandyala, R., Freeman, G. L., Pierce, G. L., & Nichols, W. W. (2010). Pulse wave analysis of the aortic pressure waveform in severe left ventricular systolic dysfunction. *Circulation: Heart Failure*, *3*(1), 149-156.

Despain, A. M. "Fourier transform computers using CORDIC iterations."*IEEE Transactions on Computers* 23.10 (1974): 993-1001.

Fetics, B., Nevo, E., Chen, C. H., & Kass, D. A. (1999). Parametric model derivation of transfer function for noninvasive estimation of aortic pressure by radial tonometry. *Biomedical Engineering, IEEE Transactions on*, *46*(6), 698-706.

Heart Outcomes Prevention Evaluation (HOPE) Study Investigators. "Effects of ramipril on cardiovascular and microvascular outcomes in people with diabetes mellitus: results of the HOPE study and MICRO-HOPE substudy."*The lancet* 355.9200 (2000): 253-259.

Hope, S. A., Meredith, I. T., & Cameron, J. D. (2004). Effect of non-invasive calibration of radial waveforms on error in transfer-function-derived central aortic waveform characteristics. *Clinical Science*, *107*(2), 205-212.

Hope, S. A., Tay, D. B., Meredith, I. T., & Cameron, J. D. (2004). Use of arterial transfer functions for the derivation of central aortic waveform characteristics in subjects with type 2 diabetes and cardiovascular disease.*Diabetes care*, *27*(3), 746-751.

Hope, S. A., Meredith, I. T., Tay, D., & Cameron, J. D. (2007). 'Generalizability'of a radial-aortic transfer function for the derivation of central aortic waveform parameters. *Journal of hypertension*, *25*(9), 1812-1820.

Karamanoglu, M., Gallagher, D. E., Avolio, A. P., & O'Rourke, M. F. (1995). Pressure wave propagation in a multibranched model of the human upper limb.*American Journal of Physiology-Heart and Circulatory Physiology*, *269*(4), H1363-H1369.

Karamanoglu, M. U. S. T. A. F. A., & Feneley, M. P. (1996). Derivation of the ascending aortic-carotid pressure transfer function with an arterial model.*American Journal of Physiology-Heart and Circulatory Physiology*, *271*(6), H2399-H2404.

Karamanoglu, M., & Feneley, M. P. (1997, October). Non-invasive estimation of wave reflection coefficient from the phase of the pressure transfer function. In *CIRCULATION* (Vol. 96, No. 8, pp. 3583-3583).

Lehmann, E. D. (2000). Regarding the accuracy of generalized transfer functions for estimating central aortic blood pressure when calibrated non-invasively. *Journal of hypertension*, *18*(3), 347-349.

Lewis, A. J. M., and D. Kotecha. "134 Peripheral Arterial Waveforms For The Prediction Of Cardiovascular Events: Carotid Versus Radial Pulse Wave Analysis." *Heart* 99.suppl 2 (2013): A79-A80.

Li, J. K-J. "A new description of arterial function: The compliance-pressure loop." *Angiology* 49.7 (1998): 543-548.

Li, J. K-J. *Comparative cardiovascular dynamics of mammals*. CRC press, 1995.

MacBrayne, J., & Webster, N. R. (2015). Oh's Intensive Care Manual. *British Journal of Anaesthesia*, *114*(2), 354-355.

Mathers, C. D., Bernard, C., Iburg, K. M., Inoue, M., Ma Fat, D., Shibuya, K., & Xu, H. (2003). Global burden of disease in 2002: data sources, methods and results. *Geneva: World Health Organization*.

Nwankwo T, Yoon SS, Burt V, Gu Q. Hypertension among adults in the US: National Health and Nutrition Examination Survey, 2011-2012. NCHS Data Brief, No. 133. Hyattsville, MD: National Center for Health Statistics, Centers for Disease Control and Prevention, US Dept of Health and Human Services, 2013.

O'Rourke, M. F., & Pauca, A. L. (2004). Augmentation of the aortic and central arterial pressure waveform. *Blood pressure monitoring*, *9*(4), 179-185.

Patlak, M. "From viper's venom to drug design: treating hypertension." *The FASEB Journal* 18.3 (2004): 421e-421e.

Pauca, A. L., O'Rourke, M. F., & Kon, N. D. (2001). Prospective evaluation of a method for estimating ascending aortic pressure from the radial artery pressure waveform. *Hypertension*, *38*(4), 932-937.

Ruiz, P., Rezaienia, M. A., Rahideh, A., Keeble, T. R., Rothman, M. T., & Korakianitis, T. (2013). In vitro cardiovascular system emulator (bioreactor) for the simulation of normal and diseased conditions with and without mechanical circulatory support. *Artificial organs*, *37*(6), 549-560.

Söderström, S., Nyberg, G., O'Rourke, M. F., Sellgren, J., & Ponten, J. (2002). Can a clinically useful aortic pressure wave be derived from a radial pressure wave?. *British journal of anaesthesia*, *88*(4), 481-488.

Software used to digitize blood pressure waveforms: http://arohatgi.info/WebPlotDigitizer/

Stergiopulos, N., Westerhof, B. E., & Westerhof, N. (1998). Physical basis of pressure transfer from periphery to aorta: a model-based study. *American Journal of Physiology-Heart and Circulatory Physiology*, *274*(4), H1386-H1392.

Takazawa, K., Tanaka, N., Fujita, M., Matsuoka, O., Saiki, T., Aikawa, M., & Ibukiyama, C. (1998). Assessment of vasoactive agents and vascular aging by the second derivative of photoplethysmogram waveform.*Hypertension*, *32*(2), 365-370.

Teo, K. K., Benedict, C. R., & Pitt, B. (1994). Emerging Role of Angiotensin-Converting Enzyme Inhibitorsin Cardiac and Vascular Protection. Visser, L. E., Stricker, B. C., Van der Velden, J., Paes, A. H. P., & Bakker, A. (1995). Angiotensin converting enzyme inhibitor associated cough: a population-based case-control study. *Journal of clinical epidemiology*, *48*(6), 851-857.

Viswanathan, P., Matonick, J. P., & Li, J. K. (1998, April). Noninvasive assessment of age-related changes in vascular elasticity and pulse wave velocity spectrum. In *Bioengineering Conference, 1998. Proceedings of the IEEE 24th Annual Northeast* (pp. 104-106). IEEE.

Williams, B., Lacy, P. S., Yan, P., Hwee, C. N., Liang, C., & Ting, C. M. (2011). Development and validation of a novel method to derive central aortic systolic pressure from the radial pressure waveform using an N-point moving average method. *Journal of the American College of Cardiology*, *57*(8), 951-961.

Zhang, G., Hahn, J. O., & Mukkamala, R. (2011). Tube-load model parameter estimation for monitoring arterial hemodynamics. *Frontiers in physiology*, *2*.

Zhang, H., Li, J. J., Wang, Q., Pompili, D., & Marsic, I. (2010, March). A distributed predictive arterial model for human vascular diagnostic applications. In *Bioengineering Conference, Proceedings of the 2010 IEEE 36th Annual Northeast* (pp. 1-2). IEEE.

Appendix

MATLAB program

The following MATLAB program was used to interpolate the digitized aortic and radial blood pressure data. The program below also outputs magnitude and phase diagrams of

```
close all
clear all
radial = dlmread('1_Radial.csv');
aortic = dlmread('1_Aortic.csv');

radial = sortrows(radial,1);
[~, ia, ~] = unique(aortic(:,1));
aortic = aortic(ia, :);

figure(); plot(radial(:,1), radial(:,2),'-o');
    title('Radial Waveform'); xlabel('Time (s)'); ylabel('Pressure
(mmHg)');
figure(); plot(aortic(:,1), aortic(:,2),'-o');
    title('Aortic Waveform'); xlabel('Time (s)'); ylabel('Pressure
(mmHg)');



f_interp = 100;
t_max = min(radial(end,1), aortic(end,1));
t_interp = 0:1/f_interp:t_max;



%t_interp = 0:0.01:0.9



radial_interp = interp1(radial(:,1),radial(:,2), t_interp)';
radial_interp(end) = radial_interp(1);
delay = 0.14/0.01; % delayed time = 140 ms/ 0.01 sec = 14
radial_delayed = circshift(radial_interp,uint64(delay));

aortic_interp = interp1(aortic(:,1),aortic(:,2), t_interp)';
figure(); plot(radial(:,1), radial(:,2),'-', t_interp, radial_interp,
'x');
    title('Interpolated Radial Waveform with X-axis Interval of 0.01
sec'); xlabel('Time (s)'); ylabel('Pressure (mmHg)');
figure(); plot(aortic(:,1), aortic(:,2),'-', t_interp, aortic_interp,
'x');
    title('Interpolated Aortic Waveform with X-axis Interval of 0.01
sec'); xlabel('Time (s)'); ylabel('Pressure (mmHg)');

% Transfer Function Portion
radial_fft = fft(radial_delayed); %FFT x
aortic_fft = fft(aortic_interp);  %FFT y
gtf_a_r = radial_fft./aortic_fft;  %magnitude

gtf_magnitude = abs(gtf_a_r); % abs(radial/aortic)
gtf_phase = unwrap(angle(gtf_a_r));   % phase( radial/aortic)
```

```
% resolving the x axis of frequency in hertz
m = length(t_interp); %91 points
fs = 100; %sampling frequency f=1/dt =1/0.01
f = (0:m-1)*(fs/m);

figure();
subplot(2,2,1);
plot(radial(:,1), radial(:,2),'-o');
    title('Radial Waveform'); xlabel('Time (s)'); ylabel('Pressure
(mmHg)');
subplot(2,2,3);
plot(aortic(:,1), aortic(:,2),'-o');
    title('Aortic Waveform'); xlabel('Time (s)'); ylabel('Pressure
(mmHg)');
subplot(2,2,2); %row,columns, 1st graph
plot(f, gtf_magnitude);
title('Magnitude (mmHg)'); xlabel('Frequency (Hz)'); ylabel('Pressure
(mmHg)');
xlim([0,10]);
subplot(2,2,4);
plot(f, gtf_phase);
title('Phase (rad)'); xlabel('Frequency (Hz)'); ylabel('Pressure
(mmHg)');
xlim([0,10]);

%%%applying the TF

radial_interp_fft = fft(radial_interp);

%% Amplitude matrix generation

gtf_r_a = 1./gtf_a_r; %Amplitude of transfer function from radial to
aorta
aortic_synthesis= radial_interp_fft.*gtf_r_a; %element by element.
aorta= radial/magnitude

%to get into time domain do inverse fourier
aortic_inv = ifft(aortic_synthesis);
shifted_aortic = circshift(aortic_inv, uint64(delay));

figure();
plot(t_interp,radial_interp,t_interp, aortic_inv, 'o', t_interp,
shifted_aortic);
legend ('Radial Waveform', 'Inverse Fourier of Aortic Waveform',
'Synthesized Aortic Waveform');

subplot(2,1,1);
plot(aortic_interp);
title ('Orginial Aortic Waveform');
subplot(2,1,2);
plot(shifted_aortic);
title ('Synthesized Aortic Waveform Through Digital Processing');

Waveform_correlation = corr2(aortic_interp, shifted_aortic)*100
```

```
close all
clear all
radial = dlmread('12_Radial.csv');
aortic = dlmread('12_Aortic.csv');

load ('Magnitude1.mat');

radial = sortrows(radial,1);

figure(); plot(radial(:,1), radial(:,2),'-o');
    title('Radial Waveform'); xlabel('Time (s)'); ylabel('Pressure
(mmHg)');

%% Interpolation of Radial Waveform

f_interp = 100;
t_max = min(radial(end,1));
t_interp = 0:1/f_interp:t_max;

radial_interp = interp1(radial(:,1),radial(:,2), t_interp)';
radial_interp(end) = radial_interp(1);
delay = 0.14/0.01; % delayed time = 140 ms/ 0.01 sec = 14
radial_delayed = circshift(radial_interp,uint64(delay));

figure(); plot(radial(:,1), radial(:,2),'-', t_interp, radial_interp,
'x');
    title('Interpolated Radial Waveform with X-axis Interval of 0.01
sec'); xlabel('Time (s)'); ylabel('Pressure (mmHg)');


[~, ia, ~] = unique(aortic(:,1));
aortic = aortic(ia, :);
aortic_interp = interp1(aortic(:,1),aortic(:,2), t_interp)';
aortic_interp(isnan(aortic_interp)) = aortic(end);

%% Transfer Function Portion
radial_fft = fft(radial_delayed); %FFT x
aortic_fft = fft(aortic_interp);  %FFT y
gtf_a_r = radial_fft./aortic_fft;  %magnitude

gtf_magnitude = abs(gtf_a_r); % abs(radial/aortic)
gtf_phase = unwrap(angle(gtf_a_r));   % phase( radial/aortic)

%% resolving the x axis of frequency in hertz
m = length(t_interp); %91 points
fs = 100; %sampling frequency f=1/dt =1/0.01
f = (0:m-1)*(fs/m);

figure();
subplot(2,2,1);
plot(radial(:,1), radial(:,2),'-o');
```

```
    title('Radial Waveform'); xlabel('Time (s)'); ylabel('Pressure
(mmHg)');
subplot(2,2,3);
plot(aortic(:,1), aortic(:,2),'-o');
    title('Aortic Waveform'); xlabel('Time (s)'); ylabel('Pressure
(mmHg)');
subplot(2,2,2); %row,columns, 1st graph
plot(f, gtf_magnitude);
title('Magnitude'); xlabel('Frequency (Hz)');
xlim([0,10]);
subplot(2,2,4);
plot(f, gtf_phase);
title('Phase (rad)'); xlabel('Frequency (Hz)');
xlim([0,10]);

%% applying the TF

radial_interp_fft = fft(radial_interp);

t_mag_max = ceil(t_max*100);

Yr = real(gtf_r_a);
Yi = imag(gtf_r_a);

gtf_r_a_interp = interpft(gtf_r_a, fix(t_mag_max));

aortic_synthesis= radial_interp_fft.*gtf_r_a_interp; %element by
element. aorta= radial/magnitude

%to get into time domain do inverse fourier
aortic_inv = ifft(aortic_synthesis);
shifted_aortic = circshift(aortic_inv, uint64(delay));

shifted_aortic = real(shifted_aortic);

figure();
plot(t_interp,radial_interp,t_interp, aortic_inv, 'o', t_interp,
shifted_aortic);
legend ('Radial Waveform', 'Inverse Fourier of Aortic Waveform',
'Synthesized Aortic Waveform');

%% Comparing to Original Aortic

subplot(2,1,1);
plot(aortic_interp);
title ('Orginial Aortic Waveform');
subplot(2,1,2);
plot(shifted_aortic);
title ('Synthesized Aortic Waveform Through Digital Processing');
%% Calculating Correlation
Waveform_correlation = corr2(aortic_interp, shifted_aortic)*100


close all
```

```
% Radial
load('Normal_Radial_TF.mat');
load('X_Radial.mat');

figure;
plot(f, NormalRadialTF);
title('TF of Radial, Carotid & Femoral Arteries'); xlabel('Frequency
(Hz)'); ylabel('Amplitude');
xlim([0,10]);
hold on

%Carotid
load('Normal_Carotid_TF.mat');
load('x_carotid.mat');


plot(x_carotid, Normal_Carotid_TF);
xlim([0,10]);
hold on

%Femoral

load('Femoral_TF.mat');
load('X_Femoral.mat');

plot(x_femoral, Femoral_TF);
xlim([0,10]);
hold on

legend('radial','carotid','femoral');

%% Normal vs. Severe Heart Failure vs. Hypertensive

figure;
load('Normal_Radial_TF.mat');
load('X_Radial.mat');

plot(f, NormalRadialTF);

title('TF of Normal, Severe Heart Failure, Hypertension');
xlabel('Frequency (Hz)'); ylabel('Amplitude');
xlim([0,10]);
hold on

load('TF_Severe_Heart_Failure.mat')
load('X_Severe_Heart_Failure.mat');

plot(x_severe_heart_failure, Severe_Heart_Failure);
xlim([0,10]);
hold on

load('TF_Hypertension.mat');
load('x_hypertension.mat');
```

```
plot(x_hypertension, TF_Hypertension);
xlim([0,10]);

legend('Normal','Severe Heart Failure','Hypertension');

%% Phase

load('Normal_Radial_Phase.mat');
load('Normal_Carotid_Phase.mat');
load('Femoral_Phase.mat');

figure;
plot(f,Normal_Radial_Phase);
xlim([0,10]);
hold on

plot(x_carotid,Normal_Carotid_Phase);
xlim([0,10]);
hold on

plot(x_femoral, Femoral_Phase);
xlim([0,10]);
hold on

title('Phase of Radial, Carotid & Femoral Arteries'); xlabel('Frequency
(Hz)'); ylabel('Radians');
legend('radial','carotid','femoral');

%% Phase for diseases

figure;
plot(f,Normal_Radial_Phase);
xlim([0,10]);
hold on

load('Severe_Heart_Failure_Phase.mat');
load('Phase_Hypertension.mat');
load('x_severe_heart_failure.mat')
load('x_hypertension.mat')

plot(x_severe_heart_failure, Severe_Heart_Failure_Phase);
xlim([0,10]);
hold on

plot(x_hypertension, Phase_Hypertension);
xlim([0,10]);
hold on

legend('Normal','Heart Failure','Hypertension');
title('Phase of Normal, Severe Heart Failure, Hypertension');
xlabel('Frequency (Hz)')
```

```
%% CAROTID


close all
clear all
carotid = dlmread('Carotid6.csv');
aortic = dlmread('Aortic_of_Carotid6.csv');

load ('Magnitude2_Carotid5_Aortic.mat');

carotid = sortrows(carotid,1);

figure(); plot(carotid(:,1), carotid(:,2),'-o');
    title('carotid Waveform'); xlabel('Time (s)'); ylabel('Pressure
(mmHg)');

%% Interpolation of carotid Waveform

f_interp = 100;
t_max = min(carotid(end,1));
t_interp = 0:1/f_interp:t_max;

carotid_interp = interp1(carotid(:,1),carotid(:,2), t_interp)';
carotid_interp(end) = carotid_interp(1);
delay = 14; % delayed time = 140 ms/ 0.01 sec = 14
carotid_delayed = circshift(carotid_interp,uint64(delay));

figure(); plot(carotid(:,1), carotid(:,2),'-', t_interp,
carotid_interp, 'x');
    title('Interpolated carotid Waveform with X-axis Interval of 0.01
sec'); xlabel('Time (s)'); ylabel('Pressure (mmHg)');



[~, ia, ~] = unique(aortic(:,1));
aortic = aortic(ia, :);
aortic_interp = interp1(aortic(:,1),aortic(:,2), t_interp)';
aortic_interp(isnan(aortic_interp)) = aortic(end);

%% Transfer Function Portion
carotid_fft = fft(carotid_delayed); %FFT x
aortic_fft = fft(aortic_interp);  %FFT y
gtf_a_r = carotid_fft./aortic_fft;  %magnitude

gtf_magnitude = abs(gtf_a_r); % abs(carotid/aortic)
gtf_phase = unwrap(angle(gtf_a_r));   % phase( carotid/aortic)

%% resolving the x axis of frequency in hertz
m = length(t_interp); %91 points
fs = 100; %sampling frequency f=1/dt =1/0.01
f = (0:m-1)*(fs/m);

figure();
subplot(2,2,1);
plot(carotid(:,1), carotid(:,2),'-o');
```

```
    title('carotid Waveform'); xlabel('Time (s)'); ylabel('Pressure
(mmHg)');
subplot(2,2,3);
plot(aortic(:,1), aortic(:,2),'-o');
    title('Aortic Waveform'); xlabel('Time (s)'); ylabel('Pressure
(mmHg)');
subplot(2,2,2); %row,columns, 1st graph
%magnitude = circshift(gtf_magnitude,81);
plot(f, gtf_magnitude);
title('Magnitude'); xlabel('Frequency (Hz)');
xlim([0,10]);
subplot(2,2,4);
plot(f, gtf_phase);
title('Phase (rad)'); xlabel('Frequency (Hz)');
xlim([0,10]);

%% applying the TF

carotid_interp_fft = fft(carotid_interp);

t_mag_max = ceil(t_max*100);

Yr = real(gtf_r_a);
Yi = imag(gtf_r_a);

gtf_r_a_interp = interpft(gtf_r_a, fix(t_mag_max));

aortic_synthesis= carotid_interp_fft.*gtf_r_a_interp; %element by
element. aorta= carotid/magnitude

%to get into time domain do inverse fourier
aortic_inv = ifft(aortic_synthesis);
shifted_aortic = circshift(aortic_inv, uint64(delay));

shifted_aortic = real(shifted_aortic);

figure();
plot(t_interp,carotid_interp,t_interp, aortic_inv, 'o', t_interp,
shifted_aortic);
legend ('carotid Waveform', 'Inverse Fourier of Aortic Waveform',
'Synthesized Aortic Waveform');

%% Comparing to Original Aortic


subplot(2,1,1);
plot(aortic_interp);
title ('Orginial Aortic Waveform');
subplot(2,1,2);
plot(shifted_aortic);
title ('Synthesized Aortic Waveform Through Digital Processing');
%% Calculating Correlation
Waveform_correlation = corr2(aortic_interp, shifted_aortic)*100
```

```
%% FEMORAL


close all
clear all
femoral = dlmread('Femoral3.csv');
aortic = dlmread('Aortic_of_Femoral3.csv');

load ('Magnitude_Femoral_Aortic.mat');

femoral = sortrows(femoral,1);

figure(); plot(femoral(:,1), femoral(:,2),'-o');
    title('femoral Waveform'); xlabel('Time (s)'); ylabel('Pressure
(mmHg)');

%% Interpolation of femoral Waveform

f_interp = 100;
t_max = min(femoral(end,1));
t_interp = 0:1/f_interp:t_max;

femoral_interp = interp1(femoral(:,1),femoral(:,2), t_interp)';
femoral_interp(end) = femoral_interp(1);
delay = 46.15; % delayed time = 140 ms/ 0.01 sec = 14
femoral_delayed = circshift(femoral_interp,uint64(delay));

figure(); plot(femoral(:,1), femoral(:,2),'-', t_interp,
femoral_interp, 'x');
    title('Interpolated femoral Waveform with X-axis Interval of 0.01
sec'); xlabel('Time (s)'); ylabel('Pressure (mmHg)');



[~, ia, ~] = unique(aortic(:,1));
aortic = aortic(ia, :);
aortic_interp = interp1(aortic(:,1),aortic(:,2), t_interp)';
aortic_interp(isnan(aortic_interp)) = aortic(end);

%% Transfer Function Portion
femoral_fft = fft(femoral_delayed); %FFT x
aortic_fft = fft(aortic_interp);  %FFT y
gtf_a_r = femoral_fft./aortic_fft;  %magnitude

gtf_magnitude = abs(gtf_a_r); % abs(femoral/aortic)
gtf_phase = unwrap(angle(gtf_a_r));   % phase( femoral/aortic)

%% resolving the x axis of frequency in hertz
m = length(t_interp); %91 points
fs = 100; %sampling frequency f=1/dt =1/0.01
f = (0:m-1)*(fs/m);

figure();
subplot(2,2,1);
```

```
plot(femoral(:,1), femoral(:,2),'-o');
    title('femoral Waveform'); xlabel('Time (s)'); ylabel('Pressure
(mmHg)');
subplot(2,2,3);
plot(aortic(:,1), aortic(:,2),'-o');
    title('Aortic Waveform'); xlabel('Time (s)'); ylabel('Pressure
(mmHg)');
subplot(2,2,2); %row,columns, 1st graph
plot(f, gtf_magnitude);
title('Magnitude'); xlabel('Frequency (Hz)');
xlim([0,10]);
subplot(2,2,4);
plot(f, gtf_phase);
title('Phase (rad)'); xlabel('Frequency (Hz)');
xlim([0,10]);

%% applying the TF

femoral_interp_fft = fft(femoral_interp);

t_mag_max = ceil(t_max*100);

Yr = real(gtf_r_a);
Yi = imag(gtf_r_a);

gtf_r_a_interp = interpft(gtf_r_a, fix(t_mag_max));

aortic_synthesis= femoral_interp_fft.*gtf_r_a_interp; %element by
element. aorta= femoral/magnitude

%to get into time domain do inverse fourier
aortic_inv = ifft(aortic_synthesis);
shifted_aortic = circshift(aortic_inv, uint64(delay));

shifted_aortic = real(shifted_aortic);

figure();
plot(t_interp,femoral_interp,t_interp, aortic_inv, 'o', t_interp,
shifted_aortic);
legend ('femoral Waveform', 'Inverse Fourier of Aortic Waveform',
'Synthesized Aortic Waveform');

%% Comparing to Original Aortic

subplot(2,1,1);
plot(aortic_interp);
title ('Orginial Aortic Waveform');
subplot(2,1,2);
plot(shifted_aortic);
title ('Synthesized Aortic Waveform Through Digital Processing');
%% Calculating Correlation
Waveform_correlation = corr2(aortic_interp, shifted_aortic)*100
```

Sample Digitized Data

Digitized data for waveform 1:

Time (ms)	Radial Pressure (mmHg)	Time (ms)	Aortic Pressure (mmHg)
-0.000934546	75.61097085	-0.001022677	75.76462486
0.017231215	78.64521008	0.022624615	79.31738666
0.022284381	81.37028987	0.030094601	81.52734793
0.027337547	84.45192216	0.035074593	83.66105309
0.032811811	87.94953236	0.040054584	85.90529691
0.037864977	92.09233279	0.045034575	88.17504965
0.042497046	95.60692168	0.050014566	90.52132915
0.045023629	98.42538427	0.054994557	93.1482068
0.047550213	101.0401026	0.060970546	96.1627118
0.050076796	103.5189914	0.064954539	98.63154239
0.053108696	106.5072409	0.072424526	101.5897654
0.057656545	109.6143412	0.079894513	104.4119408
0.060183129	112.3818677	0.090684493	107.6895147
0.062709712	114.724927	0.117036946	111.5997189
0.065741612	117.5909299	0.144634397	112.4227445
0.070289461	121.3041694	0.172024348	112.8622311
0.075342628	124.6404821	0.198456608	113.1015887
0.080395794	127.8749226	0.22680425	112.6223456
0.085954277	130.6509385	0.254194201	112.0431501
0.09302871	133.3675289	0.280339155	110.3626422
0.110714792	135.8750195	0.301504117	108.2263381
0.129664166	133.0194657	0.320179083	105.8738433
0.138507207	130.2774073	0.343834041	103.4154586
0.146086957	127.7985185	0.371223992	102.1787773
0.152403414	124.7083968	0.398613943	102.3334916
0.161246456	122.0257638	0.426003894	103.2024558
0.167562914	119.0035569	0.453393846	103.7653129
0.176405955	116.4907107	0.480783797	103.3634689
0.182722413	113.9948433	0.508173748	102.3865147
0.192828745	111.3971037	0.535563699	101.3075249
0.202935078	109.0795124	0.56295365	99.97808376
0.215567994	106.609113	0.590343601	98.41674336
0.237043951	104.3123593	0.617733552	96.68843548
0.264836366	103.6085154	0.645123503	95.01578343
0.292628781	102.9787603	0.672513454	93.61213455
0.320421196	100.8672286	0.699903405	92.05079416

0.348213611	99.20949106	0.727293356	90.62859334
0.376006026	99.81146281	0.754683308	89.41046389
0.400008566	101.9739305	0.782073259	88.45206165
0.420221231	104.2787878	0.80946321	87.56786718
0.444223771	106.2108855	0.836853161	86.66512077
0.472016186	106.1367967	0.864243112	85.74382242
0.497282018	104.2434155	0.891633063	84.92455975
0.518757975	101.9357285	0.919023014	84.04964125
0.537707349	99.71091368	0.946412965	83.37879413
0.557920014	97.49721587	0.973802916	82.68011909
0.581922554	95.22999476	1.001192867	81.75882074
0.608451678	92.99529041	1.028582818	81.04159376
0.636244093	91.30976952	1.05597277	80.38002261
0.664036508	90.44848687	1.083362721	79.57003591
0.691828922	89.73538188	1.110752672	78.7971531
0.719621337	88.91114364	1.138142623	78.07065015
0.747413752	88.00355547	1.165532574	77.45545886
0.775206167	87.21636164	1.192922525	76.81243965
0.802998582	86.39212341	1.220312476	76.16942044
0.830790997	85.54936296	1.247702427	75.4089056
0.858583412	84.55842485	1.275092378	74.37876917
0.886375827	83.71566441	1.290053817	74.11185014
0.914168242	82.77103182		
0.941960657	82.16906007		
0.969753072	81.60413274		
0.997545487	80.7613723		
1.025337902	80.11309503		
1.053130317	79.44629556		
1.080922732	78.50166297		
1.108715147	77.69594694		
1.136507561	76.94579753		
1.164299976	76.43643682		
1.192092391	75.8900317		
1.219884806	75.31584326		
1.247677221	74.59347717		
1.274206345	73.61272628		